C Petrological studies on xenoliths

In addition to the seismological investigations, xenoliths from a Quaternary tephra deposit were sampled to study the presumed source region of the CO_2-dominated gas petrologically. After the description of the sample site, an introduction into the used chemical analytical methods and into the geothermobarometry follows. Then the samples are described. Finally, the obtained petrological and mineral-chemical results are presented and discussed. Pressure-temperature (p-T) conditions of equilibration or crystallization are estimated from mineral-chemistry.

C.1 Sample site

Several (ultra-) mafic xenoliths/nodules as well as crustal xenoliths were sampled from a temporary outcrop in a tephra deposit in Mýtina (50.005°N, 12.444°E), approximately 1.5 km north of the Quaternary scoria cone Železná Hůrka (49.992°N, 12.444°E; Figures C.1, C.2) [*Kämpf et al.,* 1998; *Geissler et al.,* 2004b]. First detailed works on the tephra deposit as well as the ultramafic nodules and megacrysts were done by *Reuss* [1852] and *Proft* [1894].

The temporary outcrop was documented lithostratigraphically (Figure C.3), and samples were geochemically analysed using XRF and ICP-MS. Samples of wall rock (large blocks within the lower unit UF) and nephelinitic bombs were analysed for comparison. The excavated profile (approximately 4 m thick) consists of clayey material (weathered bedrock) at the base, tuff (lower unit with three sequences: UFa, UFb, UFc) and overlying tephra (upper unit, three sequences: OFa, OFb, OFc). The tuff is well stratified showing an average layer thickness of 1 to 3 cm. The middle part of the lower unit (UFb) contains a lot of wall rock fragments with a maximum dimension of 60 x 40 x 40 cm.

The petrochemical data (see Appendix C.i) were used to estimate the juvenile (magmatic) or wall rock content of the different tephra layers.

$$\text{(C.1)} \qquad magmatic\ component\ [\%] = \frac{X_{sample} - X_{wall\ rock}}{X_{nephelinite} - X_{wall\ rock}}$$

For this estimation contents of TiO_2, MgO, CaO, P_2O_5, Sr, Cr, Nb, and V were used (Figure C.3). Similar results can be obtained using other trace elements and REEs. Obviously, the magmatic components in UF rise from about 15% to 30 % topwards, whereas it is about 60% in OF. The reciprocal content of wall rock in UF ranges from about 85% to 70%, similar to values known from the West Eifel maar deposits (about 80%, according to *Zimanowski* [1986]).

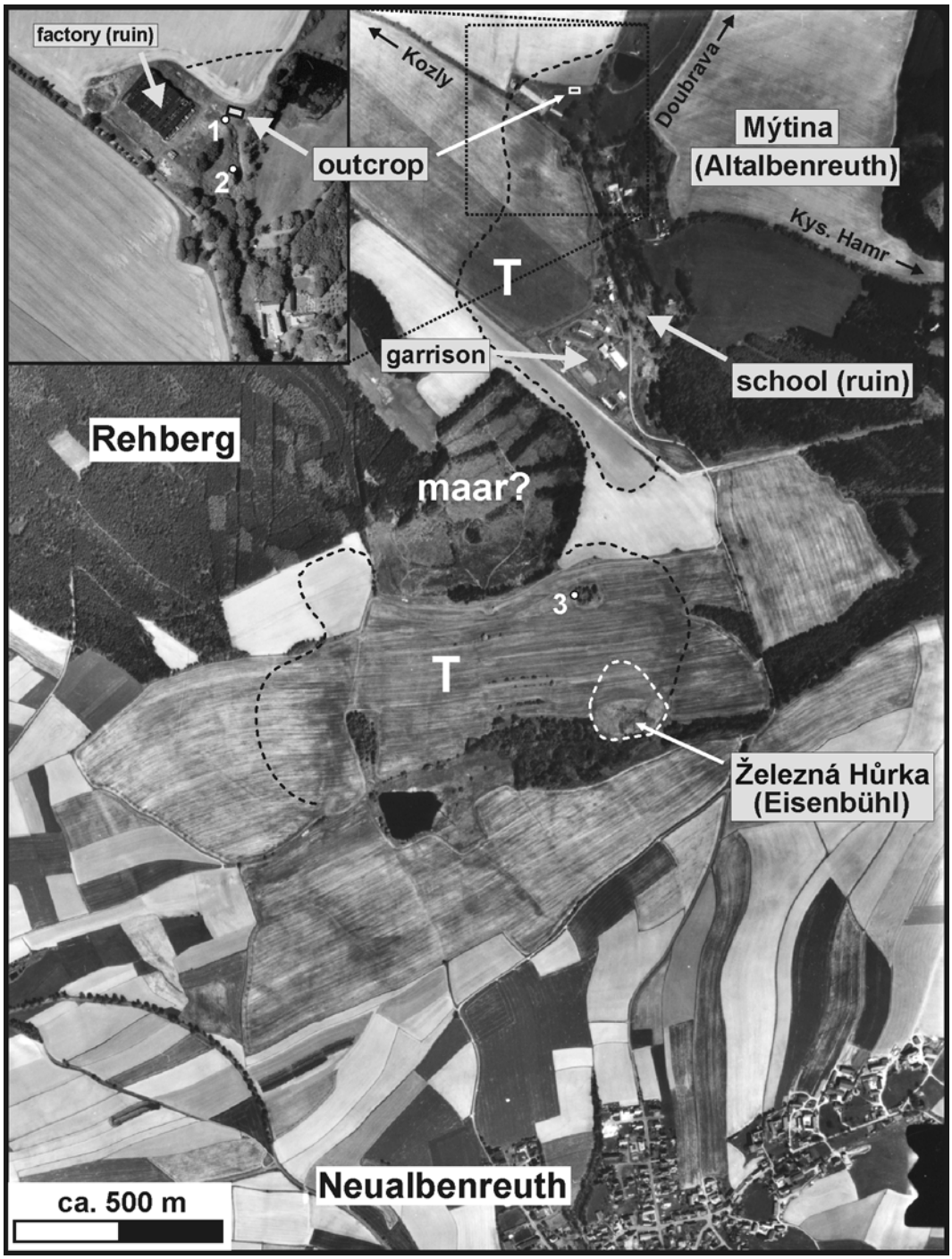

Figure C.1
Location of the temporary exploratory excavation "Mýtina", the approximate positions of previous temporary outcrops are marked (1 – sampling by *Kämpf* 1996; 2 – sampling by *Schwarzkopf* 1997), supposed tephra deposits (T) in the surrounding of the Železná Hůrka (3 – outcrops of tephra in a former quarry). The assumed boundaries of the tephra deposits are supported by the interpretation of field studies and aerial photographs (*Bayerisches Landesvermessungsamt* 1993 and 2001, nr. 93101/0 014 and 101007/0 316). From *Geissler et al.* [2004b].

The age of the tephra deposit was determined by *Wagner et al.* [2002] to about 300 ky using fission track and alpha-recoil track measurements on apatites and phlogopite [*Geissler et al.,* 2004b]. The Železná Hůrka scoria cone (lower unit) is approximately 500 ky old according to *Wagner et al.* [2002], however the uncertainties of the dating methods used are very high.

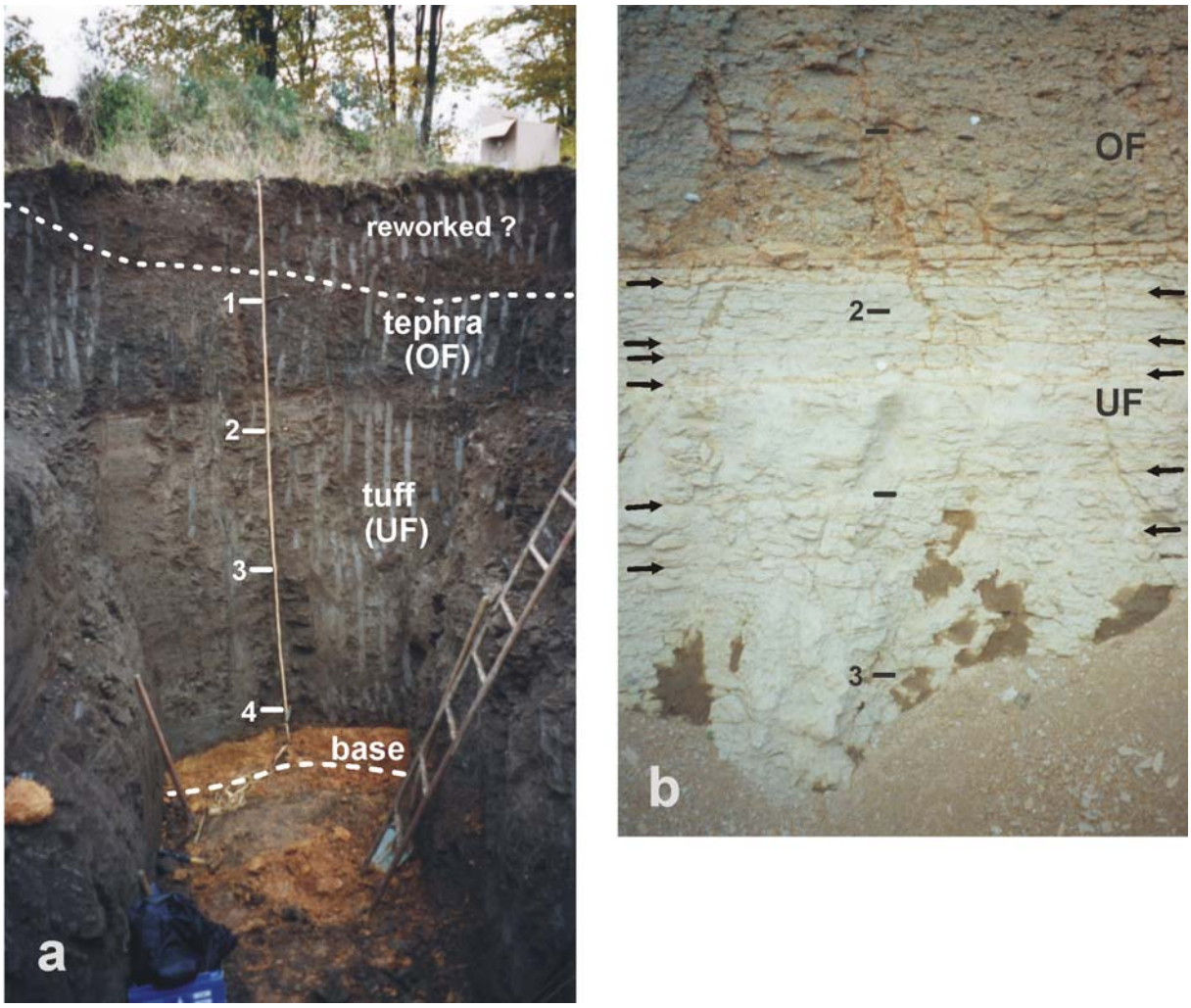

Figure C.2
The tephra-tuff deposit north of Mýtina, (temporary exploratory excavation); location in Figure C.1 (photographs by W.H. Geissler). **(a)** Total view (October 2002, fresh), **(b)** Total view (June 2003, weathered); note the high number of thin layers within the Lower Unit (arrows). From *Geissler et al.* [2004b].

C.2 Analytical methods and basics of geothermobarometry

Samples from nephelinitic host rock, ultramafic nodules/xenoliths, and crustal xenoliths were analysed for their chemical and mineralogical composition by microscopy and several chemical procedures, including X-ray fluorescence (XRF), inductively coupled plasma mass-spectrometry (ICP-MS), and mineral-chemical analyses by electron-microprobe analysis (EMPA). Whole-rock chemistry, both major and trace elements including rare earth elements (REE), were analysed in the laboratories of the GeoForschungsZentrum Potsdam. Results from mineral-chemical investigations can be used for geothermobarometric calculations, which are mainly based on empirically and experimentally calibrated formulas.

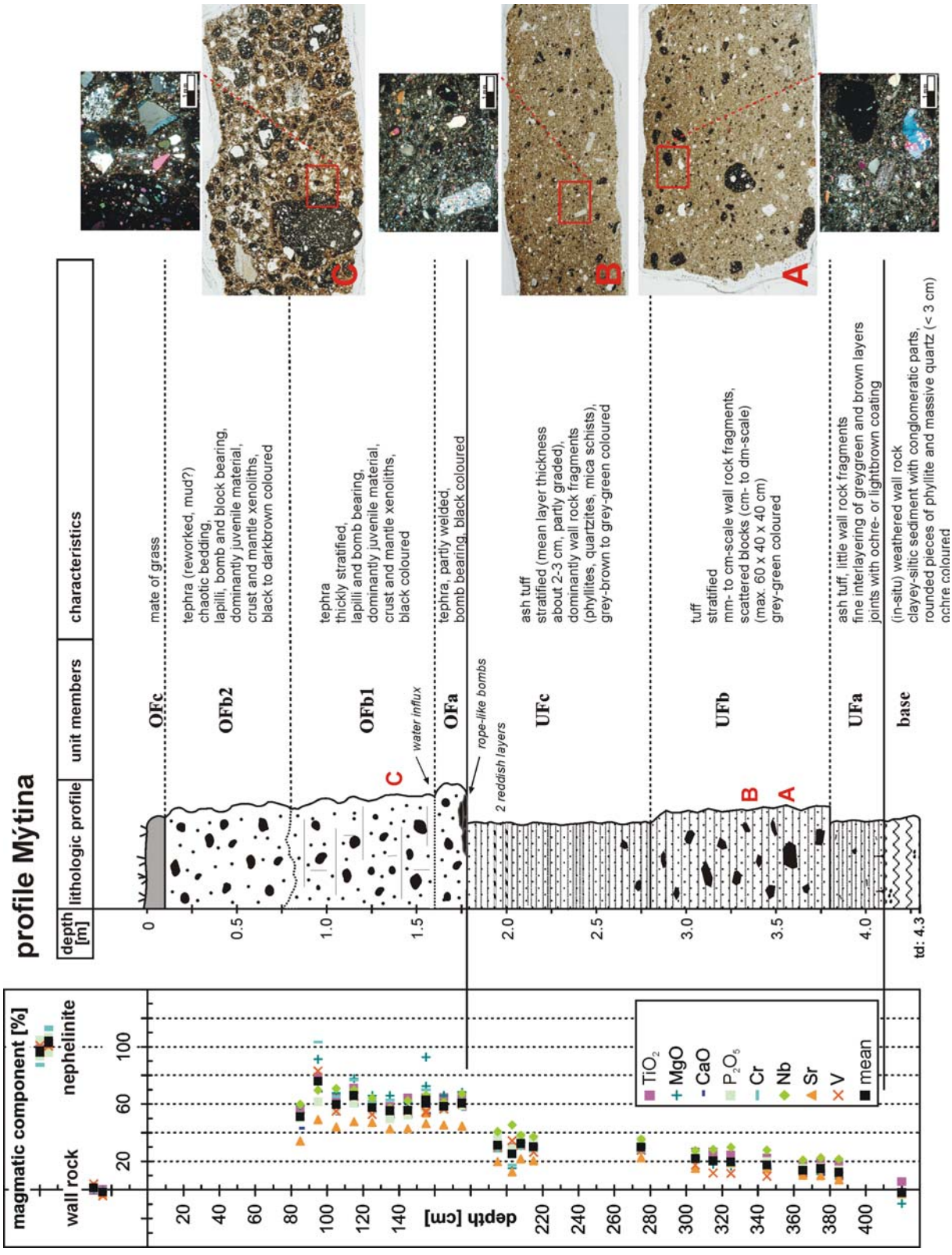

Figure C.3
Lithostratigraphy of the tephra-tuff-deposit within the excavation Mýtina (central part; from *Geissler et al.* [2004b]) together with photographs of thin-sections (right; made by E. Gantz, B. Stöcker, and W.H. Geissler). Thin-sections are about 4 cm long. Also shown is a "geochemistry" log (left) to demonstrate the content of juvenile magmatic material within the tephra-tuff layers (for data see Appendix C.i). UF - lower unit (tuff), OF - upper unit (tephra). The juvenile clasts of UF are vesicle free/poor. The country rock clasts of UF range in size from fine ash to 60 x 40 x 40 cm.

Sample preparation for whole-rock chemical analyses (ICP-MS, XRF) includes crushing to a grain size <62 µm and homogenisation. Thin-sections for microscopy and electron-microprobe analyses were made by the preparation laboratory of the GFZ Potsdam. The sections have commonly a thickness of 25 µm.

C.2.1 Geochemical (XRF, ICP-MS) and mineral-chemical (EMPA) investigations

In this chapter the basics of the analytical methods for rock and mineral chemistry will be introduced. A more detailed description of the theories, instruments, and analytical procedures can be found, e.g., in *Zussmann* [1977], *Gray* [1988], *Klein and Hurlbut* [1993], and *Dulski* [2001].

C.2.1.1 X-ray fluorescence spectrometry (XRF)

The sample, grounded to a fine powder, is compressed into a circular pellet or fused into a glass disc. This pellet/disc is shortly irradiated with primary X-rays. X-rays are absorbed by the sample according to Beer's law. The absorbed X-ray energy cause generation of a secondary X-ray emission spectrum, which is characteristic for each element in the sample. During absorption of the primary X-rays electrons in the inner shell are displaced. Vacancies will most probably be filled by electrons from the next outer shell creating a new vacancy. "Electron jumps" cause emission of energy in the form of the characteristic secondary X-radiation. The emission phenomenon is called X-ray fluorescence. Each element has characteristic spectral lines. The secondary X-ray spectrum (consisting of a low-intensity continuous background and element peaks) is resolved into spectral lines by an X-ray spectrometer, consisting of a diffracting crystal and an X-ray detector (X-ray counting device: scintillation counter or flow proportional counter).

C.2.1.2 Inductively coupled plasma mass-spectrometry (ICP-MS)

ICP-MS is a multi-element analytical method, which allows the quantification of concentrations of many trace elements, including the rare earth elements (REE) within rocks, minerals and natural waters [*Dulski*, 2001]. The method is described by *Gray* [1988] in more detail.

Inductively coupled plasma is produced, if energy is transmitted via an induction coil to a gas. The soluted sample is transformed into a gas-supported aerosol using a pneumatolytic nebulizer and is subsequently introduced into the plasma. The reproducible extraction of ions from the plasma to the

mass-spectrometer is complicated, because both have totally different temperature and pressure conditions (1 atm, 7000K and $\leq 10^{-5}$ mbar, 300K, respectively). The ions are collected by a conic collector and separated by mass using a quadrupol mass filter. The counting of ions is done in an electron multiplicator in the impulse counting mode.

C.2.1.3 Electron microprobe analysis (EMPA)

The methodology of electron microprobe analysis is similar to the XRF method. Only the primary X-radiation is replaced by a sharply focused electron beam, which allows the qualitative and quantitative analysis of a minute volume of material (10-20 μm^3 or 10^{-11}g minimum for silicate materials). The heart of the electron microprobe is an X-ray spectrometer. X-rays within the sample volume are excitated by an electron beam, which is sharply focused by electromagnetic lenses down to a diameter of 2 to 10 (20) µm. A heated tungsten filament serves as the source of the free electrons (energy source). The electron beam has enough energy to displace inner-shell electrons of the constituent atoms of the sample. Outer shell electrons fill inner-shell vacancies and loose their energy, which is emitted as characteristic X-rays. The characteristic X-ray spectrum of the elements within a crystal or glass is recorded wavelength dispersive by a crystal spectrometer or energy dispersive by a semiconductor spectrometer. The duration of point measurements range between 2 and 7 min depending on the number of analysed elements and required accuracy (counting times).

Using the electron microprobe two-dimensional element scans or line scans are possible to study the zoning of elements within minerals (e.g., Al or Ti in clinopyroxene). The focused electron beam causes heating of the sample analysis area. Therefore, the beam diameter should be greater analysing samples with a higher content of H_2O, F, and alkalis (e.g., feldspars, mica and glass analyses).

C.2.2 Geothermobarometry of xenoliths

To combine petrologic and seismic data, it is necessary to estimate the depth of origin of the xenoliths. In the past, strong efforts were made to calibrate geothermobarometer, empirically and experimentally, for mineral assemblages equilibrated under pressures typical for the lower crust (garnet-bearing metamorphic rocks) and upper mantle (spinel and garnet lherzolites [see *Pearson et al.,* 2004]). Unfortunately, the Mýtina (ultra-) mafic xenolith suite provides no possibility to use these standard upper mantle geothermobarometers, which are calibrated for orthopyroxene- and garnet-bearing upper mantle rocks. Calibrations for other assemblages are rare, however, *Ernst and Liu* [1998] and *Huckenholz et al.* [1992] proposed geothermobarometers for amphibole-bearing xenoliths. *Nimis and*

Ulmer [1998] and *Nimis* [1999] published barometric formulations for clinopyroxenes. Temperature of equilibration can be estimated using the Mg^{2+} - Fe^{2+} partitioning between coexisting olivine and spinel. Geothermobarometers used in this study are outlined below.

C.2.2.1 Amphibole thermobarometry

Ti-rich amphiboles, found as phenocrysts and xenocrysts in many alkali basaltic rocks, are a near-liquidus phases, stable up to ca. 31 kbar and 1100°C [*Schulze*, 1987]. Several studies showed that the chemistry of amphiboles is sensitive to pressure, temperature, oxygen and water fugacities [e.g., *Helz,* 1982; *Spear,* 1981; *Wones and Gilbert,* 1981]. There exist a lot of empirical and experimentally calibrated thermo/barometers for mostly amphibole-bearing quartz-rich intrusions [e.g., *Otten,* 1984; *Hammarstrom and Zen,* 1986; *Hollister et al.,* 1987; *Johnson and Rutherford,* 1989; *Schmidt,* 1992]. They are calibrated for a mineral assemblage of hornblende, melt, fluid, biotite, quartz, sanidine, plagioclase, sphene, magnetite or ilmenite.

Ernst and Liu [1998] compiled a p-T scheme based on the Al_2O_3 and TiO_2 contents in amphiboles. This scheme can be used for metabasaltic assemblages containing coexisting Al-rich (e.g., plagioclase, epidote, garnet) and Ti-rich phases (e.g., ilmenite, titanite, rutile), and closely approached chemical equilibrium under crustal or uppermost mantle conditions. It should be also applicable, with caution, to inhomogeneous specimens. Al increases with both p and T, but also compositional variations (high proportions of melt) seem to influence partitioning of Al_2O_3 in Ca-amphibole. TiO_2 content correlates positively with temperature and can be used as a geothermometer above 500°C, where solubility of Ti in calcic amphiboles becomes substantial. According to *Ernst and Liu* [1998], the Al- and Ti-contents of amphibole can give an estimate for the solidification depth of an intrusion, or the equilibrium pressure of a magma chamber before eruption. This thermobarometer should be especially applicable at crustal/lithospheric pressures (up to ~1.2 GPa).

Huckenholz et al. [1992] studied the exchange reactions of Ca, Ti and Na between coexisting calcic amphiboles (potassian and titanian pargasites) and clinopyroxenes (diopside), which crystallized from a melt with magnesio-hastingsite composition. Their results provide pressure constraints for calcic amphiboles (potassian and titanian pargasites) coexisting with clinopyroxenes. *Huckenholz et al.* [1992] proposed that the Na/Ca exchange between both minerals could be used for pressure estimates in alkali basalt systems (4-45 kbar).

$$P[kbar] \pm 2\ kbar = 48.04 - 23.94 \ln \frac{(Na/Ca)_{amph}}{(Na/Ca)_{cpx}} \quad \text{(C.2)}$$

Pressure estimates of natural amphibole-clinopyroxene pairs can be made, when alkali basalts close to nepheline basanite, olivine nephelinite, or pargasite composition is available with Na/Ca ratios of 0.25 to 0.60, and they bear both amphibole and clinopyroxene. The barometer is not applicable for peridotite systems and alkali basalts + H_2O-excess systems (then $K_D > 6$).

C.2.2.2 Olivine-spinel thermometry (spinel barometry)

Mg^{2+} - Fe^{2+} partitioning between coexisting spinel and olivine (formula C.3) was first suggested as potential geothermometer by *Irvine* [1965]:

$$(C.3) \qquad 1/2\,Fe_2SiO_4 + Mg(Cr_\alpha Al_\beta Fe^{3+}_\gamma)_2O_4 = 1/2\,Mg_2SiO_4 + Fe(Cr_\alpha Al_\beta Fe^{3+}_\gamma)_2O_4$$

where α, β, and γ are the atomic fractions of the respective trivalent cations. This exchange is temperature-sensitive, especially for Cr-rich spinels. The first calibration was made by *Jackson* [1969] from available thermo-chemical data. *Roeder et al.* [1979] re-evaluated this formulation of the *Irvine* olivine-spinel geothermometer using a different free energy value of $FeCr_2O_4$. Their equation to estimate the temperature of equilibration is:

$$(C.4) \qquad T\,[K] = \frac{3480\alpha + 1018\beta - 1720\gamma + 2400}{2.23\alpha + 2.56\beta - 3.08\gamma - 1.47 + 1.987 \ln K_D}$$

where $\alpha = \frac{Cr}{Cr + Al + Fe^{3+}}$, $\beta = \frac{Al}{Cr + Al + Fe^{3+}}$, $\gamma = \frac{Fe^{3+}}{Cr + Al + Fe^{3+}}$, and

$$(C.5) \qquad K_D = \frac{(X_{Mg} / X_{Fe^{2+}})_{olivine}}{(X_{Mg} / X_{Fe^{2+}})_{spinel}}$$

is the equilibrium constant for the Mg^{2+}/Fe^{2+} exchange between coexisting olivine and spinel. *Fabries* [1979] pointed out that there are problems with end-member spinels, especially spinels with low Cr/(Cr+Al) ratios as common in lherzolitic rocks. In this case the calculated temperatures could be too high. His formulation of the olivine-spinel thermometer is given below:

$$(C.6) \qquad T\,[K] = \frac{4250\,Y^{sp}_{Cr} + 1343}{\ln K^0_D + 1.825\,Y^{sp}_{Cr} + 0.571}$$

$$\ln K^0_D = \ln K_D - 4.0\,Y^{sp}_{Fe^{3+}} \qquad \text{[according to } \textit{Irvine}\text{, 1965]}$$

$$\ln K^0_D = \ln K_D - 2.0\,Y^{sp}_{Fe^{3+}} \qquad \text{(T = 1200°C, } \textit{Roeder et al.}\text{ [1979])}$$

According to *Fabries* [1979], the uncertainty due to analytical errors in the determination of Mg and Fe^{2+} in spinel and olivine, and Cr, Al, and Fe^{3+} in spinel is about ±50 K [see also *Jackson,* 1969]. These first versions of olivine-spinel thermometer did not take into account the influence of oxygen fugacity f_{O2} [*O'Neill,* 1981]. *Ballhaus et al.* [1991] calibrated a oxygen geobarometer and provided a corrected and simplified version of the olivine-spinel thermometer from *O'Neill and Wall* [1987]:

(C.7)

$$T[K] = \frac{(6530 + 280p + 7000 + 108p)(1 - 2X_{Fe}^{ol}) - 1960(X_{Mg}^{sp} - X_{Fe^{2+}}^{sp}) + 16150X_{Cr}^{sp} + 25150(X_{Fe^{3+}}^{sp} + X_{Ti}^{sp})}{R \ln K_D \{Mg / Fe^{2+}\}_{ol/sp} + 4.705}$$

X_{Ti}^{sp} is the number of Ti cations in spinel to 4 oxygens, $K_D\{Mg/Fe^{2+}\}_{ol/sp} = \frac{(X_{Mg}/X_{Fe^{2+}})_{olivine}}{(X_{Mg}/X_{Fe^{2+}})_{spinel}}$,

X_{Cr}^{sp} and $X_{Fe^{3+}}^{sp}$ are the $\frac{Cr^{3+}}{\Sigma R^{3+}}$ and $\frac{Fe^{3+}}{\Sigma R^{3+}}$ ratios in spinel, respectively. R is the molar constant R = 8.3143 $J \cdot mol^{-1}K^{-1}$. p is in GPa.

The formulation of *O'Neill and Wall* [1987] is:

(C.8)

$$T[K] = \frac{6530 + 28p + (5000 + 10.8p)(X_{Mg}^{ol} - 2X_{Fe}^{ol}) - 1960(1 + X_{Ti}^{sp})(X_{Mg}^{sp} - X_{Fe^{2+}}^{sp}) + 18620X_{Cr}^{sp} + 25150(X_{Fe^{3+}}^{sp} + X_{Ti}^{sp})}{R \ln K_D \{Mg / Fe^{2+}\}_{ol/sp} + 4.705}$$

The pressure dependence of the olivine-spinel thermometer resulted from the work of *O'Neill* [1981]. *O'Neill* [1981] found that the Cr-content of spinels influences the depth (pressure) of the transition between spinel and garnet lherzolite and can be used as a maximum pressure (depth) indicator:

(C.9) $$p = p^0 + 27.9\,(X_{Cr}^{sp} + X_{Fe^{3+}}^{sp})$$

whereas p^0 is approximately 17.6-19.8 kbar at 1100°C, and X_{Cr}^{sp} and $X_{Fe^{3+}}^{sp}$ are the mole fractions of chromium and ferric iron in spinel.

Medaris et al. [1999] used the olivine-spinel thermometer as a barometer. They fitted temperature data derived with the formulation of *Ballhaus et al.* [1991] to a model geotherm (underplating scenario with subsequent cooling) to get depth estimates for spinel peridotite nodules from the Kozákov volcano (Elbe Zone, CZ).

There are several limitations of the olivine-spinel geothermometry, which have to be kept in mind. The equilibrium exchange of Mg^{2+} and Fe^{2+} between spinel and olivine is one of the fastest exchange reactions. It is still effectively during cooling down to relatively low temperature (subsolidus), while other exchange reactions in peridotites (e.g., pyroxene exchange reactions) are blocked at higher temperatures (*Fabries,* 1979). The decision if olivine and spinel are coexistent equilibrium phases and the estimation of Fe^{3+} contents from electron microprobe data via stoichiometric derivation are further problems.

C.2.2.3 Pyroxene thermometry

Furthermore, the chemical composition of coexisting clinopyroxene and orthopyroxene can be used as a geothermometer. On the basis of experiments and ability tests *Brey and Koehler* [1990] formulated new versions of the two-pyroxene thermometer:

$$T_{BKN}\,[K] = \frac{23664 + (24.9 + 126.3\,X_{Fe}^{cpx})\,p}{13.38 + (\ln K_D^*)^2 + 11.59\,X_{Fe}^{opx}} \qquad \text{(C.10)}$$

with $K_D^* = \frac{(1 - Ca^*)^{cpx}}{(1 - Ca^*)^{opx}}$, $Ca^* = \frac{Ca^{M2}}{1 - Na^{M2}}$ and $X_{Fe}^{opx,cpx} = \frac{Fe}{Fe + Mg}$.

The Ca content of orthopyroxene alone can be used as a geothermometer:

$$T_{Ca-in-opx}\,[K] = \frac{6425 + 26.4p}{-\ln Ca^{opx} + 1.843} \qquad \text{(C.11)}$$

The partitioning of Na between orthopyroxene and clinopyroxene is also temperature sensitive (thermometer calibrated from natural rock data):

$$T_{Na}^{cpx/opx}\,[K] = \frac{35000 + 61.5p}{(\ln D_{Na})^2 + 19.8} \qquad \text{(C.12)}$$

p is in kbar, $D_{Na} = \frac{Na^{opx}}{Na^{cpx}}$.

An older version of the pyroxene thermometer was suggested by *Wells* [1977], however *Lindsley* [1983] pointed out, that it should not be used any longer. *Brey and Koehler* [1990] pointed out that *Well*'s formulation reproduces the experimental results at 900°C, but increasingly underestimates them at higher temperatures.

C.2.2.4 Phlogopite-liquid (glass) thermobarometry

Righter and Carmichael [1996] published results from experiments on olivine and augite minette powders at 1 bar to 2 kbar (water-saturated) and 900 to 1300°C. The oxygen fugacity was controlled between the nickel-nickel oxide (NNO) and hematite-magnetite (HM) oxygen buffers. *Righter and Carmichael* [1996] showed that the partitioning of TiO_2 between biotite and liquid is temperature dependent (uncertainty of ±50 K), whereas the BaO partitioning is pressure and temperature dependent (uncertainty of ±4 kbar).

(C.13) $$\ln D_{TiO_2}^{phl/liq} = \frac{a}{T} + b$$

with the TiO_2 partition coefficient $D_{TiO_2}^{phl/liq} = \frac{TiO_2^{phl}[wt\%]}{TiO_2^{glass}[wt\%]}$

and a, b as regression coefficients (a = 17600, b = -12.1). T is in Kelvin.

(C.14) $$p = \frac{T}{c}(\ln D_{BaO} - a - \frac{b}{T} - d \ln a_{H_2O})$$

with the BaO partitioning coefficient $D_{BaO}^{phl/liq} = \frac{BaO^{phl}[wt\%]}{BaO^{glass}[wt\%]}$,

and the regression coefficients a = -2.167, b = 4553, c = -130.7, and d = -0.388. T is in Kelvin; p is in kbar. Where phlogopite is close to liquidus a_{H2O} can be set to 1 (phlogopite/biotite as phenocrysts together with either olivine or augite). Reducing a_{H2O} to 0.8 the calculated pressure increases by 10% [*Righter and Carmichael,* 1996].

C.2.2.5 Olivine-clinopyroxene barometry

Köhler and Brey [1990] established a geobarometer, which is based on the calcium exchange between olivine $(\frac{Mg}{Mg+Fe})^{ol} \approx 0.9$ coexisting with clinopyroxene in natural lherzolitic compositions:

(C.15) $$p[kbar] = \frac{-T \ln D_{Ca} - 11982 + 3.61T}{56.2}, \qquad T \geq (1275.25 + 2.827\,p)\ [\mathrm{K}]$$

(C.16) $$p[kbar] = \frac{-T \ln D_{Ca} - 5792 - 1.25T}{42.5}, \qquad T \leq (1275.25 + 2.827\,p)\ [\mathrm{K}]$$

where $D_{Ca} = \frac{Ca^{ol}}{Ca^{cpx}}$, and Ca^{ol}, Ca^{cpx} are the atomic proportions of Ca in the structural formulae of olivine and clinopyroxene based on 4 and 6 oxygens, respectively. According to *Köhler and Brey* [1990] the uncertainties are in the range of ±1.7 kbar (1σ).

O'Reilly et al. [1997] described the limitations of the above geobarometer. The Ca and Ti contents in olivines in spinel peridotites are well correlated with one another and with temperature, whereas the Ca content is poorly correlated with pressure. A strong temperature dependence of the Ca-in-olivine barometer exists. A temperature uncertainty of ±50 K results in a pressure uncertainty of ±8 kbar. Therefore, pressure estimates span the entire width of the spinel-lherzolite field at 900-1200°C.

C.2.2.6 Clinopyroxene barometry

Nimis and Ulmer [1998] performed crystal structure modelling of Ca-rich clinopyroxene coexisting with basic and ultrabasic melts and calibrated a geobarometer that is based on the structural parameters unit-cell volume (V_{cell}) and M1-site volume (V_{M1}). It should be applicable to anhydrous and hydrous melt compositions (quartz-normative basalts to nephelinite, excluding melts coexisting with garnet or melilite), pressure conditions pertinent to the crust and upper mantle (0 to 24 kbar), as well as a variety of f_{O2} conditions. At a given melt composition, V_{cell} and V_{M1} decrease linearly as pressure increases. The expanded version of the geobarometer (valid for an/hydrous compositions) is very temperature sensitive (underestimating T by 20 K cause 1 kbar increase of calculated p).

The best way is using of X-ray diffraction data as input for the calculations, however another approach is the calculation from mineral chemical analyses (atomic fractions from microprobe data, via chemistry-structure coefficients; for details see *Nimis* [1995] and *Nimis and Ulmer* [1998]). For pressure calculations the Excel-Worksheet provided by *Nimis* [1999] was used.

According to *Nimis and Ulmer* [1998], most useful results can be obtained for cumulitic products (pyroxenitic xenoliths, megacrysts), but the geobarometer should also be applicable to mantle equilibrium partial-melting residua. Clinopyroxenes that re-equilibrated after magmatic crystallization or melting during subsolidus processes are unsuitable for geobarometric purposes, unless their primary composition can be recovered. *Nimis* [1999] discussed the uncertainties of the clinopyroxene barometry. The errors for the expanded version of the barometer are about 3.1 kbar; low-pressure data (≤15 kbar) are better reproduced (standard deviation σ = 2.6 kbar) than high-pressure data (>18 kbar; σ = 6.1 kbar). The standard deviation is about 1.75 kbar for anhydrous basic or ultrabasic systems. In comparison to the uncertainties of the barometric formulation, the uncertainties in chemical analyses (e.g., by electron microprobe) cause negligible errors.

C.3 Sample description

C.3.1 Mantle xenoliths (ultramafic nodules)

Mantle xenoliths can generally be divided into two groups according to *Lloyd and Bailey* [1975], *Frey and Prinz* [1978], and *Lloyd* [1981, 1987]:

Group I: spinel lherzolites, spinel harzburgites, wehrlites, dunites (composed of olivine, ortho- and clinopyroxene and minor amounts of amphibole and dark mica).

Group II: pyroxenites (mainly clinopyroxene, minor amounts of orthopyroxene and olivine) containing significant amounts of hydrous minerals (titaniferous phlogopite, amphibole) and titanite, (perovskite), titanomagnetite (ilmenite?), apatite, rarely calcite and feldspar.

The (ultra-) mafic xenolith-suite (nodules; further mostly referred as mantle xenoliths) sampled from the Mýtina tephra deposit includes wehrlites, clinopyroxenites, hornblendites (Table C.I; for nomenclature see Figure C.4), chromite-bearing olivine-clinopyroxene aggregates, and megacrysts of olivine, clinopyroxene, amphibole and phlogopite (Plate 1). The xenoliths and megacrysts are commonly coated by the host rock and form cored bombs.

The volcanic host rock (dark grey, vesicular scoria and bombs) can be classified as olivine melanephelinite [*Le Bas,* 1987; *Le Bas et al.,* 1992; *Le Maitre,* 1989]. The only partly re-crystallized glassy groundmass contains olivine and strongly zoned titanian diopside phenocrysts, euhedral in form and commonly up to 1 mm maximal size. No feldspathic minerals (plagioclase, alkali-feldspar, nepheline) can be observed by optical microscopy. Additionally to the phenocrysts olivine and clinopyroxene xenocrysts with fragmented or irregular edges in contact to the host rock also occur.

Most of the xenoliths show cumulus textures (Plates 2, 3). No (shear) deformation textures could be observed in the Mýtina samples, but some samples exhibit high porosity (only partly filled with glass).

Wehrlites (MXZH1, -2, -3, -4, -67; Plates 1, 2)
Several wehrlitic samples were identified. The main components are green clinopyroxene and olivine; minor constituents are brown mica (phlogopite) and glass. All samples show a cumulus texture and contain some percent open pore space (in some thin-sections filled with coloured glue) [see *Kämpf et al*., 1999b]. Euhedral to anhedral crystals occur together in one sample. Grain size is variable in different samples (from less then 1 mm up to more than 1 cm). Boundaries of some nodules imply that the samples have a xenolithic origin rather than being cumulates from the host magma. Spongy zones (sieve texture) can be observed in some clinopyroxenes, especially near the rim.

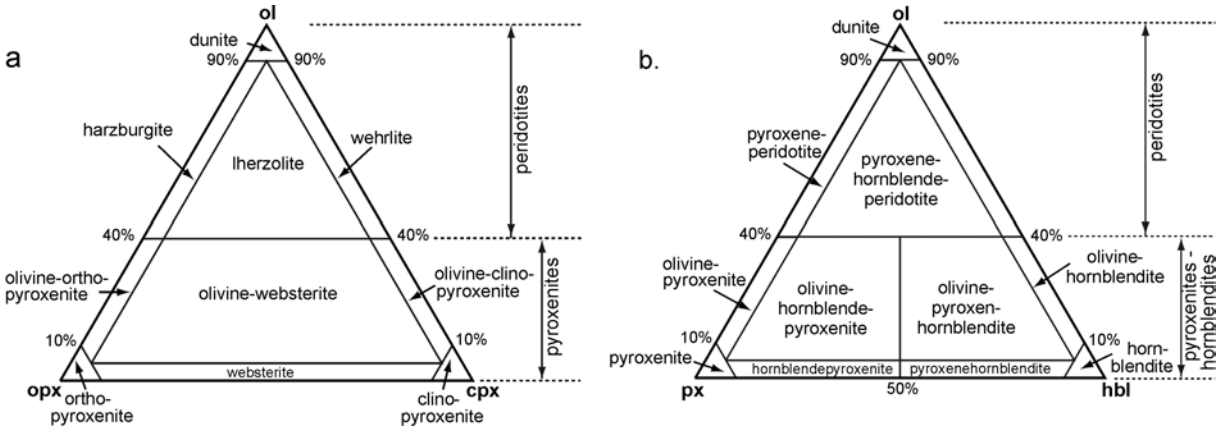

Figure C.4
IUGS classification of ultramafic plutonic rocks [after *Le Maitre,* 1989].
No modal composition was determined, however most of the analysed xenoliths are olivine-clinopyroxene-bearing samples and would plot in the wehrlite and olivine-clinopyroxenite fields (no orthopyroxene) **(a)**. Amphibole and clinopyroxene rich samples (no or minor amounts of olivine) plot in the hornblende- (hbl-) pyroxenite and pyroxene- (cpx-) hornblendite fields **(b)**. Sample MXZH66 can be classified as (pyroxene-) hornblende- (hbl-) peridotite; sample MXZH68 is a hornblendite (almost 100% amphibole). The olivine-orthopyroxene-clinopyroxene-bearing samples from Gottleuba (Go01-1) and Zinst (Zinst-1) would plot in the harzburgite and lherzolite fields, respectively.

Hornblende-peridotite (MXZH66; Plates 1, 3)

Sample MXZH66 contains olivine, clinopyroxene, amphibole and spinel as main phases and shows an equigranular, cumulus texture. This sample is classified as hornblende-peridotite to distinguish it from the typical wehrlites containing olivine, clinopyroxene and phlogopite (± glass). Amphibole and spinel are partly euhedral, whereas olivine and clinopyroxene are anhedral. The average grain size is up to 5 mm. Only one sample was found up to now.

Olivine-clinopyroxene-spinel cumulates (MXZH8, -18, -61, -64; Plate 2)

Additionally to the wehrlitic samples, olivine-clinopyroxene-spinel aggregates were investigated. Commonly there are smaller than the wehrlitic samples and show no regular boundaries, indicating crystallization from the melt (at least for some of the constituents). They also contain dark-brown Cr-rich spinel. Clinopyroxenes have a less spongy appearance than that in the wehrlites. They show titanian diopsidic rims towards the melt (nephelinite).

Clinopyroxenites (MXZH5, -11, -33; Plate 3)

There are several samples containing clinopyroxene as the main constituent. Further minerals are amphibole (up to 50%), ilmenite (± titano-magnetite), apatite (MXZH5), and titanite (MXZH11). They are equigranular and show cumulus textures; the average grain size is several mm, but may reach up to 1 cm. There seem to exist two generations of amphibole in sample MXZH33.

Hornblendites (MXZH12, -13, -68; Plate 3)

Hornblendites are mainly composed of pitch-black amphibole (brown in thin-sections; euhedral to anhedral crystals). Minor phases are clinopyroxene, ilmenite (± titano-magnetite), phlogopite, and sulphide inclusions. Normal grain size is some mm. In samples MXZH12 and MXZH13 up to cm-size amphibole crystals overgrow small clinopyroxene crystals. Glass, phlogopite, skeletal olivine, titano-magnetite, and clinopyroxene phenocrysts occur in vugs in both samples.

Spinel lherzolites/harzburgites (Zinst-1, Go01-1; Plate 2)

Spinel lherzolites are the typical upper mantle xenoliths in the mafic Cainozoic volcanics of Central Europe [e.g., *Menzies and Bodinier,* 1993]. Up to now, such rock fragments could not be found within the Quaternary volcanics in the area under study. For comparison, two spinel peridotite xenoliths from the Mariengründel, about 1km south-southeast of Bad Gottleuba, Saxony (50.842°N, 13.952°E; Elbe Zone; late Miocene?), and from the Wunschenberg quarry near Zinst, NE-Bavaria (49.90°N, 11.94°E; Franconian Lineament; K-Ar whole rock age 28.8±1.8 Ma, according to *Todt and Lippolt* [1975]), are investigated. The average grain size in both samples is up to 5 mm. Most crystals have anhedral grain boundaries. Sample Zinst-1 contains several volume percent clinopyroxene, whereas Go01-1 has only a small amount of clinopyroxene.

Table C.I. Mineral parageneses of studied samples. (Mineral abbreviation according to *Kretz,* 1983; am - amphibole, fsp - feldspar, gl - glass, sp - spinel, sulph - sulphide).

sample	paragenese														rock type
	ol fo%	cpx	opx	fsp	am	phl	sp	ilm	mag	ap	ttn	rt	gl	sulph	
Železná Hůrka															
EB1	82..85				x										ol-megacryst
EB5-ol9	89..85						x								ol-phenocryst
Mýtina															
XKZH1		x	x	x	x	x			(x)			x			norite
XKZH2				x					x						?
XKZH3		x		x						x					? (+zrn)
MXZH66	82	x			x		x		(x)						hbl-peridotite
MXZH5		x			x			x		x					hbl-clinopyroxenite
MXZH11		x			x				x		x				hbl-clinopyroxenite
MXZH33		x			x	(x)		x	x						hbl-clinopyroxenite
MXZH12	(x)	x			x	x		x	x						cpx-hornblendite
MXZH13		x			x	?		x	x						cpx-hornblendite
MXZH68					x				(x)					x	hornblendite
MXZH1,3	88	x				x									wehrlite
MXZH2	88	x													wehrlite
MXZH4	88	x													wehrlite
MXZH8	88	x					x						x		ol-cpx-cumulate
MXZH18	88	x				?	x						x		ol-cpx-cumulate
MXZH64	86..88	x					x								ol-cpx-cumulate
MXZH61	83..87	x					x						x		ol-cpx-cumulate
MXZH17 (gm)	88						x								ol-phenocryst
MXZH24	82..87	(x)				x							x		ol-megacryst
MXZH69	86	x				x	x						x		ol-megacryst
sp-lherzolites															
Zinst-1	90	x	x				x								sp-lherzolite
Go01-1	90	x	x	?			x								sp-lherzolite (harzburgite)

C.3.2 Megacrysts

The Železná Hůrka and the tephra deposit in Mýtina have been known at least since the 19th century for the occurrence of megacrysts (large single crystals), several cm in size [*Reuss*, 1852; *Proft*, 1894]. A number of samples from both localities, including olivine, clinopyroxene, amphibole and phlogopite crystals, were investigated (Plates 1, 3).

Olivine (MXZH7, -19, -24, -69; EB1)
Some olivine megacrysts occur as euhedral crystals, partly showing skeletal growth. Other samples have irregular grain boundaries. Rounded samples are a third group, indicating disequilibrium with the host melt (e.g., MXZH19). Composite megacryst samples consist of three ore more large olivine crystals (e.g., MXZH69). Most of the olivine megacrysts are porous. Pore boundaries are crystal faces only in a few samples. The vugs are partly filled with glass and groundmass crystals (mostly clinopyroxene); bigger exemplars are empty showing only a thin coating of the pore walls by glass and micro-phenocrysts. One olivine megacryst from Železná Hůrka (EB-1) contains an amphibole inclusion [see *Kämpf et al.,* 1993].

Clinopyroxene (MXZH9, -14, -17, -62; EB2, -6, -7)
Two types of clinopyroxene megacrysts occur, black and green in colour, the latter ones mostly in olivine-clinopyroxene-spinel aggregates. Almost all samples are zoned/rimmed. One sample from the Železná Hůrka shows sector zoning (EB2). Some samples have a spongy appearance, which stems from small melt pockets. Also composite samples (spongy + not spongy crystals) occur (MXZH62). Clinopyroxene megacrysts show all kinds of grain boundaries (subhedral to anhedral, broken, rounded).

Amphibole (MXZH10, -15, -32, -35, -39, -42, -1a, -9)
Amphibole megacrysts look pitch-black in hand specimen and dark-brown in thin-sections. Almost all samples are rounded, indicating disequilibrium with the host melt, at least under conditions during the ascent within the magma column. Only a few samples show well developed crystal faces in hand specimen. But most samples show perfect cleavage under the microscope. Some of the amphibole megacrysts are also porous, containing vugs, partly filled with glass.

Phlogopite (MXZH21, -22, -74)
Thin black mica flakes are very common in the tephra and as inclusions in volcanic bombs. Their length is up to 7 cm. Flake boundaries are rounded. One sample with dimensions of 35x35x35 mm was found (MXZH74).

Plate 1
Photographs of typical hand specimen of (ultra-) mafic nodules from the Mýtina tephra. **(a)** Amphibole megacrysts are commonly rounded and have vugs filled with nephelinitic glass; **(b)** phlogopite megacrysts can normally be found as flakes; **(c)** and **(d)** olivine megacryst MXZH19 showing atypically large vugs, which are only partly filled with nephelinitic glass; **(e)** porous wehrlitic xenolith MXZH3, consisting mainly of olivine and clinopyroxene and minor phlogopite; **(f)** black coloured clinopyroxene megacryst showing typical conchoidal fracture; **(g)** amphibole-bearing peridotite (olivine, clinopyroxene, amphibole, spinel); **(h)** porous wehrlitic xenoliths MXZH67 consisting only of olivine and clinopyroxene. (Photographs by E. Gantz, GFZ Potsdam)

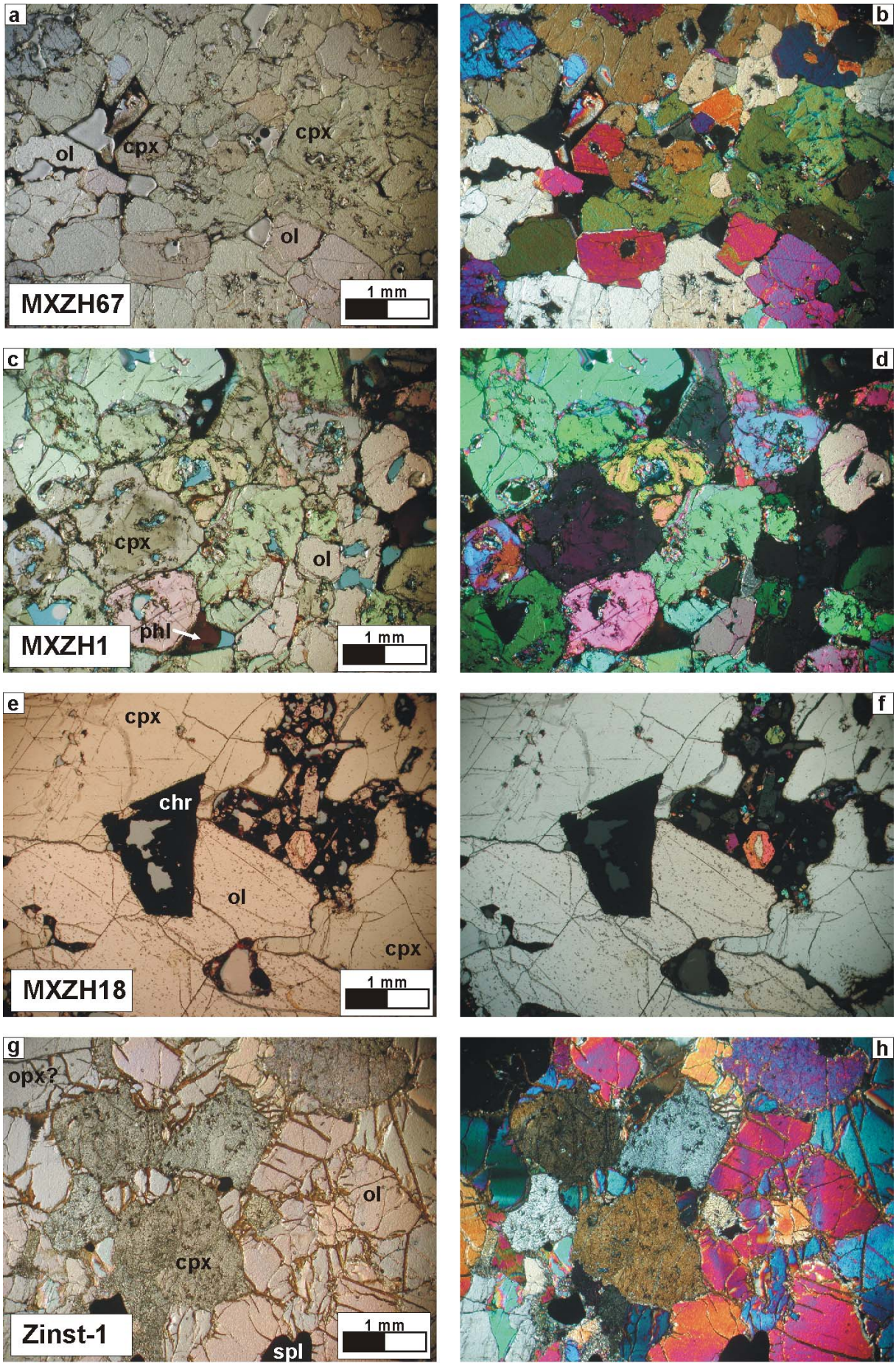
a
ol
cpx
cpx
ol
MXZH67
1 mm
b
c
cpx
ol
phl
MXZH1
1 mm
d
e
cpx
chr
ol
cpx
MXZH18
1 mm
f
g
opx?
ol
cpx
Zinst-1
spl
1 mm
h

Plate 2

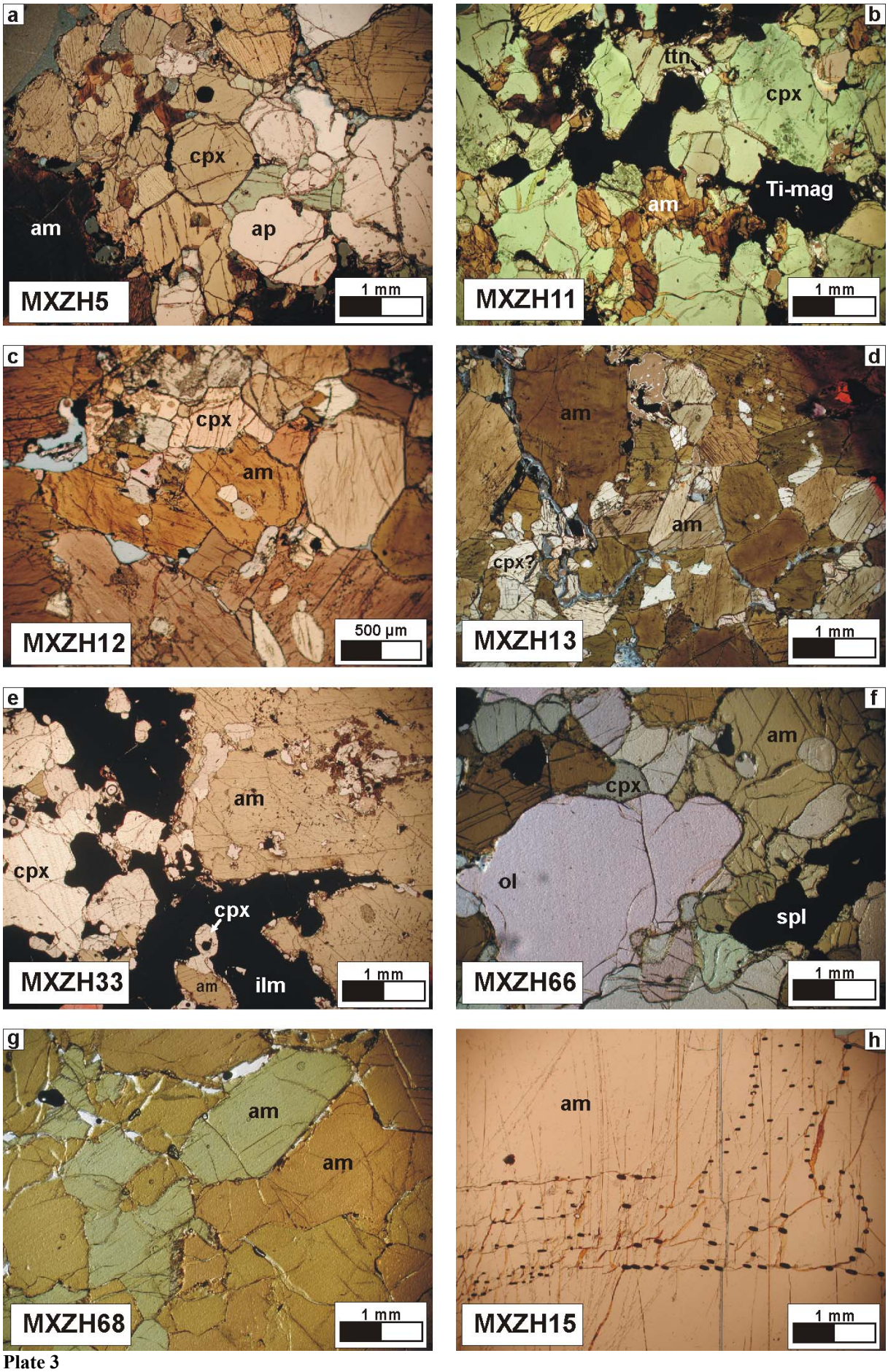
a
cpx
am
ap
MXZH5
1 mm
b
ttn
cpx
Ti-mag
am
MXZH11
1 mm
c
cpx
am
MXZH12
500 µm
d
am
am
cpx?
MXZH13
1 mm
e
am
cpx
cpx
MXZH33
am
ilm
1 mm
f
am
cpx
ol
spl
MXZH66
1 mm
g
am
am
MXZH68
1 mm
h
am
MXZH15
1 mm

Plate 3

Plate 2
Photographs of thin-sections (left: single, and right: crossed nicols) of typical wehrlitic xenoliths or olivine-clinopyroxene cumulates from the Mýtina tephra **(a)** to **(f);** and a spinel lherzolite xenolith from the Wunschenberg (Zinst, NE-Bavaria).
Samples MXZH67 **(a+b)** and MXZH1 **(c+d)** consist of olivine and clinopyroxene up to several millimetre in grain size. Both samples are porous. MXZH1 further contains phlogopite; and some clinopyroxene grains show zoning (mainly in Ti and Cr, from microprobe measurements). This is probably an indication for an overprinting of sample MXZH1 by heating or metasomatic reactions. MXZH18 **(e+f)** consists of olivine, clinopyroxene (both up to cm-size) and dark-brown chromium-rich spinel. The space in-between the mineral grains is partly filled with nephelinitic groundmass containing phenocrysts; some "pores" contain scoriaceous glass. Spinel lherzolite sample Zinst-1 **(g+h)** consists of olivine, clinopyroxene, orthopyroxene, and dark-brown spinel.

Plate 3
Photographs of thin-sections of amphibole-bearing xenoliths and an amphibole megacryst.
(a) MXZH5: apatite- and amphibole-bearing clinopyroxenite; **(b)** MXZH11: amphibole- and Ti-magnetite-bearing clinopyroxenite, containing also minor titanite (sphene); **(c)** and **(d)** MXZH12, MXZH13: hornblendite samples, consisting mainly of amphibole, which partly overgrows small clinopyroxene grains (poikilitic), as well as of phlogopite and magnetite; **(e)** MXZH33: ilmenite-bearing hornblende-clinopyroxenite; **(f)** MXZH66: amphibole-bearing peridotite consisting of olivine, clinopyroxene and dark-brown spinel; **(g)** MXZH68: hornblendite, consisting only of amphibole and minor magnetite and sulphide inclusion; **(h)** MXZH15: amphibole megacrysts showing inclusion (magnetite and sulphide) trails.

C.3.3 Crustal xenoliths

Crustal xenoliths in the lower unit of the tephra deposit range in size from ash particles up to several decimetre big samples [see *Geissler et al.,* 2004b]. Within the upper unit, their size is up to 10 cm; most samples are coated with the host rock, forming cored bombs. Many samples show primary sedimentary layering (bedding), overprinted by foliation. Main components are quartz and mica (muscovite and biotite); minor constituents are feldspar, garnet, and zircon and others (see Appendix C.ii). Commonly the samples show small grain sizes of the minerals. Samples can be classified by their textures and mineral composition into the following groups: quartzitic (quartz-rich) rocks, phyllitic rocks and mica schists, and feldspar-rich rocks (Plates 4, 5). A transition exists from phyllitic quartzites to quartzitic phyllites/mica schists.

Quartzitic xenoliths show generally an alternated stratification of quartz-rich and mica-rich (mostly muscovite) layers. These rocks have light-grey colours; some samples are whitish. Minor components beside quartz and muscovite are feldspar, biotite, and rounded zircon (sometimes enriched in specific layers/samples; e.g., XKZH58, XKZH61). The phyllitic and mica schist xenoliths are more mica-rich (muscovite, biotite) than the quartzitic samples. They mostly have dark-grey (greenish) colours. Minor components are feldspar, garnet, staurolite, and (?) cordierite.

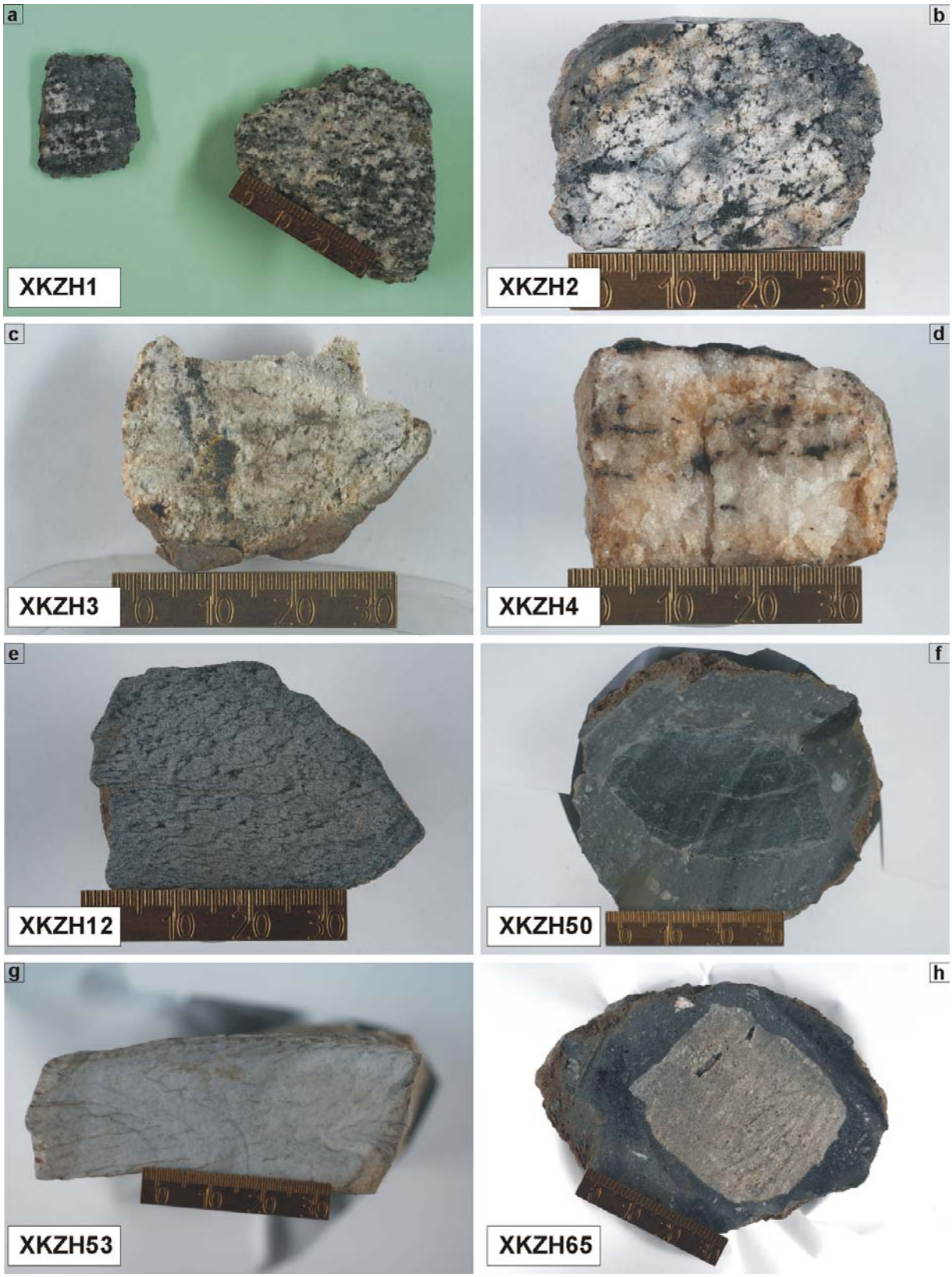

Plate 4
Photographs of typical hand specimen of crustal xenoliths from the Mýtina tephra. **(a)** XKZH1: noritic sample (mainly plagioclase + orthopyroxene ± clinopyroxene) showing weak layering of the main components; **(b)** and **(c)** XKZH2, XKZH3: feldspar rich samples; **(d)** XKZH4: quartz-rich xenolith, probably a fragment of a quartz vein; **(e)** XKZH12: quartzitic mica-schist; **(f)** XKZH50: mica-schist; **(g)** XKZH53: quartzite; **(h)** XKZH65: quartz-feldspar-bearing xenolith, which may belong to meta-tuff layers (within the "Neualbenreuth layers"). (Photographs by E. Gantz, GFZ Potsdam).

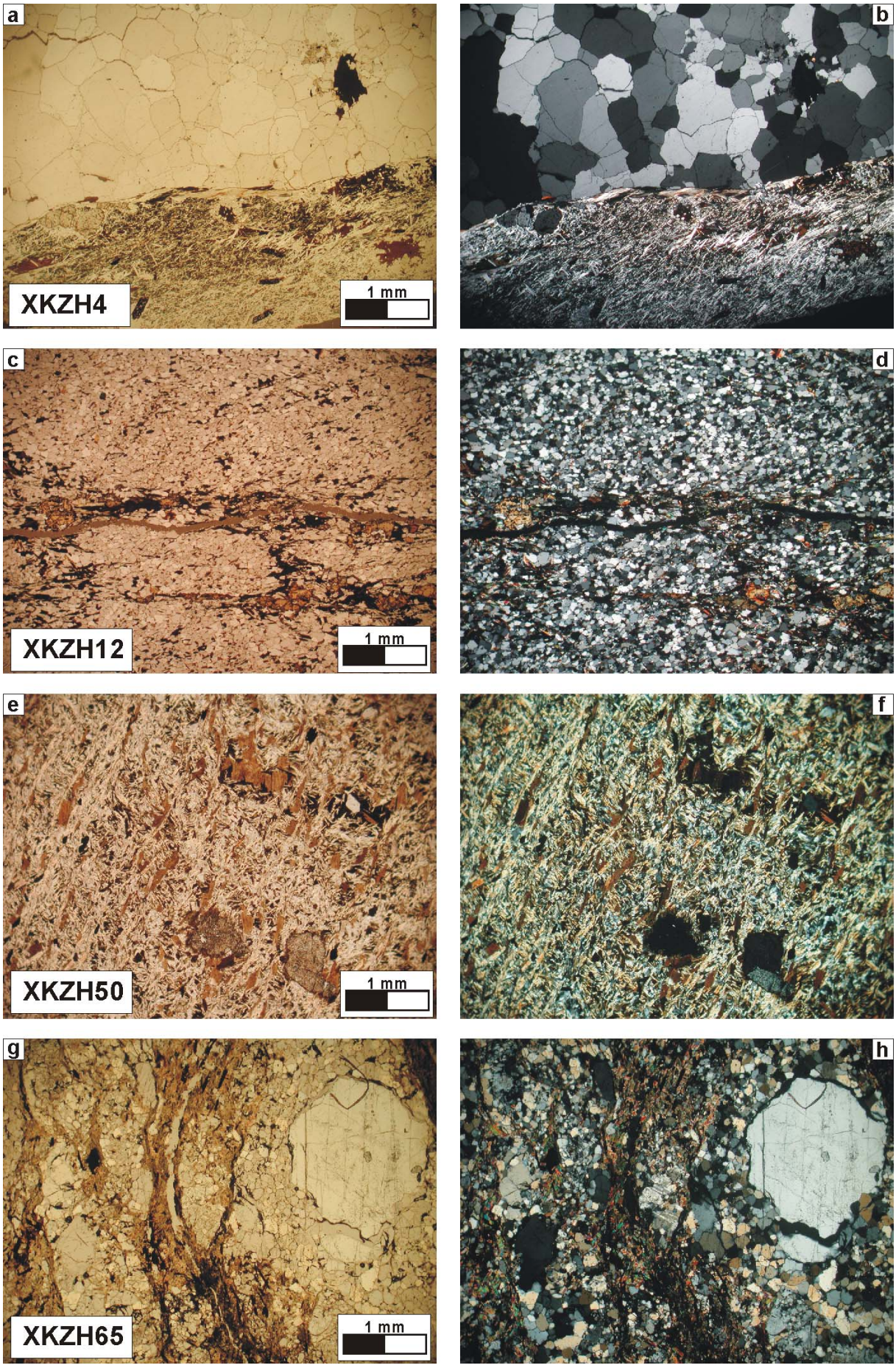

Plate 5

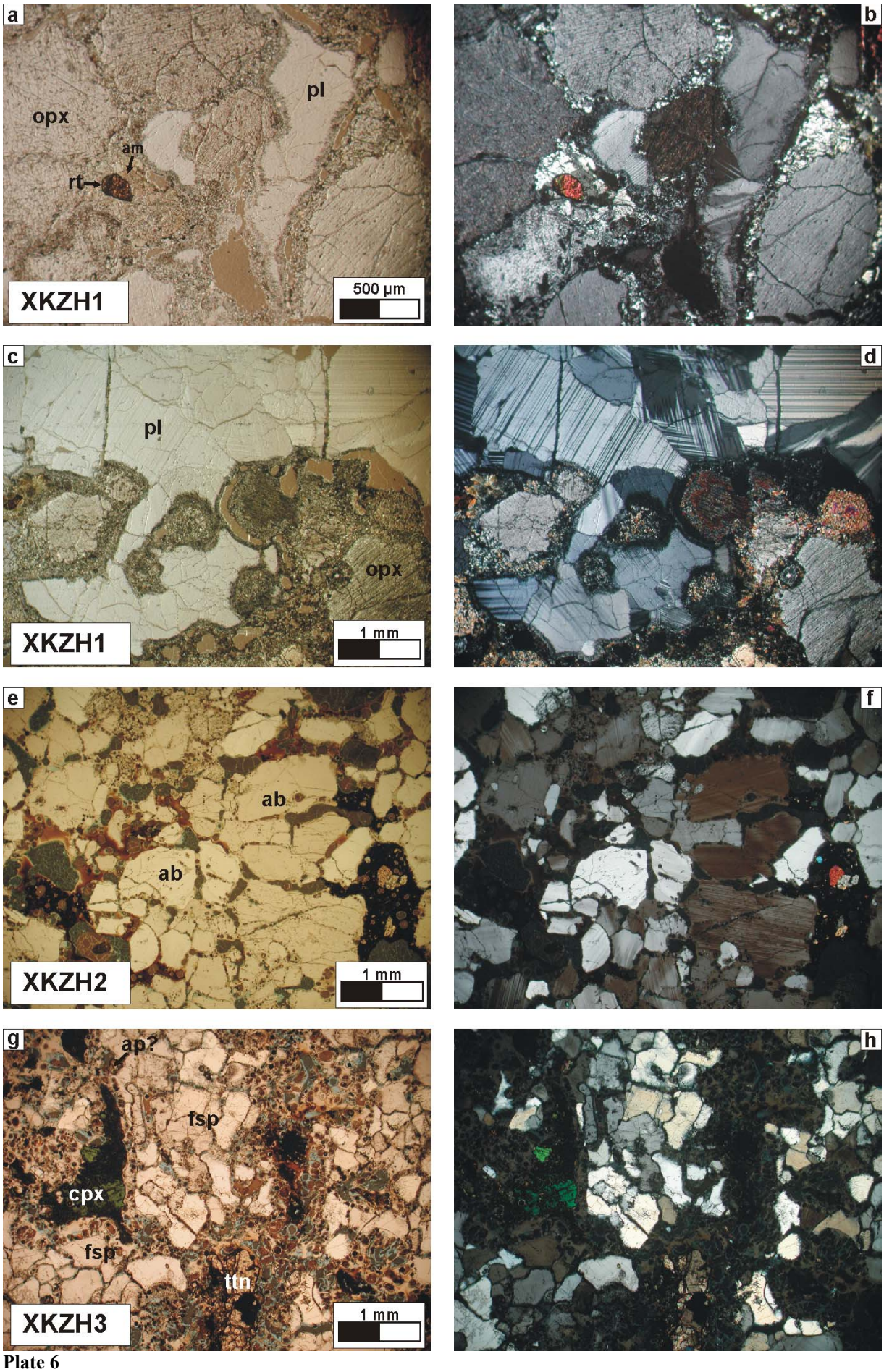
a
opx
pl
am
rt
XKZH1
500 µm
b
c
pl
opx
XKZH1
1 mm
d
e
ab
ab
XKZH2
1 mm
f
g
ap?
fsp
cpx
fsp
ttn
XKZH3
1 mm
h

Plate 6

Plate 5
Photographs of thin-sections (left: single, and right: crossed nicols) of typical crustal xenoliths.
Sample XKZH4 **(a+b)** shows a sharp contact between quartzite and garnet-bearing mica schist. XKZH4 might be a fragment of a quartz vein or dike ("Pfahl"), which are common in the area; **(c+d)** XKZH12: garnet- and staurolite-bearing quartzitic mica schist; **(e+f)** XKZH50: garnet-bearing mica schist; **(g+h)** XKZH65: porphyroclastic quartz-feldspar-bearing rock (meta-tuff?).

Plate 6
Photographs of thin-sections (single and crossed nicols) of feldspar-dominated crustal xenoliths.
Noritic sample XKZH1 **(a-d)** consists mainly of plagioclase and orthopyroxene, minor components are amphibole, rutile, brown mica, and fine grained intergrowth of orthopyroxene and clinopyroxene; **(e+f)** XKZH2: glass- (brown) bearing sample mainly composed of albite; contains also minor amounts of zircon and a Nb-Ta-bearing ore [*Kämpf,* personal communication]; **(g+h)** XKZH3: feldspar rich sample, which additionally contains pyroxene (green), zircon (?), apatite, and titanite.
The porous texture of sample XKZH2 and XKZH3 as well as the glass formation in XKZH2 is most probable related to the heating in the host magma, whereas the origin of fine grained orthopyroxene-clinopyroxene intergrowth might be related to previous metamorphic/metasomatic overprinting.

Besides the majority of quartz- and mica-rich crustal xenoliths also light grey more feldspar-rich samples could be found (XKZH1, -2, -3, -6, -65, -66; Plates 4, 6). Three analysed feldspar-rich xenoliths are strongly influenced by heating in the host magma. One of them (XKZH1) shows layering of the major components feldspar and orthopyroxene indicating some metamorphic overprinting of a probable primary magmatic texture. Minor components in sample XKZH1 (Plate 6) are clinopyroxene, dark mica, rutile and amphibole. In the two other analysed feldspar-rich samples (XKZH2, XKZH3) the heating in the host magma resulted into glass formation. This might be an indication for a deeper than uppermost crust origin of these xenoliths (due to a longer residence time in the magma).
Light grey samples XKZH65, XKZH66 (Plates 4, 5) and XKZH6 show coarse feldspar and quartz remnants resting in a (partly re-crystallized) matrix of quartz, feldspar, and mica.

C.4 Data

C.4.1 Whole-rock major and trace element chemistry

Samples were grounded in an agate mill to less than 62 µm and homogenised. Major element oxides and most trace elements were analysed by X-ray fluorescence spectrometry on fused glass pellets on a Siemens SRS 303 spectrometer at the GFZ Potsdam by Dipl.-Krist. Rudolf Naumann. H_2O and CO_2 were determined by IR-spectrometry (LECO CH elemental analyser) or thermal conductivity measurements (vario EL) after decomposition of the rock powder in a 1000°C oxygen stream. FeO was analysed by potentiometric titration using a modification of the Wilson procedure [*Wilson,* 1955]. Trace and Rare Earth (REE) elements were analysed by inductively-coupled plasma mass-spectrometry (ICP-MS) on a Perkin-Elmer/SCIEX Elan 5000 ICP mass-spectrometer at the GFZ Potsdam by Dr. Peter Dulski. For details on ICP-MS sample preparation (mixed acid digestion procedure), calibration, conditions of measurement, and error discussion see *Dulski* [2001].

Table C.II. Whole-rock chemistry of (ultra-) mafic nodules and host rock samples (XRF, ICP-MS).

sample		wehrlites, ol-cpx-aggregates								hbl-pt
		MXZH1	MXZH2	MXZH3	MXZH4	MXZH8	MXZH18	MXZH18D	MXZH67	MXZH66
SiO_2 (wt.%)		47.4	46.2	46.3	43.7	47.5	47.5	47.5	46.0	40.3
TiO_2		0.897	0.534	0.957	0.482	0.741	1.166	1.166	0.704	1.032
Al_2O_3		4.9	3.4	5.1	2.7	4.3	6.5	6.4	3.8	5.2
Fe_2O_3(t)		1.77	1.10	2.09	1.66	1.47	2.07	6.31	1.80	2.80
FeO		4.13	5.52	4.39	6.91	4.27	3.81		5.16	10.27
MnO		0.110	0.115	0.117	0.135	0.109	0.116	0.115	0.114	0.166
MgO		22.69	29.48	24.52	35.48	24.69	17.85	17.83	27.03	31.14
CaO		16.36	12.69	14.91	8.80	15.28	17.54	17.54	13.11	6.30
Na_2O		0.52	0.38	0.46	0.26	0.49	0.85	0.86	0.50	0.53
K_2O		0.06	<0,02	0.12	<0,02	0.01	0.24	0.24	0.04	0.47
P_2O_5		0.114	0.042	0.153	0.076	0.073	0.190	0.193	0.075	0.047
H_2O		0.90	0.66	0.85	0.89	0.53	1.04	1.04	0.72	0.76
CO_2		0.26	0.33	0.19	0.37	0.33	0.22	0.22	0.12	0.14
Total		100.11	100.45	100.16	101.46	99.80	99.09	99.41	99.74	100.32
Cs (ppm)	ICP-MS	0.05	< 0.01	0.08	0.02	0.06	0.34		0.03	0.10
Rb	XRF								<10	<10
	ICP-MS	4.7	0.4	6.5	0.7	3.1	19.5		2.2	5.4
Sr	XRF								101	85
	ICP-MS	148	56	181	48	97	255		108	91
Ba	XRF								53	91
	ICP-MS	108	34	199	36	64	215		68	86.3
Zr	XRF								41	35
	ICP-MS	46	19	49	22	33	73		33	26
Nb	XRF									
	ICP-MS								14	10
Ta	ICP-MS								1.2	< 1
Th	ICP-MS	1.03	0.31	1.35	0.51	0.68	2.14		1.02	0.59
U	ICP-MS	0.23	0.07	0.29	0.12	0.13	0.51		0.18	0.15
Pb	ICP-MS	0.43	0.25	0.67	0.39	0.36	0.91		0.57	0.49
V	XRF								160	176
Cr	XRF								3485	2622
Ni	XRF								681	562
Zn	XRF								37	67
Y	XRF								<10	<10
	ICP-MS	6.1	3.6	6.5	3.0	5.1	9.0		4.9	4.2
La	ICP-MS	9.84	3.69	11.9	4.32	6.16	16.9		7.34	4.94
Ce	ICP-MS	21.1	7.98	24.1	9.67	14.1	34.0		16.2	11.0
Pr	ICP-MS	2.73	1.27	3.16	1.36	2.02	4.28		2.08	1.50
Nd	ICP-MS	11.2	5.61	12.4	5.57	8.39	17.0		9.18	6.96
Sm	ICP-MS	2.41	1.33	2.59	1.26	2.04	3.38		1.93	1.57
Eu	ICP-MS	0.75	0.46	0.81	0.40	0.62	1.07		0.60	0.48
Gd	ICP-MS	2.24	1.38	2.32	1.17	1.89	3.15		1.72	1.49
Tb	ICP-MS	0.27	0.18	0.29	0.14	0.24	0.40		0.22	0.19
Dy	ICP-MS	1.46	0.87	1.51	0.77	1.26	2.10		1.17	0.98
Ho	ICP-MS	0.25	0.14	0.26	0.12	0.21	0.36		0.19	0.16
Er	ICP-MS	0.55	0.34	0.60	0.29	0.48	0.86		0.48	0.46
Tm	ICP-MS	0.07	0.04	0.07	0.03	0.05	0.10		0.05	0.04
Yb	ICP-MS	0.46	0.25	0.51	0.25	0.39	0.69		0.32	0.33
Lu	ICP-MS	0.05	0.03	0.06	0.02	0.05	0.08		0.04	0.04
Hf	ICP-MS	1.43	0.71	1.42	0.71	1.16	1.99		1.02	0.97

Table C.II. (continued).

sample		hornblendites, clinopyroxenites					am-X	cpx-X	ol-X	phl-X
		MXZH5	MXZH12	MXZH11	MXZH13	MXZH68	MXZH15	MXZH16	MXZH19	MXZH22
SiO_2 (wt.%)		39.5	39.6	39.2	40.0	40.5	40.8	49.5	39.2	
TiO_2		2.487	3.430	3.846	3.280	3.233	3.131	1.076	0.082	
Al_2O_3		9.8	12.5	6.0	12.6	13.6	14.4	6.6	0.5	
Fe_2O_3(t)		5.44	6.00	11.43	5.28	4.28	2.64	1.95	3.51	
FeO		5.46	6.34	8.55	6.61	5.36	4.84	3.34	15.18	
MnO		0.155	0.128	0.228	0.126	0.097	0.075	0.104	0.226	
MgO		10.79	13.35	10.06	13.28	14.35	15.70	14.88	46.39	
CaO		19.40	12.74	18.88	13.03	11.55	11.56	20.46	0.38	
Na_2O		1.34	1.97	0.76	1.94	2.29	1.96	0.85	<0,1	
K_2O		0.68	1.65	0.06	1.67	1.98	2.21	<0,02	<0,02	
P_2O_5		2.524	0.005	0.111	0.006	0.042	0.031	0.031	0.029	
H_2O		1.53	1.48	0.66	1.20	1.18	1.35	0.80	0.27	
CO_2		0.23	0.24	0.19	0.18	0.09	0.35	0.33	0.14	
Total		99.34	99.44	99.97	99.21	99.11	99.05	99.92	105.91	
Cs (ppm)	ICP-MS	0.67	0.16	0.10	0.22	0.04	0.01	< 0.01	0.03	1.81
Rb	XRF					15				
	ICP-MS	42.0	21.8	8.6	23.8	18.2	14.5	< 0.2	1.0	321
Sr	XRF					321				
	ICP-MS	474	419	240	427	344	282	93	11.3	142
Ba	XRF					254				
	ICP-MS	320	342	107	380	242	185	4.6	12.3	2379
Zr	XRF					73				
	ICP-MS	236	222	201	235	54	37	43	4.4	6.6
Nb	XRF									
	ICP-MS					16				
Ta	ICP-MS					1.8				
Th	ICP-MS	3.05	0.50	1.97	0.56	0.37	0.10	0.08	0.15	0.17
U	ICP-MS	0.73	0.13	0.46	0.14	0.09	0.04	0.02	0.04	0.02
Pb	ICP-MS	1.12	0.67	0.62	0.76	0.60	0.25	0.18	0.21	0.60
V	XRF					365				
Cr	XRF					13				
Ni	XRF					75				
Zn	XRF					35				
Y	XRF					11				
	ICP-MS	17.7	11.0	11.9	11.1	9.4	8.2	8.9	0.45	0.18
La	ICP-MS	33.8	9.02	18.0	9.70	6.93	3.55	2.68	1.14	0.44
Ce	ICP-MS	78.0	28.2	45.4	29.3	20.6	11.8	9.56	2.10	0.86
Pr	ICP-MS	10.6	4.60	6.41	4.83	3.29	2.12	1.86	0.25	0.09
Nd	ICP-MS	43.3	21.2	26.9	22.2	16.3	10.5	9.46	0.87	0.33
Sm	ICP-MS	8.34	4.96	5.39	5.04	3.99	2.86	2.69	0.15	0.06
Eu	ICP-MS	2.51	1.53	1.66	1.59	1.30	0.99	0.95	0.05	< 0.008
Gd	ICP-MS	7.07	4.37	4.57	4.46	3.60	2.89	2.99	0.13	0.04
Tb	ICP-MS	0.82	0.54	0.56	0.55	0.45	0.37	0.40	0.01	< 0.008
Dy	ICP-MS	4.19	2.70	2.90	2.82	2.38	2.01	2.15	0.09	0.04
Ho	ICP-MS	0.69	0.44	0.48	0.46	0.40	0.33	0.36	0.02	0.01
Er	ICP-MS	1.62	1.03	1.15	1.08	0.93	0.80	0.83	0.04	0.02
Tm	ICP-MS	0.20	0.12	0.14	0.13	0.09	0.10	0.10	0.01	< 0.006
Yb	ICP-MS	1.34	0.84	0.96	0.87	0.60	0.63	0.65	0.04	0.03
Lu	ICP-MS	0.16	0.10	0.13	0.10	0.08	0.07	0.07	< 0.009	< 0.009
Hf	ICP-MS	4.26	7.49	6.75	8.07	2.23	1.69	2.17	0.10	0.19

Table C.II. (continued).

sample		host rock (nephelinite)							
		My1	My1-B	My2	My2-B	BK-2	BK-2B	Go-01	Go-02
SiO_2 (wt.%)		40.0	39.8	41.3	41.1	39.9	39.4	41.8	42.0
TiO_2		2.958	2.933	2.898	2.869	2.840	2.906	2.377	2.385
Al_2O_3		11.5	11.4	11.6	11.6	11.2	11.3	12.2	12.2
Fe_2O_3(t)		5.58	5.63	5.68	5.39	12.35	7.02	3.45	4.05
FeO		5.26	5.11	5.05	5.27		4.00	7.85	7.41
MnO		0.188	0.187	0.185	0.185	0.210	0.198	0.182	0.182
MgO		13.64	13.70	12.60	12.68	13.05	12.25	11.72	11.93
CaO		12.67	12.54	12.41	12.31	12.69	13.15	11.54	11.35
Na_2O		2.53	2.61	2.30	2.40	3.40	3.47	3.00	3.10
K_2O		1.55	1.53	1.42	1.42	2.11	2.17	1.38	1.29
P_2O_5		0.667	0.724	0.654	0.714	0.740	0.757	0.755	0.751
H_2O		2.21	2.28	2.51	2.75	0.75	1.07	1.80	1.80
CO_2		0.11	0.10	0.11	0.10	0.10	0.17	0.68	0.31
Total		99.38	98.49	99.33	98.78	99.30	97.81	98.75	98.69
Cs (ppm)	ICP-MS	0.91	0.89	2.09	2.03		0.81	1.14	1.03
Rb	XRF	61	59	208	208		58	54	56
	ICP-MS	71	69	246	241	71	64	59	64
Sr	XRF	707	708	681	687		868	842	830
	ICP-MS	759	748	738	724	943	874	916	906
Ba	XRF	780	770	752	738		734	559	569
	ICP-MS	776	761	740	708	678	730	554	542
Zr	XRF	225	220	247	243		259	202	197
	ICP-MS	237	239	242	243	218	269	212	211
Nb	XRF		93		91		105		
	ICP-MS	134	116	73	112		126	109	109
Ta	ICP-MS	9.8	6.7	5.9	6.4		7.3	7.7	12
Th	ICP-MS	8.9	9.0	9.5	9.6	8.9	9.6	7.7	7.6
U	ICP-MS	2.4	2.4	2.4	2.5	2.4	2.8	2.3	2.3
Pb	ICP-MS	2.9	3.1	3.7	4.0		2.7	4.6	4.6
V	XRF	315	320	316	306		308	220	220
Cr	XRF	726	735	586	582		495	317	309
Ni	XRF	249	n.a.	225	n.a.		n.a.	246	255
Zn	XRF	70	72	74	75		76	89	88
Y	XRF	21	22	22	24		23	23	24
	ICP-MS	21	21	23	22	23	24	24	24
La	ICP-MS	68.4	68.3	70.3	68.2		73.9	60.9	60.4
Ce	ICP-MS	131	128	135	129		141	113	112
Pr	ICP-MS	14.8	14.8	15.6	14.7		16.1	12.6	12.5
Nd	ICP-MS	56.2	55.7	59.0	55.6		61.1	47.7	47.6
Sm	ICP-MS	9.61	9.65	10.2	9.66		10.6	8.64	8.58
Eu	ICP-MS	2.92	2.83	2.90	2.77		3.09	2.60	2.61
Gd	ICP-MS	7.69	7.42	8.17	7.73		8.40	7.50	7.37
Tb	ICP-MS	0.97	0.97	1.03	1.00		1.08	1.00	1.01
Dy	ICP-MS	4.94	4.89	5.22	4.98		5.40	5.36	5.36
Ho	ICP-MS	0.81	0.83	0.86	0.84		0.94	0.96	0.93
Er	ICP-MS	2.06	2.05	2.23	2.10		2.32	2.43	2.43
Tm	ICP-MS	0.25	0.26	0.28	0.27		0.28	0.30	0.31
Yb	ICP-MS	1.51	1.51	1.66	1.59		1.73	1.88	1.84
Lu	ICP-MS	0.21	0.20	0.24	0.23		0.25	0.27	0.27
Hf	ICP-MS	5.26	5.35	5.30	5.34		6.10	4.64	4.73

The analytical precision for all methods is better than 10% and was checked against international rock and in-house laboratory standards. The accuracy of ICP-MS measurements is in the range of ±5% [*Dulski,* 2001]. The analyses of Nb and Ta are less accurate due to the unstable behaviour of these elements in solution. The results are listed in Table C.II and Appendix C.ii for mantle and crustal xenoliths, respectively. Figure C.5 and Appendix C.iii show the chondrite (C1)-normalized REE patterns of the investigated samples.

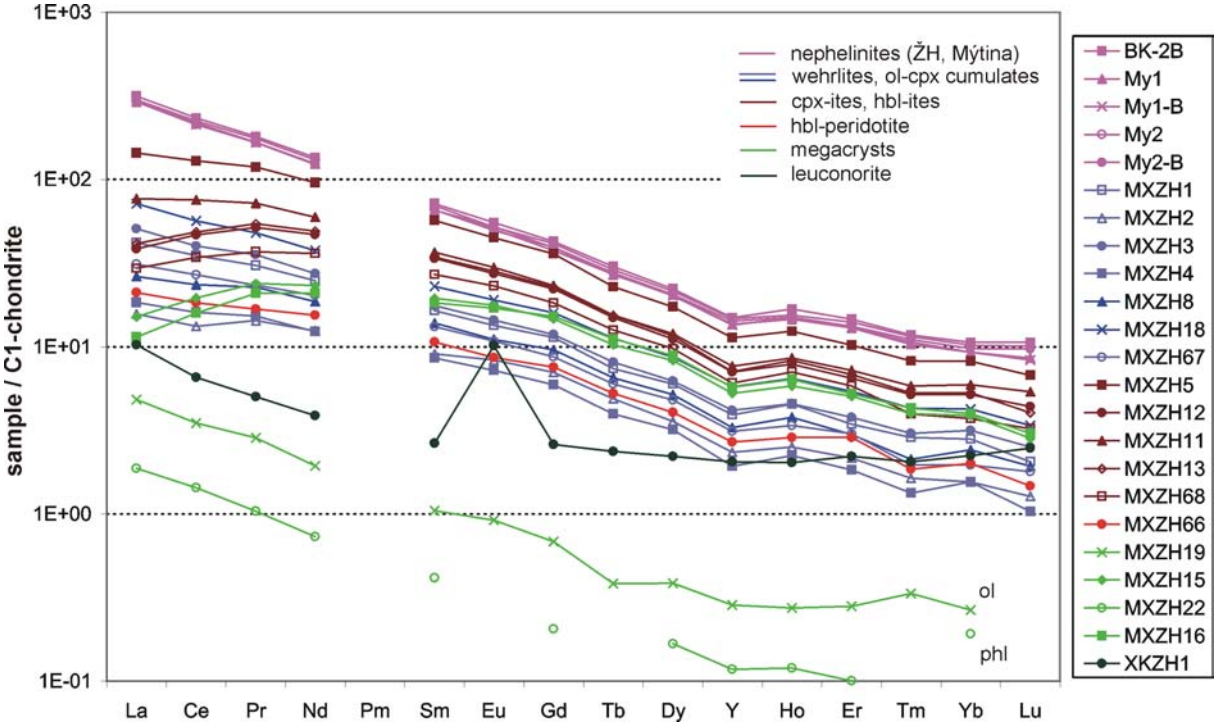

Figure C.5
Chondrite (C1)-normalized REE patterns of host mela-nephelinites and (ultra-) mafic nodules from the tephra deposit in Mýtina (see Table C.II). REE values of C1-chondrites are taken from *Anders and Grevesse* [1989].

C.4.2 Mineral-chemical analyses (EMPA)

Minerals of several mantle xenoliths, megacrysts, and three crustal xenoliths were analysed for their chemical composition. Major and minor elements of minerals (olivine, clinopyroxene, amphibole, phlogopite, spinel, titanite, ilmenite, apatite) were determined with the CAMECA SX50 and CAMECA SX100 microprobes of the GFZ Potsdam, which are equipped with four wave-length dispersive spectrometers, using an acceleration voltage of 15 kV, a beam current of 20 nA, and a beam diameter of 2 µm (for mica, feldspar, and glass analyses 10 µm, because of the higher concentration of diffusion endangered elements like Na, F, K). Counting time for the peak was 20 seconds, and for the background 10 seconds on each side of the peak. Ca in olivine was measured as a trace element (50.2 nA, 15 kV, 300s counting time for peak and background) in selected samples to perform pressure estimations with the olivine-clinopyroxene barometer.

Table C.III. Mineral-chemical composition and structural formulae for peridotites (average and standard deviation; n: number of analyses).

sample	MXZH66				Zinst-1				Go01-1			
	ol	cpx	am	sp	ol	cpx	opx	sp	ol	cpx	opx	sp
n	22	10	10	5	10	10	6	5	3	3	4	3
SiO_2	**38.72** ± 0.19	**49.58** ± 0.29	**41.72** ± 0.17	**0.12** ± 0.01	**40.76** ± 0.20	**53.48** ± 0.23	**56.21** ± 0.14	**0.07** ± 0.01	**40.88** ± 0.08	**52.78** ± 0.38	**55.85** ± 0.53	**0.02** ± 0.01
TiO_2	**0.02** ± 0.01	**1.12** ± 0.03	**3.24** ± 0.05	**1.56** ± 0.01	**0.01** ± 0.01	**0.32** ± 0.03	**0.13** ± 0.01	**0.62** ± 0.02	**0.01** ± 0.01	**0.02** ± 0.01	**0.01** ± 0.01	**0.01** ± 0.01
Al_2O_3	**0.04** ± 0.01	**6.45** ± 0.07	**14.60** ± 0.07	**41.61** ± 0.07	**0.01** ± 0.01	**3.88** ± 0.08	**3.65** ± 0.03	**31.69** ± 0.20	**0.01** ± 0.00	**3.90** ± 0.53	**2.66** ± 0.05	**40.22** ± 0.31
Cr_2O_3	**0.01** ± 0.02	**0.65** ± 0.04	**0.79** ± 0.05	**14.27** ± 0.09	**0.05** ± 0.02	**1.24** ± 0.04	**0.79** ± 0.03	**34.55** ± 0.10	**0.01** ± 0.01	**0.95** ± 0.22	**0.38** ± 0.02	**26.39** ± 0.18
Fe_2O_3				**13.56** ± 0.43				**6.07** ± 0.39				**5.39** ± 0.48
FeO	**16.44** ± 0.19	**5.63** ± 0.09	**7.21** ± 0.15	**15.19** ± 0.07	**8.96** ± 0.08	**3.00** ± 0.05	**5.73** ± 0.11	**11.14** ± 0.17	**8.99** ± 0.07	**2.63** ± 0.12	**6.00** ± 0.09	**10.38** ± 0.31
MgO	**44.64** ± 0.11	**14.86** ± 0.07	**15.60** ± 0.05	**15.35** ± 0.06	**49.87** ± 0.25	**17.06** ± 0.09	**33.44** ± 0.10	**16.90** ± 0.10	**49.95** ± 0.10	**16.99** ± 0.28	**34.17** ± 0.14	**18.22** ± 0.24
MnO	**0.23** ± 0.03	**0.12** ± 0.04	**0.07** ± 0.03	**0.17** ± 0.03	**0.14** ± 0.03	**0.08** ± 0.02	**0.14** ± 0.03	**0.10** ± 0.03	**0.12** ± 0.02	**0.09** ± 0.03	**0.13** ± 0.01	**0.08** ± 0.03
NiO	**0.15** ± 0.04			**0.15** ± 0.05	**0.41** ± 0.04			**0.27** ± 0.05	**0.39** ± 0.02			**0.22** ± 0.03
CaO	**0.15** ± 0.02	**20.74** ± 0.17	**11.63** ± 0.11	**0.01** ± 0.01	**0.09** ± 0.02	**19.64** ± 0.12	**0.99** ± 0.02	**0.02** ± 0.02	**0.04** ± 0.01	**21.59** ± 0.59	**0.51** ± 0.02	**0.01** ± 0.00
BaO												
Na_2O		**1.03** ± 0.03	**2.29** ± 0.02			**1.43** ± 0.05	**0.15** ± 0.01			**0.86** ± 0.05	**0.05** ± 0.01	
K_2O		**0.01** ± 0.00	**2.26** ± 0.06			**0.00** ± 0.01	**0.01** ± 0.01			**0.00** ± 0.00	**0.00** ± 0.00	
P_2O_5												
Cl			**0.02** ± 0.01									
F			**0.07** ± 0.03									
H_2O												
Total	**100.40** ± 0.29	**100.18** ± 0.39	**99.45** ± 0.18	**101.98** ± 0.50	**100.30** ± 0.42	**100.13** ± 0.32	**101.23** ± 0.19	**101.42** ± 0.19	**100.40** ± 0.10	**99.81** ± 0.06	**99.76** ± 0.54	**100.94** ± 0.30
Atomic formulae												
Si	0.978	1.823	5.974	0.026	0.994	1.931	1.917	0.017	0.996	1.917	1.931	0.005
Ti	0.000	0.031	0.349	0.261	0.000	0.009	0.004	0.107	0.000	0.001	0.00	0.002
Al	0.001	0.280	2.463	10.876	0.000	0.165	0.147	8.547	0.000	0.167	0.109	10.480
Cr	0.000	0.004	0.090	2.502	0.001	0.035	0.021	6.251	0.000	0.027	0.010	4.613
Fe^{3+}				2.262				1.045				0.897
Fe^{2+}	0.347	0.173	0.863	2.817	0.183	0.091	0.164	2.132	0.183	0.080	0.174	1.919
Mg	1.681	0.814	3.329	5.074	1.813	0.918	1.700	5.767	1.813	0.920	1.762	6.003
Mn	0.005	0.019	0.008	0.031	0.003	0.002	0.004	0.019	0.003	0.003	0.004	0.015
Ni	0.003			0.026	0.008			0.049	0.008			0.039
Ca	0.004	0.817	1.784	0.003	0.002	0.759	0.036	0.005	0.001	0.84	0.019	0.003
Ba												
Na		0.074	0.635			0.100	0.010			0.060	0.003	
K		0.000	0.413			0.000	0.000			0.000	0.000	
P												
Total	3.020	4.034	15.907	23.878	3.004	4.011	4.001	23.937	3.004	4.014	4.011	23.976
Ca (trace)	0.0038				0.0020				0.0010			
Cr/(Cr+Al)				0.187				0.422				0.306
Mg/(Mg+Fe)	0.829	0.825	0.794	0.643	0.908	0.910	0.912	0.730	0.908	0.920	0.910	0.758
Fo	82.4				90.3				90.3			
Wo		43.1				40.6	1.9			44.1	1.0	
En		42.9				49.1	88.8			48.4	89.8	
Fs		10.1				5.0	8.7			4.3	9.0	
Ac		3.9				5.4	0.5			3.2	0.2	

Table C.IV. Mineral-chemical composition and structural formulae for clinopyroxenites.

sample	MXZH11				MXZH5					MXZH33		
	cpx	am	mag	ttn	cpx	am	ilm	mag	ap	cpx	am	ilm
n	13	10	13	5	5	5	3	3	5	11	9	8
SiO_2	**47.52** ± 0.23	**40.03** ± 0.20	**0.04** ± 0.02	**30.43** ± 0.12	**47.92** ± 0.58	**39.76** ± 0.16	**0.01** ± 0.01	**0.07** ± 0.01	**0.30** ± 0.02	**51.09** ± 0.18	**39.84** ± 0.23	**0.02** ± 0.01
TiO_2	**1.87** ± 0.09	**2.54** ± 0.05	**9.78** ± 0.15	**39.14** ± 0.10	**1.45** ± 0.16	**2.36** ± 0.02	**41.25** ± 0.08	**9.15** ± 0.02	**0.01** ± 0.01	**0.84** ± 0.05	**2.51** ± 0.03	**42.09** ± 0.29
Al_2O_3	**5.84** ± 0.11	**13.43** ± 0.13	**2.28** ± 0.04	**1.00** ± 0.02	**6.29** ± 0.42	**14.26** ± 0.17	**0.31** ± 0.02	**3.20** ± 0.03	**0.00** ± 0.00	**3.56** ± 0.09	**12.70** ± 0.10	**0.39** ± 0.07
Cr_2O_3	**0.01** ± 0.01	**0.01** ± 0.02	**0.04** ± 0.01	**0.02** ± 0.02	**0.01** ± 0.01	**0.01** ± 0.01	**0.02** ± 0.01	**0.04** ± 0.01	**0.01** ± 0.01	**0.01** ± 0.01	**0.00** ± 0.01	**0.02** ± 0.02
Fe_2O_3			**58.07** ± 0.30	**0.86** ± 0.06				**59.00** ± 0.20				
FeO	**9.09** ± 0.14	**14.38** ± 0.19	**28.37** ± 0.11		**9.60** ± 0.09	**14.90** ± 0.32	**54.14** ± 0.33	**28.88** ± 0.53	**0.14** ± 0.02	**6.98** ± 0.17	**11.71** ± 0.11	**51.25** ± 0.66
MgO	**11.29** ± 0.08	**11.85** ± 0.10	**1.65** ± 0.03	**0.00** ± 0.00	**11.13** ± 0.22	**11.15** ± 0.27	**2.46** ± 0.12	**1.97** ± 0.25	**0.04** ± 0.01	**13.35** ± 0.11	**13.53** ± 0.05	**3.83** ± 0.43
MnO	**0.21** ± 0.04	**0.21** ± 0.05	**0.72** ± 0.04	**0.03** ± 0.03	**0.19** ± 0.03	**0.19** ± 0.02	**0.55** ± 0.04	**0.53** ± 0.07	**0.05** ± 0.01	**0.14** ± 0.02	**0.13** ± 0.03	**0.41** ± 0.03
NiO			**0.05** ± 0.04	**0.03** ± 0.02	**0.02** ± 0.02	**0.01** ± 0.01	**0.03** ± 0.02	**0.01** ± 0.01	**0.00** ± 0.00			**0.04** ± 0.03
CaO	**22.50** ± 0.09	**11.88** ± 0.08	**0.01** ± 0.01	**28.99** ± 0.04	**22.66** ± 0.09	**12.01** ± 0.20	**0.06** ± 0.01	**0.03** ± 0.02	**56.05** ± 0.15	**23.57** ± 0.09	**12.04** ± 0.10	**0.03** ± 0.02
BaO												
Na_2O	**1.19** ± 0.04	**2.97** ± 0.04		**0.04** ± 0.01	**0.95** ± 0.02	**2.30** ± 0.08			**0.11** ± 0.02	**0.88** ± 0.02	**2.74** ± 0.04	
K_2O	**0.01** ± 0.01	**1.35** ± 0.05			**0.00** ± 0.00	**1.69** ± 0.02			**0.00** ± 0.00	**0.01** ± 0.01	**1.48** ± 0.03	
P_2O_5				**0.13** ± 0.02					**42.15** ± 0.33			
Cl		**0.04** ± 0.01				**0.02** ± 0.01			**0.17** ± 0.01		**0.01** ± 0.01	
F		**0.00** ± 0.01		**0.14** ± 0.03		**0.00** ± 0.00			**0.80** ± 0.03		**0.00** ± 0.00	
H_2O												
Total	**99.53** ± 0.27	**98.68** ± 0.26	**101.01** ± 0.37	**100.81** ± 0.20	**100.22** ± 0.28	**98.64** ± 0.71	**98.83** ± 0.36	**102.86** ± 0.56	**99.83** ± 0.28	**100.44** ± 0.26	**96.70** ± 0.31	**98.08** ± 0.14
Atomic formulae												
Si	1.804	5.978	0.012		1.806	5.949		0.019		1.895	6.009	
Ti	0.053	0.286	2.112		0.041	0.265		1.935		0.024	0.285	
Al	0.262	2.364	0.772		0.280	2.514		1.060		0.156	2.257	
Cr	0.000	0.002	0.008		0.000	0.001		0.008		0.000	0.001	
Fe^{3+}			12.558					12.491				
Fe^{2+}	0.289	1.796	6.819		0.303	1.865		6.793		0.217	1.477	
Mg	0.639	2.637	0.709		0.625	2.486		0.825		0.738	3.042	
Mn	0.007	0.026	0.176		0.006	0.024		0.126		0.004	0.017	
Ni			0.011		0.001	0.001		0.002				
Ca	0.915	1.901	0.002		0.916	1.925		0.009		0.937	1.945	
Ba											0.001	
Na	0.088	0.859			0.069	0.668				0.063	0.801	
K	0.000	0.257			0.000	0.322				0.000	0.285	
P												
Total	4.056	16.106	23.178		4.047	16.021		23.268		4.035	16.119	
Ca (trace)												
Cr/(Cr+Al)			0.010					0.007				
Mg/(Mg+Fe)	0.689	0.595	0.094		0.674	0.571	0.07	0.108		0.773	0.673	0.12
Fo												
Wo	47.2				47.7					47.8		
En	33.0				32.6					37.7		
Fs	15.3				16.1					11.3		
Ac	4.5				3.6					3.2		

Table C.V. Mineral-chemical composition and structural formulae for hornblendites.

sample	MXZH12					MXZH13			MXZH68
	cpx	am	phl	ilm	mag	cpx	am	ilm	am
n	4	5	10	10	10	5	12	5	10
SiO_2	**49.18** ± 0.15	**40.87** ± 0.15	**37.52** ± 0.12	**0.02** ± 0.01	**0.08** ± 0.04	**50.29** ± 0.19	**39.42** ± 0.17	**0.02** ± 0.01	**41.34** ± 0.16
TiO_2	**1.59** ± 0.05	**3.06** ± 0.06	**3.85** ± 0.03	**46.29** ± 0.22	**13.95** ± 0.58	**1.06** ± 0.03	**3.02** ± 0.02	**48.93** ± 1.35	**3.37** ± 0.04
Al_2O_3	**5.02** ± 0.14	**13.13** ± 0.05	**15.87** ± 0.07	**0.27** ± 0.03	**4.48** ± 2.90	**3.99** ± 0.09	**12.76** ± 0.08	**0.77** ± 0.05	**13.75** ± 0.11
Cr_2O_3	**0.01** ± 0.01	**0.00** ± 0.00	**0.00** ± 0.01	**0.02** ± 0.02	**0.03** ± 0.01	**0.01** ± 0.01	**0.01** ± 0.01	**0.02** ± 0.01	**0.02** ± 0.02
Fe_2O_3					**54.04** ± 3.05				
FeO	**7.43** ± 0.10	**11.81** ± 0.12	**11.95** ± 0.13	**46.67** ± 0.92	**23.75** ± 2.54	**6.92** ± 0.11	**11.64** ± 0.20	**40.51** ± 1.44	**9.47** ± 0.15
MgO	**12.75** ± 0.06	**13.14** ± 0.02	**18.17** ± 0.06	**4.99** ± 0.64	**5.41** ± 1.91	**12.98** ± 0.06	**13.25** ± 0.06	**8.66** ± 0.91	**14.39** ± 0.13
MnO	**0.15** ± 0.01	**0.12** ± 0.03	**0.09** ± 0.03	**0.58** ± 0.08	**0.32** ± 0.07	**0.15** ± 0.01	**0.13** ± 0.03	**0.37** ± 0.05	**0.09** ± 0.03
NiO				**0.03** ± 0.03	**0.03** ± 0.03			**0.03** ± 0.04	
CaO	**22.83** ± 0.06	**11.97** ± 0.09	**0.16** ± 0.04	**0.02** ± 0.01	**0.04** ± 0.04	**23.49** ± 0.11	**12.05** ± 0.08	**0.09** ± 0.02	**11.62** ± 0.07
BaO			**0.46** ± 0.04				**0.02** ± 0.02		
Na_2O	**1.03** ± 0.01	**2.63** ± 0.02	**0.63** ± 0.02			**0.93** ± 0.01	**2.55** ± 0.04		**2.51** ± 0.04
K_2O	**0.01** ± 0.00	**1.80** ± 0.03	**8.36** ± 0.09			**0.01** ± 0.00	**1.81** ± 0.03		**1.97** ± 0.03
P_2O_5									
Cl		**0.02** ± 0.00	**0.01** ± 0.00				**0.02** ± 0.01		**0.02** ± 0.01
F		**0.00** ± 0.00	**0.00** ± 0.00				**0.00** ± 0.00		**0.02** ± 0.03
H_2O			**4.15** ± 0.01						
Total	**99.99** ± 0.19	**98.54** ± 0.26	**101.22** ± 0.27	**98.89** ± 0.41	**102.13** ± 0.36	**99.84** ± 0.44	**96.66** ± 0.24	**99.40** ± 0.39	**98.55** ± 0.24
Atomic formulae									
Si	1.839	6.039	5.419		0.022	1.879	5.961		6.029
Ti	0.045	0.340	0.418		2.836	0.030	0.343		0.370
Al	0.221	2.287	2.701		1.405	0.176	2.274		2.364
Cr	0.001	0.000	0.000		0.006	0.000	0.001		0.002
Fe^{3+}					11.016				
Fe^{2+}	0.233	1.459	1.443		5.388	0.216	1.472		1.155
Mg	0.711	2.894	3.913		2.164	0.723	2.987		3.129
Mn	0.005	0.015	0.011		0.073	0.005	0.017		0.011
Ni					0.006				
Ca	0.915	1.895	0.025		0.011	0.941	1.952		1.815
Ba			0.026				0.001		
Na	0.075	0.753	0.176			0.068	0.748		0.708
K	0.001	0.339	1.539			0.000	0.350		0.367
P									
Total	4.044	16.022	15.670		22.928	4.037	16.105		15.949
Ca (trace)									
Cr/(Cr+Al)									
Mg/(Mg+Fe)	0.754	0.665	0.731	0.16	0.287	0.770	0.670	0.28	0.730
Fo									
Wo	47.2					48.2			
En	36.7					37.0			
Fs	12.2					11.3			
Ac	3.9					3.5			

Table C.VI. Mineral-chemical composition and structural formulae for wehrlites and ol-cpx-aggregates (c - core; r - rim composition).

sample	MXZH1				MXZH2				MXZH4		MXZH8	
	ol	cpx1	cpx2	phl	ol1	ol2	cpx1	cpx2	ol	cpx	ol	cpx
n	4	5	6	7	6	4	4	3	9	5	10	8
SiO_2	**40.42** ± 0.13	**51.77** ± 0.21	**51.24** ± 0.34	**38.45** ± 0.31	**40.01** ± 0.09	**40.28** ± 0.06	**51.26** ± 0.25	**52.81** ± 0.06	**40.37** ± 0.12	**52.63** ± 0.14	**40.18** ± 0.16	**51.27** ± 0.26
TiO_2	**0.01** ± 0.01	**0.75** ± 0.01	**1.09** ± 0.08	**4.74** ± 0.12	**0.02** ± 0.01	**0.01** ± 0.01	**0.81** ± 0.02	**0.60** ± 0.02	**0.01** ± 0.01	**0.63** ± 0.03	**0.01** ± 0.01	**0.64** ± 0.04
Al_2O_3	**0.04** ± 0.01	**5.01** ± 0.02	**6.23** ± 0.30	**16.99** ± 0.21	**0.03** ± 0.01	**0.04** ± 0.01	**5.28** ± 0.03	**3.85** ± 0.10	**0.03** ± 0.01	**3.91** ± 0.09	**0.04** ± 0.01	**4.37** ± 0.23
Cr_2O_3	**0.04** ± 0.01	**1.29** ± 0.03	**0.13** ± 0.02	**0.09** ± 0.04	**0.04** ± 0.01	**0.03** ± 0.01	**1.47** ± 0.03	**1.09** ± 0.02	**0.03** ± 0.02	**1.13** ± 0.03		**1.18** ± 0.11
Fe_2O_3												
FeO	**11.15** ± 0.07	**3.76** ± 0.07	**4.55** ± 0.12	**6.75** ± 0.05	**11.69** ± 0.12	**11.21** ± 0.12	**3.90** ± 0.06	**3.97** ± 0.11	**11.67** ± 0.13	**3.95** ± 0.03	**11.25** ± 0.26	**3.64** ± 0.12
MgO	**48.61** ± 0.11	**16.23** ± 0.09	**15.65** ± 0.23	**20.63** ± 0.19	**48.20** ± 0.20	**48.61** ± 0.12	**15.71** ± 0.18	**17.06** ± 0.10	**48.35** ± 0.21	**16.83** ± 0.04	**47.93** ± 0.16	**16.38** ± 0.22
MnO	**0.17** ± 0.01	**0.09** ± 0.01	**0.10** ± 0.01	**0.03** ± 0.02	**0.16** ± 0.01	**0.17** ± 0.01	**0.08** ± 0.02	**0.09** ± 0.02	**0.16** ± 0.02	**0.10** ± 0.03	**0.12** ± 0.01	**0.05** ± 0.03
NiO	**0.25** ± 0.05	**0.03** ± 0.03	**0.01** ± 0.02		**0.20** ± 0.04	**0.20** ± 0.01	**0.02** ± 0.02	**0.05** ± 0.01	**0.20** ± 0.04	**0.03** ± 0.03	**0.23** ± 0.03	
CaO	**0.18** ± 0.01	**20.87** ± 0.08	**21.05** ± 0.12	**0.19** ± 0.09	**0.16** ± 0.01	**0.17** ± 0.01	**20.91** ± 0.09	**20.73** ± 0.06	**0.17** ± 0.01	**21.15** ± 0.13	**0.17** ± 0.01	**20.46** ± 0.21
BaO				**0.36** ± 0.06								
Na_2O		**0.93** ± 0.03	**0.95** ± 0.03	**0.49** ± 0.02			**0.96** ± 0.02	**0.83** ± 0.03		**0.86** ± 0.02		**0.88** ± 0.02
K_2O		**0.00** ± 0.00	**0.01** ± 0.01	**8.56** ± 0.38			**0.01** ± 0.01	**0.01** ± 0.00		**0.01** ± 0.01		**0.01** ± 0.00
P_2O_5												
Cl				**0.03** ± 0.01								
F				**0.00** ± 0.00								
H_2O				**4.27** ± 0.04								
Total	**100.88** ± 0.16	**100.74** ± 0.15	**101.01** ± 0.20	**101.56** ± 1.10	**100.50** ± 0.35	**100.71** ± 0.20	**100.41** ± 0.50	**101.09** ± 0.27	**101.01** ± 0.31	**101.23** ± 0.23	**99.94** ± 0.35	**98.89** ± 0.34
Atomic formulae												
Si	0.990	1.874	1.852	5.392	0.986	0.988	1.865	1.903	0.989	1.897	0.993	1.888
Ti	0.000	0.020	0.029	0.500	0.000	0.000	0.022	0.017	0.000	0.017	0.000	0.018
Al	0.001	0.214	0.265	2.808	0.001	0.001	0.226	0.163	0.001	0.166	0.001	0.190
Cr	0.005	0.037	0.004	0.010	0.001	0.001	0.042	0.031	0.001	0.032		0.035
Fe^{3+}												
Fe^{2+}	0.228	0.114	0.138	0.792	0.241	0.230	0.119	0.120	0.239	0.119	0.233	0.112
Mg	1.774	0.876	0.844	4.313	1.771	1.778	0.852	0.916	1.766	0.905	1.766	0.899
Mn	0.004	0.003	0.003	0.004	0.003	0.003	0.002	0.003	0.003	0.003	0.003	0.002
Ni	0.005	0.001	0.000		0.004	0.004	0.001	0.002	0.004	0.001	0.005	
Ca	0.005	0.809	0.815	0.029	0.004	0.004	0.815	0.801	0.004	0.817	0.005	0.807
Ba				0.020								
Na		0.065	0.067	0.133			0.068	0.058		0.060		0.063
K		0.000	0.000	1.530			0.000	0.000		0.000		0.000
P												
Total	3.012	4.013	4.017	15.530	3.011	3.010	4.012	4.014	3.008	4.017	3.005	4.014
Ca (trace)	0.0045				0.0044	0.0042						
Cr/(Cr+Al)												
Mg/(Mg+Fe)	0.886	0.885	0.860	0.845	0.880	0.885	0.878	0.884	0.881	0.884	0.884	0.889
Fo	88.0				87.5	88.0			87.6		87.8	
Wo		43.4	43.7				43.9	42.2		42.9		42.9
En		46.9	45.2				45.9	48.3		47.5		47.7
Fs		6.2	7.5				6.5	6.5		6.4		6.1
Ac		3.5	3.6				3.7	3.1		3.2		3.3

Table C.VI. (continued).

sample	MXZH18						MXZH61					
	ol1	ol3	cpx1	cpx2-r	cpx2-c	sp	ol-a	ol-b	cpx1-c	cpx1-r	cpx2	sp
n	13	6	14	10	7	10	16	5	11	8	17	5
SiO_2	**40.29** ± 0.12	**40.13** ± 0.16	**51.71** ± 0.32	**43.94** ± 1.24	**51.94** ± 0.33	**0.12** ± 0.07	**40.33** ± 0.15	**39.54** ± 0.12	**52.06** ± 0.12	**43.24** ± 1.96	**51.12** ± 0.12	**0.08** ± 0.01
TiO_2	**0.02** ± 0.01	**0.02** ± 0.01	**0.60** ± 0.04	**3.63** ± 0.45	**0.58** ± 0.03	**1.39** ± 0.03	**0.02** ± 0.01	**0.03** ± 0.01	**0.70** ± 0.02	**4.27** ± 0.76	**1.01** ± 0.03	**1.48** ± 0.03
Al_2O_3	**0.04** ± 0.01	**0.04** ± 0.01	**4.15** ± 0.16	**8.45** ± 0.92	**3.90** ± 0.04	**28.36** ± 0.14	**0.04** ± 0.01	**0.04** ± 0.01	**4.73** ± 0.07	**9.05** ± 1.56	**6.02** ± 0.06	**30.19** ± 0.20
Cr_2O_3	**0.07** ± 0.04	**0.04** ± 0.02	**1.29** ± 0.06	**0.05** ± 0.04	**1.20** ± 0.02	**34.38** ± 0.20	**0.03** ± 0.01	**0.01** ± 0.01	**1.40** ± 0.02	**0.04** ± 0.02	**0.66** ± 0.12	**33.11** ± 0.28
Fe_2O_3						**8.35** ± 0.24						**8.69** ± 0.11
FeO	**10.87** ± 0.09	**11.72** ± 0.20	**3.54** ± 0.08	**7.03** ± 0.32	**3.66** ± 0.06	**12.25** ± 0.13	**12.50** ± 0.55	**15.95** ± 0.17	**3.71** ± 0.06	**7.97** ± 0.55	**5.20** ± 0.08	**12.56** ± 0.20
MgO	**48.27** ± 0.13	**47.74** ± 0.23	**17.12** ± 0.16	**12.56** ± 0.51	**17.42** ± 0.13	**15.82** ± 0.10	**47.93** ± 0.47	**45.27** ± 0.13	**16.46** ± 0.06	**11.57** ± 0.85	**15.32** ± 0.05	**16.09** ± 0.14
MnO	**0.11** ± 0.02	**0.13** ± 0.01	**0.06** ± 0.03	**0.05** ± 0.02	**0.07** ± 0.02	**0.07** ± 0.02	**0.18** ± 0.02	**0.22** ± 0.02	**0.10** ± 0.02	**0.08** ± 0.01	**0.11** ± 0.02	**0.14** ± 0.02
NiO	**0.25** ± 0.04	**0.21** ± 0.02				**0.17** ± 0.03	**0.21** ± 0.04	**0.18** ± 0.02	**0.04** ± 0.03	**0.01** ± 0.02	**0.04** ± 0.02	**0.17** ± 0.05
CaO	**0.16** ± 0.01	**0.17** ± 0.01	**20.38** ± 0.20	**23.06** ± 0.16	**20.19** ± 0.05	**0.01** ± 0.01	**0.17** ± 0.01	**0.14** ± 0.01	**20.86** ± 0.09	**23.92** ± 0.13	**20.50** ± 0.09	**0.01** ± 0.01
BaO												
Na_2O			**0.84** ± 0.03	**0.33** ± 0.02	**0.84** ± 0.03		**0.01** ± 0.01	**0.01** ± 0.01	**0.91** ± 0.02	**0.35** ± 0.04	**1.07** ± 0.02	
K_2O			**0.01** ± 0.01	**0.00** ± 0.00	**0.00** ± 0.00		**0.00** ± 0.00	**0.00** ± 0.00	**0.01** ± 0.01	**0.01** ± 0.01	**0.00** ± 0.01	
P_2O_5							**0.01** ± 0.01	**0.02** ± 0.02				
Cl												
F												
H_2O												
Total	**100.07** ± 0.20	**100.19** ± 0.22	**99.70** ± 0.36	**99.11** ± 0.28	**99.81** ± 0.47	**100.90** ± 0.36	**101.41** ± 0.26	**101.41** ± 0.28	**100.97** ± 0.17	**100.51** ± 0.15	**101.05** ± 0.18	**102.51** ± 0.16
Atomic formulae												
Si	0.993	0.992	1.888	1.668	1.893	0.028	0.988	0.985	1.879	1.632	1.853	0.019
Ti	0.000	0.000	0.017	0.104	0.016	0.245	0.000	0.001	0.019	0.121	0.027	0.254
Al	0.001	0.001	0.179	0.378	0.168	7.824	0.001	0.001	0.201	0.403	0.257	8.158
Cr	0.001	0.001	0.037	0.002	0.035	6.363	0.001	0.000	0.040	0.001	0.019	6.001
Fe^{3+}						1.471						1.500
Fe^{2+}	0.224	0.242	0.108	0.224	0.111	2.398	0.256	0.332	0.112	0.252	0.158	2.408
Mg	1.774	1.759	0.932	0.711	0.946	5.520	1.751	1.681	0.886	0.651	0.828	5.498
Mn	0.002	0.003	0.002	0.002	0.002	0.014	0.004	0.005	0.003	0.003	0.003	0.027
Ni	0.005	0.004				0.031	0.004	0.004	0.001	0.000	0.001	0.031
Ca	0.004	0.004	0.797	0.938	0.789	0.003	0.004	0.004	0.807	0.968	0.796	0.002
Ba												
Na			0.059	0.024	0.060				0.064	0.026	0.075	
K			0.000	0.000	0.000				0.000	0.000	0.000	
P												
Total	3.005	3.007	4.018	4.051	4.020	23.897	3.010	3.012	4.013	4.057	4.019	23.897
Ca (trace)	0.0039											
Cr/(Cr+Al)						0.449						0.424
Mg/(Mg+Fe)	0.888	0.879	0.896	0.761	0.895	0.697	0.872	0.835	0.888	0.721	0.840	0.695
Fo	88.3	87.4					86.7	83.0				
Wo			42.0	49.4	41.3				43.1	51.0	42.8	
En			49.1	37.4	49.6				47.3	34.3	44.5	
Fs			5.8	11.9	6.0				6.2	13.4	8.7	
Ac			3.1	1.3	3.1				3.4	1.3	4.1	

Table C.VI. (continued).

sample	MXZH64				
	ol-a	ol-b	sp	cpx-c	cpx-r
n	17	10	10	25	28
SiO_2	**40.47** ± 0.13	**39.78** ± 0.18	**0.10** ± 0.01	**52.29** ± 0.25	**42.96** ± 0.73
TiO_2	**0.02** ± 0.02	**0.02** ± 0.01	**1.39** ± 0.03	**0.62** ± 0.03	**4.03** ± 0.31
Al_2O_3	**0.04** ± 0.01	**0.04** ± 0.04	**27.10** ± 0.26	**4.46** ± 0.19	**9.67** ± 0.56
Cr_2O_3	**0.08** ± 0.06	**0.02** ± 0.02	**35.36** ± 0.34	**1.38** ± 0.07	**0.03** ± 0.03
Fe_2O_3			**8.51** ± 0.32		
FeO	**10.81** ± 0.18	**13.17** ± 0.37	**12.15** ± 0.29	**3.46** ± 0.09	**7.56** ± 0.36
MgO	**48.42** ± 0.17	**46.72** ± 0.38	**15.58** ± 0.18	**16.34** ± 0.14	**11.36** ± 0.40
MnO	**0.15** ± 0.03	**0.16** ± 0.03	**0.12** ± 0.03	**0.11** ± 0.03	**0.08** ± 0.04
NiO	**0.25** ± 0.04	**0.18** ± 0.03	**0.18** ± 0.04		
CaO	**0.16** ± 0.02	**0.16** ± 0.01	**0.02** ± 0.03	**20.93** ± 0.15	**23.73** ± 0.14
BaO					
Na_2O	**0.03** ± 0.02	**0.02** ± 0.02		**0.92** ± 0.04	**0.41** ± 0.02
K_2O	**0.01** ± 0.01	**0.01** ± 0.01		**0.01** ± 0.01	**0.00** ± 0.00
P_2O_5					
Cl					
F					
H_2O					
Total	**100.43** ± 0.28	**100.26** ± 0.30	**100.51** ± 0.41	**100.53** ± 0.32	**99.83** ± 0.22
Atomic formulae					
Si	0.994	0.989	0.023	1.893	1.629
Ti	0.000	0.000	0.247	0.017	0.115
Al	0.001	0.001	7.543	0.190	0.432
Cr	0.001	0.000	6.604	0.040	0.001
Fe^{3+}			1.513		
Fe^{2+}	0.222	0.274	2.401	0.105	0.240
Mg	1.773	1.732	5.487	0.882	0.642
Mn	0.003	0.003	0.024	0.003	0.002
Ni	0.005	0.004	0.034		
Ca	0.004	0.004	0.005	0.812	0.964
Ba					
Na				0.065	0.030
K				0.000	0.000
P					
Total	3.004	3.009	23.880	4.007	4.055
Ca (trace)	0.0039				
Cr/(Cr+Al)			0.467		
Mg/(Mg+Fe)	0.889	0.863	0.696	0.894	0.728
Fo	88.3	85.9			
Wo				43.5	51.3
En				47.3	34.2
Fs				5.8	12.9
Ac				3.5	1.6

Table C.VII. Chemical composition and structural formulae of olivine megacrysts and associated minerals (c - core; r - rim).

sample	MXZH7		MXZH19		MXZH24					MXZH69		
	ol	ol	ol	cpx-in-gl	ol-a	ol-b	phl1	phl2	cpx-in-gl	ol	phl	
n	6 r	10 c	20	6	9 r	10 c	3	5	10	9	5	
SiO_2	**39.34** ± 0.24	**39.02** ± 0.19	**39.16** ± 0.09	**37.13** ± 0.48	**39.96** ± 0.15	**39.11** ± 0.17	**38.23** ± 0.14	**38.61** ± 0.06	**37.95** ± 0.41	**39.97** ± 0.15	**38.54** ± 0.24	
TiO_2	**0.02** ± 0.01	**0.02** ± 0.01	**0.02** ± 0.01	**6.59** ± 0.14	**0.02** ± 0.01	**0.03** ± 0.01	**4.70** ± 0.03	**4.64** ± 0.05	**6.50** ± 0.16	**0.03** ± 0.01	**5.09** ± 0.07	
Al_2O_3	**0.03** ± 0.01	**0.04** ± 0.01	**0.03** ± 0.01	**12.57** ± 0.17	**0.03** ± 0.01	**0.04** ± 0.01	**17.14** ± 0.03	**17.12** ± 0.09	**11.86** ± 0.28	**0.04** ± 0.01	**17.13** ± 0.08	
Cr_2O_3	**0.03** ± 0.02	**0.00** ± 0.00		**0.12** ± 0.08	**0.03** ± 0.02	**0.00** ± 0.00	**0.12** ± 0.00	**0.84** ± 0.15	**0.32** ± 0.17	**0.02** ± 0.01	**0.56** ± 0.02	
Fe_2O_3												
FeO	**14.24** ± 0.18	**16.61** ± 0.17	**16.31** ± 0.16	**9.13** ± 0.19	**12.46** ± 0.21	**16.41** ± 0.12	**7.21** ± 0.25	**5.53** ± 0.10	**8.02** ± 0.19	**13.12** ± 0.80	**5.99** ± 0.10	
MgO	**45.70** ± 0.23	**43.85** ± 0.15	**43.89** ± 0.18	**9.01** ± 0.22	**47.13** ± 0.34	**43.98** ± 0.14	**19.99** ± 0.03	**20.76** ± 0.12	**10.30** ± 0.14	**47.14** ± 0.56	**21.12** ± 0.06	
MnO	**0.22** ± 0.03	**0.22** ± 0.04	**0.17** ± 0.02	**0.08** ± 0.02	**0.12** ± 0.02	**0.17** ± 0.03	**0.05** ± 0.02	**0.02** ± 0.03	**0.05** ± 0.02	**0.17** ± 0.02	**0.05** ± 0.01	
NiO	**0.16** ± 0.03	**0.14** ± 0.03	**0.13** ± 0.02		**0.14** ± 0.02	**0.10** ± 0.04	**0.08** ± 0.01	**0.14** ± 0.02		**0.18** ± 0.03		
CaO	**0.25** ± 0.06	**0.14** ± 0.01	**0.14** ± 0.01	**22.54** ± 0.12	**0.19** ± 0.01	**0.16** ± 0.01	**0.05** ± 0.02	**0.03** ± 0.01	**23.05** ± 0.14	**0.16** ± 0.01	**0.01** ± 0.00	
BaO							**0.25** ± 0.02	**0.27** ± 0.05			**0.30** ± 0.04	
Na_2O				**0.45** ± 0.02			**0.72** ± 0.02	**0.45** ± 0.02	**0.34** ± 0.02		**0.48** ± 0.02	
K_2O				**0.00** ± 0.00			**9.09** ± 0.13	**9.57** ± 0.07	**0.02** ± 0.01		**8.89** ± 0.06	
P_2O_5												
Cl							**0.02** ± 0.00	**0.03** ± 0.01			**0.02** ± 0.01	
F							**0.00** ± 0.00	**0.00** ± 0.00			**0.00** ± 0.00	
H_2O							**4.26** ± 0.01	**4.30** ± 0.01			**4.32** ± 0.01	
Total	**100.00** ± 0.33	**100.03** ± 0.38	**99.85** ± 0.31	**97.62** ± 0.33	**100.07** ± 0.28	**100.01** ± 0.23	**101.89** ± 0.33	**102.28** ± 0.21	**98.42** ± 0.33	**100.87** ± 0.19	**102.49** ± 0.32	
Atomic formulae												
Si	0.987	0.989	0.992	1.463	0.992	0.990	5.372	5.382	1.477	0.988	5.350	
Ti	0.000	0.000	0.000	0.195	0.000	0.000	0.496	0.486	0.190	0.001	0.531	
Al	0.001	0.001	0.001	0.584	0.001	0.001	2.839	2.813	0.544	0.001	2.802	
Cr	0.001	0.000	0.000	0.004	0.001	0.000	0.013	0.092	0.010	0.000	0.061	
Fe^{3+}												
Fe^{2+}	0.299	0.352	0.346	0.301	0.259	0.347	0.847	0.644	0.261	0.271	0.695	
Mg	1.709	1.656	1.658	0.529	1.744	1.660	4.189	4.313	0.597	1.737	4.371	
Mn	0.005	0.005	0.004	0.003	0.003	0.004	0.006	0.003	0.002	0.004	0.005	
Ni	0.003	0.003	0.003		0.003	0.002	0.009	0.016		0.004		
Ca	0.007	0.004	0.004	0.952	0.005	0.004	0.007	0.004	0.961	0.004	0.002	
Ba							0.014	0.015			0.016	
Na				0.035			0.195	0.120	0.025		0.129	
K				0.000			1.630	1.701	0.001		1.575	
P												
Total	3.011	3.009	3.011	4.065	3.007	3.009	15.618	15.590	4.069	3.010	15.539	
Ca (trace)												
Cr/(Cr+Al)												
Mg/(Mg+Fe)	0.851	0.825	0.827	0.638	0.871	0.827	0.832	0.870	0.696	0.865	0.863	
Fo	84.5	82.0	82.3		86.6	82.3				86.0		
Wo				52.3					52.1			
En				29.1					32.3			
Fs				16.7					14.2			
Ac				1.9					1.4			

Table C.VIII. Chemical composition and structural formulae of clinopyroxene megacrysts and associated minerals (HK - analyses by H. Kämpf; c - core; r - rim; s - sector).

sample	MXZH14		MXZH9		MXZH62				EB2			
	cpx-r	cpx-c	cpx-r	cpx-c	cpx-c	cpx-r1	cpx-r2	cpx-old	cpx-r	cpx-s1	cpx-s2	ol
n	5 (HK)	15 (HK)	3	8	2	6	2	2	7	17	20	22
SiO_2	**46.74** ± 2.30	**50.49** ± 0.45	**46.76** ± 2.95	**51.29** ± 0.15	**50.25** ± 0.05	**50.76** ± 0.18	**42.29** ± 0.33	**52.40** ± 0.05	**43.52** ± 0.92	**50.73** ± 0.18	**49.78** ± 0.24	**39.24** ± 0.22
TiO_2	**2.90** ± 0.87	**1.03** ± 0.06	**2.70** ± 1.08	**0.93** ± 0.02	**1.27** ± 0.01	**1.16** ± 0.02	**4.39** ± 0.03	**0.66** ± 0.04	**3.57** ± 0.29	**0.86** ± 0.03	**1.05** ± 0.03	**0.02** ± 0.01
Al_2O_3	**6.69** ± 1.89	**5.95** ± 0.19	**6.60** ± 2.26	**5.49** ± 0.07	**6.58** ± 0.05	**6.08** ± 0.03	**10.00** ± 0.08	**4.36** ± 0.07	**8.00** ± 0.95	**5.05** ± 0.07	**6.18** ± 0.07	**0.04** ± 0.02
Cr_2O_3	**0.21** ± 0.11	**0.11** ± 0.02	**0.20** ± 0.15	**0.40** ± 0.01	**0.05** ± 0.02	**0.07** ± 0.01	**0.01** ± 0.00	**0.88** ± 0.15	**0.02** ± 0.01	**0.29** ± 0.02	**0.34** ± 0.03	
Fe_2O_3												
FeO	**6.09** ± 0.66	**5.63** ± 0.11	**6.25** ± 1.24	**5.27** ± 0.07	**5.91** ± 0.07	**5.81** ± 0.10	**8.04** ± 0.00	**3.50** ± 0.02	**7.53** ± 0.24	**5.17** ± 0.05	**5.31** ± 0.07	**14.85** ± 0.50
MgO	**13.54** ± 1.18	**15.29** ± 0.13	**13.36** ± 1.44	**15.53** ± 0.09	**14.44** ± 0.01	**14.83** ± 0.13	**11.29** ± 0.16	**16.46** ± 0.10	**12.03** ± 0.45	**15.63** ± 0.07	**14.96** ± 0.08	**44.85** ± 0.40
MnO	**0.07** ± 0.02	**0.11** ± 0.04	**0.06** ± 0.04	**0.14** ± 0.02	**0.12** ± 0.01	**0.13** ± 0.02	**0.09** ± 0.00	**0.10** ± 0.00	**0.06** ± 0.02	**0.09** ± 0.02	**0.09** ± 0.02	**0.14** ± 0.02
NiO	**0.01** ± 0.01	**0.02** ± 0.02										**0.18** ± 0.03
CaO	**23.60** ± 0.12	**20.41** ± 0.20	**23.68** ± 0.14	**20.18** ± 0.08	**20.46** ± 0.02	**20.57** ± 0.11	**23.33** ± 0.04	**21.42** ± 0.03	**23.31** ± 0.16	**20.11** ± 0.08	**20.24** ± 0.10	**0.14** ± 0.01
BaO												
Na_2O	**0.37** ± 0.03	**1.02** ± 0.03	**0.37** ± 0.04	**1.02** ± 0.03	**1.17** ± 0.00	**1.09** ± 0.02	**0.42** ± 0.00	**0.84** ± 0.02	**0.35** ± 0.35	**0.93** ± 0.02	**1.02** ± 0.04	
K_2O	**0.00** ± 0.00	**0.00** ± 0.00	**0.00** ± 0.00	**0.00** ± 0.00	**0.01** ± 0.01	**0.01** ± 0.01	**0.00** ± 0.00	**0.00** ± 0.00	**0.01** ± 0.01	**0.01** ± 0.01	**0.00** ± 0.00	
P_2O_5												
Cl												
F												
H_2O												
Total	**100.21** ± 0.20	**100.06** ± 0.51	**99.99** ± 0.17	**100.25** ± 0.16	**100.24** ± 0.08	**100.49** ± 0.43	**99.85** ± 0.55	**100.62** ± 0.13	**98.39** ± 0.35	**98.86** ± 0.24	**98.97** ± 0.27	**99.46** ± 0.23
Atomic formulae												
Si	1.740	1.851	1.748	1.871	1.842	1.855	1.607	1.896	1.672	1.877	1.844	0.991
Ti	0.080	0.030	0.076	0.026	0.035	0.032	0.125	0.018	0.103	0.024	0.029	0.000
Al	0.296	0.257	0.292	0.236	0.284	0.262	0.448	0.186	0.362	0.220	0.270	0.001
Cr			0.006	0.012	0.002	0.002	0.000	0.025	0.000	0.008	0.010	
Fe^{3+}												
Fe^{2+}	0.188	0.171	0.196	0.161	0.181	0.177	0.256	0.106	0.242	0.160	0.165	0.314
Mg	0.752	0.832	0.744	0.845	0.789	0.807	0.640	0.888	0.689	0.862	0.826	1.690
Mn			0.002	0.004	0.004	0.004	0.003	0.003	0.002	0.003	0.003	0.003
Ni												0.004
Ca	0.942	0.802	0.949	0.789	0.804	0.805	0.950	0.831	0.960	0.797	0.803	0.004
Ba												
Na	0.028	0.072	0.027	0.072	0.083	0.077	0.031	0.059	0.026	0.067	0.073	
K			0.000	0.000	0.001	0.000	0.000	0.000	0.000	0.000	0.000	
P												
Total	4.026	4.015	4.039	4.015	4.023	4.021	4.059	4.011	4.057	4.018	4.023	3.007
Ca (trace)												
Cr/(Cr+Al)												
Mg/(Mg+Fe)	0.800	0.829	0.792	0.840	0.813	0.820	0.715	0.893	0.740	0.843	0.834	0.843
Fo												83.9
Wo	49.3	42.7	49.5	42.2	43.2	43.0	50.6	44.0	50.0	42.2	43.0	0.2
En	39.4	44.3	38.8	45.2	42.4	43.2	34.0	47.1	35.9	45.6	44.2	84.1
Fs	9.8	9.1	10.3	8.8	9.9	9.7	13.8	5.8	12.7	8.6	8.9	15.8
Ac	1.5	3.8	1.4	3.9	4.5	4.1	1.6	3.1	1.3	3.5	3.9	0.0

Table C.VIII. (continued).

sample	EB6		EB7	
	cpx-r	cpx-c	cpx-r	cpx-c
n	5	25	12	13
SiO_2	**39.39** ± 0.25	**51.59** ± 0.25	**45.62** ± 0.90	**50.32** ± 0.31
TiO_2	**5.93** ± 0.11	**0.86** ± 0.03	**3.04** ± 0.31	**1.05** ± 0.04
Al_2O_3	**11.65** ± 0.58	**4.82** ± 0.12	**6.64** ± 0.87	**5.99** ± 0.10
Cr_2O_3	**0.01** ± 0.02	**0.29** ± 0.02	**0.06** ± 0.10	**0.28** ± 0.03
Fe_2O_3				
FeO	**8.77** ± 0.07	**4.17** ± 0.09	**6.83** ± 0.49	**5.34** ± 0.12
MgO	**10.12** ± 0.25	**16.23** ± 0.11	**12.91** ± 0.54	**15.03** ± 0.10
MnO	**0.10** ± 0.02	**0.09** ± 0.03	**0.10** ± 0.02	**0.11** ± 0.03
NiO				
CaO	**23.38** ± 0.26	**21.40** ± 0.10	**23.67** ± 0.11	**20.23** ± 0.09
BaO				
Na_2O	**0.42** ± 0.02	**0.82** ± 0.02	**0.37** ± 0.03	**1.15** ± 0.03
K_2O	**0.01** ± 0.00	**0.01** ± 0.01	**0.00** ± 0.00	**0.01** ± 0.01
P_2O_5				
Cl				
F				
H_2O				
Total	**99.78** ± 0.27	**100.27** ± 0.24	**99.23** ± 0.35	**99.51** ± 0.33
Atomic formulae				
Si	1.512	1.878	1.728	1.854
Ti	0.171	0.023	0.087	0.029
Al	0.527	0.207	0.297	0.260
Cr	0.000	0.008	0.002	0.008
Fe^{3+}				
Fe^{2+}	0.281	0.127	0.216	0.164
Mg	0.579	0.881	0.729	0.826
Mn	0.003	0.003	0.003	0.004
Ni				
Ca	0.962	0.835	0.961	0.798
Ba				
Na	0.031	0.058	0.027	0.082
K	0.000	0.000	0.000	0.000
P				
Total	4.068	4.020	4.050	4.025
Ca (trace)				
Cr/(Cr+Al)				
Mg/(Mg+Fe)	0.673	0.874	0.771	0.834
Fo				
Wo	51.8	43.9	49.6	42.6
En	31.2	46.3	37.6	44.1
Fs	15.3	6.8	11.3	9.0
Ac	1.7	3.0	1.4	4.4

Table C.IX. Chemical composition and structural formulae of amphibole and mica megacrysts (HK - analyses by H. Kämpf).

sample	EB1	MXZH15			MXZH1a	MXZH9	MXZH10	MXZH32			MXZH35	MXZH42
	incl. in olivine	rim	core_sulphides	core			core	rim		near vug		
n	41	20	10	10	5	5	6	5	10	2	10	10
SiO_2	**41.92** ± 0.11	**40.52** ± 0.36	**41.12** ± 0.18	**41.47** ± 0.09	**42.05** ± 0.02	**41.82** ± 0.23	**41.60** ± 0.16	**41.74** ± 0.08	**41.47** ± 0.49	**41.29** ± 0.06	**41.66** ± 0.33	**41.75** ± 0.32
TiO_2	**3.28** ± 0.05	**3.26** ± 0.05	**3.31** ± 0.05	**3.30** ± 0.07	**3.49** ± 0.06	**3.39** ± 0.07	**3.24** ± 0.06	**3.26** ± 0.05	**3.42** ± 0.05	**3.36** ± 0.01	**3.27** ± 0.03	**3.42** ± 0.11
Al_2O_3	**14.57** ± 0.06	**14.67** ± 0.06	**14.62** ± 0.08	**14.56** ± 0.07	**13.89** ± 0.07	**14.32** ± 0.07	**14.78** ± 0.07	**14.62** ± 0.05	**13.80** ± 0.09	**14.36** ± 0.07	**14.73** ± 0.07	**14.22** ± 0.24
Cr_2O_3	**0.22** ± 0.02	**0.26** ± 0.03	**0.11** ± 0.02	**0.11** ± 0.03	**0.05** ± 0.01	**0.06** ± 0.02	**0.24** ± 0.02	**0.18** ± 0.02	**0.01** ± 0.01	**0.02** ± 0.02	**0.22** ± 0.01	**0.06** ± 0.02
Fe_2O_3												
FeO	**7.37** ± 0.10	**7.17** ± 0.14	**7.35** ± 0.13	**7.62** ± 0.12	**8.86** ± 0.18	**7.98** ± 0.06	**7.38** ± 0.13	**7.41** ± 0.20	**8.15** ± 0.17	**6.74** ± 0.14	**7.41** ± 0.12	**7.84** ± 0.19
MgO	**15.32** ± 0.08	**15.64** ± 0.07	**15.65** ± 0.05	**15.51** ± 0.05	**14.80** ± 0.09	**15.20** ± 0.07	**15.46** ± 0.06	**15.45** ± 0.06	**15.40** ± 0.10	**16.45** ± 0.02	**15.64** ± 0.09	**15.37** ± 0.13
MnO	**0.07** ± 0.03	**0.08** ± 0.04	**0.08** ± 0.04	**0.07** ± 0.03	**0.08** ± 0.03	**0.08** ± 0.03	**0.10** ± 0.03	**0.09** ± 0.03	**0.09** ± 0.03	**0.07** ± 0.02	**0.07** ± 0.03	**0.08** ± 0.03
NiO	**0.04** 0.02				**0.02** 0.02							
CaO	**11.53** ± 0.06	**11.44** ± 0.07	**11.51** ± 0.06	**11.46** ± 0.12	**11.75** ± 0.09	**11.52** ± 0.06	**11.59** ± 0.09	**11.55** ± 0.11	**11.77** ± 0.10	**11.71** ± 0.07	**11.63** ± 0.06	**11.66** ± 0.06
BaO												
Na_2O	**2.18** ± 0.06	**2.24** ± 0.03	**2.28** ± 0.03	**2.28** ± 0.02	**2.43** ± 0.04	**2.32** ± 0.02	**2.25** ± 0.03	**2.25** ± 0.03	**2.44** ± 0.04	**2.27** ± 0.06	**2.29** ± 0.03	**2.38** ± 0.05
K_2O	**2.08** ± 0.02	**2.28** ± 0.04	**2.22** ± 0.04	**2.22** ± 0.05	**1.90** ± 0.04	**2.18** ± 0.02	**2.28** ± 0.02	**2.25** ± 0.02	**2.07** ± 0.04	**2.09** ± 0.02	**2.25** ± 0.02	**2.19** ± 0.09
P_2O_5												
Cl	**0.02** ± 0.01	**0.02** ± 0.01	**0.02** ± 0.01	**0.02** ± 0.01	**0.02** ± 0.00	**0.02** ± 0.01	**0.02** ± 0.01	**0.01** ± 0.00	**0.01** ± 0.01	**0.01** ± 0.00	**0.02** ± 0.01	**0.02** ± 0.01
F	**0.00** ± 0.00	**0.06** ± 0.02	**0.05** ± 0.02	**0.04** ± 0.02	**0.00** ± 0.00	**0.00** ± 0.00	**0.04** ± 0.04	**0.05** ± 0.03	**0.03** ± 0.03	**0.09** ± 0.03	**0.06** ± 0.03	**0.05** ± 0.02
Total	**98.61** ± 0.23	**97.60** ± 0.37	**98.30** ± 0.29	**98.63** ± 0.21	**99.34** ± 0.07	**98.89** ± 0.26	**98.95** ± 0.17	**98.84** ± 0.30	**98.65** ± 0.52	**98.41** ± 0.05	**99.22** ± 0.40	**99.02** ± 0.44
Atomic formulae on the basis of 23 oxygens												
Si	6.037	5.916	5.956	5.988	6.056	6.029	5.983	6.006	6.010	5.955	5.976	6.013
Ti	0.356	0.358	0.361	0.358	0.378	0.368	0.351	0.353	0.373	0.364	0.353	0.370
Al	2.473	2.524	2.495	2.477	2.358	2.433	2.506	2.480	2.358	2.441	2.490	2.414
Cr	0.025	0.030	0.013	0.013	0.006	0.007	0.027	0.020	0.002	0.002	0.025	0.007
Fe^{3+}												
Fe^{2+}	0.888	0.876	0.891	0.920	1.067	0.962	0.887	0.892	0.988	0.814	0.889	0.945
Mg	3.288	3.404	3.379	3.338	3.177	3.267	3.314	3.315	3.327	3.537	3.345	3.300
Mn	0.009	0.010	0.010	0.009	0.010	0.010	0.012	0.011	0.011	0.009	0.008	0.010
Ni	0.005				0.002							
Ca	1.780	1.790	1.787	1.772	1.813	1.779	1.786	1.781	1.827	1.809	1.788	1.800
Ba												
Na	0.609	0.634	0.641	0.639	0.680	0.648	0.627	0.627	0.687	0.634	0.636	0.665
K	0.381	0.425	0.410	0.410	0.350	0.400	0.418	0.412	0.383	0.385	0.412	0.402
P												
Total	15.850	15.965	15.942	15.923	15.896	15.904	15.910	15.897	15.964	15.948	15.923	15.925
Cr/(Cr+Al)	0.010	0.012	0.005	0.005	0.002	0.003	0.011	0.008	0.001	0.001	0.010	0.003
Mg/(Mg+Fe)	0.787	0.795	0.791	0.784	0.749	0.773	0.789	0.788	0.771	0.813	0.790	0.777
p - S92 [kbar]	8.8	9.0	8.9	8.8	8.2	8.6	8.9	8.8	8.2	8.6	8.8	8.5
p - Ho87 [kbar]	9.2	9.5	9.3	9.2	8.5	9.0	9.4	9.2	8.5	9.0	9.3	8.9
p - HZ86 [kbar]	8.5	8.8	8.6	8.5	7.9	8.3	8.7	8.6	7.9	8.4	8.6	8.2
p - JR89 [kbar]	7.0	7.2	7.1	7.0	6.5	6.8	7.1	7.0	6.5	6.9	7.1	6.8

S92 - *Schmidt,* 1992; Ho87 - *Hollister et al.,* 1987; HZ86 - *Hammarstrom and Zen,* 1986; JR89 - *Johnson and Rutherford,* 1989.

Table C.IX. (continued).

sample	MXZH39		MXZH21	
	core	rim	phl	
n	20	10	11	11 (HK)
SiO_2	**41.54** ± 0.21	**41.55** ± 0.13	**37.74** ± 0.32	**37.30** ± 0.39
TiO_2	**3.32** ± 0.03	**3.28** ± 0.03	**4.25** ± 0.06	**4.23** ± 0.05
Al_2O_3	**14.51** ± 0.06	**14.53** ± 0.08	**16.93** ± 0.25	**16.72** ± 0.18
Cr_2O_3	**0.30** ± 0.02	**0.22** ± 0.02	**0.03** ± 0.02	
Fe_2O_3				
FeO	**7.22** ± 0.15	**7.19** ± 0.14	**7.54** ± 0.14	**7.39** ± 0.19
MgO	**15.48** ± 0.08	**15.51** ± 0.08	**19.12** ± 0.24	**19.31** ± 0.17
MnO	**0.08** ± 0.03	**0.09** ± 0.02		**0.05** ± 0.02
NiO				
CaO	**11.52** ± 0.10	**11.51** ± 0.05	**0.14** ± 0.12	**0.03** ± 0.03
BaO			**0.13** ± 0.02	***0.33*** ± *0.09*
Na_2O	**2.28** ± 0.03	**2.26** ± 0.02	**0.67** ± 0.05	**0.67** ± 0.03
K_2O	**2.19** ± 0.05	**2.20** ± 0.03	**8.59** ± 0.54	**8.98** ± 0.14
P_2O_5			**0.00** ± 0.00	**0.02** ± 0.02
Cl	**0.02** ± 0.01	**0.02** ± 0.01	**0.02** ± 0.01	**0.02** ± 0.01
F	**0.05** ± 0.02	**0.06** ± 0.04	**0.00** ± 0.00	**0.00** ± 0.00
Total	**98.48** ± 0.29	**98.40** ± 0.18	**95.17** ± 0.54	**95.05** ± 0.82
Atomic formulae on the basis of 23 oxygens				
Si	5.997	6.001		
Ti	0.360	0.357		
Al	2.470	2.473		
Cr	0.035	0.026		
Fe^{3+}				
Fe^{2+}	0.872	0.868		
Mg	3.331	3.340		
Mn	0.010	0.011		
Ni				
Ca	1.783	1.782		
Ba				
Na	0.639	0.633		
K	0.403	0.406		
P				
Total	15.898	15.896		
Cr/(Cr+Al)	0.014	0.010		
Mg/(Mg+Fe)	0.793	0.794	0.819	0.823
p - S92 [kbar]	8.7	8.8		
p - Ho87 [kbar]	9.2	9.2		
p - HZ86 [kbar]	8.5	8.5		
p - JR89 [kbar]	7.0	7.0		

Table C.X. Chemical composition and structural formulae of groundmass (gm) minerals (c- core, r - rim).

sample	MXZH2		MXZH18	MXZH9	MXZH8			EB2	MXZH64	MXZH69		MXZH17	
	ol-gm	ol-gm	ol-gm	ol-gm	ol-gm1	ol-gm1	ol-gm2	ol-gm	ol-gm	ol-gm	ol-gm	ol-gm	sp(ol)
n	4 c	1 r	7	8	9 c	6 r	8	4	3	3 c	2 r	1	1
SiO_2	**40.50** ± 0.06	**39.81**	**40.52** ± 0.11	**40.50** ± 0.14	**39.94** ± 0.41	**39.48** ± 0.22	**39.06** ± 0.20	**39.61** ± 0.10	**39.30** ± 0.18	**40.18** ± 0.09	**39.42** ± 0.03	**40.44**	**0.11**
TiO_2	**0.01** ± 0.00	**0.04**	**0.02** ± 0.01	**0.01** ± 0.01	**0.02** ± 0.01	**0.04** ± 0.02	**0.03** ± 0.02	**0.02** ± 0.01	**0.03** ± 0.01	**0.02** ± 0.01	**0.03** ± 0.01	**0.01**	**1.40**
Al_2O_3	**0.04** ± 0.00	**0.04**	**0.04** ± 0.01	**0.04** ± 0.01	**0.04** ± 0.02	**0.03** ± 0.01	**0.20** ± 0.27	**0.03** ± 0.01	**0.02** ± 0.01	**0.04** ± 0.01	**0.02** ± 0.00	**0.03**	**29.17**
Cr_2O_3	**0.04** ± 0.01	**0.04**	**0.06** ± 0.03	**0.08** ± 0.02					**0.03** ± 0.02	**0.04** ± 0.01	**0.02** ± 0.01	**0.06**	**33.66**
Fe_2O_3													**9.02**
FeO	**10.91** ± 0.11	**14.32**	**10.04** ± 0.34	**10.05** ± 0.09	**10.39** ± 0.56	**12.87** ± 0.40	**13.60** ± 0.24	**13.54** ± 0.19	**13.25** ± 0.39	**11.11** ± 0.08	**13.98** ± 0.02	**11.24**	**11.84**
MgO	**48.78** ± 0.07	**46.46**	**48.76** ± 0.18	**48.95** ± 0.05	**48.34** ± 0.64	**46.29** ± 0.36	**45.38** ± 0.41	**45.69** ± 0.22	**45.34** ± 0.24	**48.70** ± 0.08	**46.01** ± 0.10	**48.43**	**16.28**
MnO	**0.16** ± 0.02	**0.27**	**0.11** ± 0.02	**0.16** ± 0.03	**0.11** ± 0.02	**0.16** ± 0.03	**0.14** ± 0.02	**0.16** ± 0.01	**0.31** ± 0.15	**0.15** ± 0.01	**0.27** ± 0.01	**0.20**	**0.09**
NiO	**0.24** ± 0.02	**0.04**	**0.32** ± 0.05	**0.37** ± 0.03	**0.31** ± 0.04	**0.14** ± 0.05	**0.15** ± 0.03	**0.13** ± 0.03	**0.14** ± 0.11	**0.24** ± 0.02	**0.09** ± 0.01	**0.24**	**0.22**
CaO	**0.18** ± 0.01	**0.35**	**0.17** ± 0.04	**0.14** ± 0.01	**0.19** ± 0.02	**0.31** ± 0.12	**0.22** ± 0.03	**0.24** ± 0.03	**0.43** ± 0.11	**0.18** ± 0.01	**0.35** ± 0.00	**0.17**	**0.01**
BaO													
Na_2O													
K_2O													
P_2O_5													
Cl													
F													
H_2O													
Total	**100.85** ± 0.11	**101.37**	**100.04** ± 0.25	**100.29** ± 0.20	**99.33** ± 0.77	**99.32** ± 0.40	**98.77** ± 0.35	**99.42** ± 0.35	**98.89** ± 0.55	**100.66** ± 0.20	**100.20** ± 0.09	**100.83**	**101.79**
Atomic formulae													
Si	0.990	0.985	0.995	0.993	0.991	0.990	0.989	0.995	0.993	0.986	0.986	0.991	0.026
Ti	0.000	0.001	0.000	0.000	0.000	0.001	0.001	0.000	0.001	0.000	0.001	0.000	0.244
Al	0.001	0.001	0.001	0.001	0.001	0.001	0.006	0.001	0.001	0.001	0.001	0.001	7.944
Cr	0.001	0.001	0.001	0.001					0.001	0.001	0.001	0.001	6.149
Fe^{3+}													1.568
Fe^{2+}	0.223	0.296	0.206	0.206	0.216	0.270	0.288	0.284	0.280	0.228	0.292	0.231	2.287
Mg	1.778	1.713	1.786	1.789	1.787	1.731	1.713	1.711	1.709	1.782	1.715	1.770	5.608
Mn	0.003	0.006	0.002	0.003	0.002	0.003	0.003	0.003	0.007	0.003	0.006	0.004	0.017
Ni	0.005	0.001	0.006	0.007	0.006	0.003	0.003	0.003	0.003	0.005	0.002	0.005	0.040
Ca	0.005	0.009	0.004	0.004	0.005	0.008	0.006	0.007	0.012	0.005	0.010	0.005	0.003
Ba													
Na													
K													
P													
Total	3.007	3.012	3.003	3.005	3.008	3.008	3.008	3.004	3.005	3.011	3.012	3.007	23.886
Ca (trace)													
Cr/(Cr+Al)													0.436
Mg/(Mg+Fe)	0.889	0.853	0.896	0.897	0.892	0.865	0.856	0.857	0.859	0.887	0.854	0.885	0.710
Fo	88.3	84.6	89.1	89.0	88.6	85.9	85.1	85.2	85.0	88.1	84.7	87.9	
Wo													
En													
Fs													
Ac													

Table C.X. (continued).

sample	MXZH8		MXZH24		MXZH69	EB1	EB5	MXZH64	MXZH17	MXZH69
	cpx-gm	cpx-gm	cpx-gm	cpx-gm	cpx-gm	cpx-gm	cpx-gm	mag-gm	sp-gm	sp-gm
n	9 c	4 r	11 c	4 r	1	6	4	1	1	2
SiO_2	**45.59** ± 0.42	**39.14** ± 1.48	**49.57** ± 0.44	**44.86** ± 2.57	**39.82**	**38.30** ± 0.83	**41.75** ± 0.78	**3.32**	**0.10**	**0.09** ± 0.00
TiO_2	**2.88** ± 0.07	**5.69** ± 0.68	**1.05** ± 0.04	**3.08** ± 0.74	**5.58**	**6.18** ± 0.32	**4.83** ± 0.54	**10.99**	**1.16**	**1.42** ± 0.02
Al_2O_3	**6.29** ± 0.25	**11.28** ± 1.24	**6.07** ± 0.05	**7.23** ± 1.87	**11.66**	**11.97** ± 0.48	**9.66** ± 0.57	**6.48**	**25.24**	**30.28** ± 0.12
Cr_2O_3	**0.03** ± 0.02	**0.16** ± 0.16	**0.05** ± 0.02	**0.08** ± 0.11	**0.01**	**0.00** ± 0.01	**0.23** ± 0.14	**0.13**	**40.82**	**33.05** ± 0.21
Fe_2O_3								**48.33**	**7.16**	**8.43** ± 0.14
FeO	**7.11** ± 0.14	**8.21** ± 0.44	**5.57** ± 0.06	**6.83** ± 1.02	**8.68**	**8.75** ± 0.38	**7.72** ± 0.55	**21.89**	**11.85**	**12.40** ± 0.13
MgO	**12.99** ± 0.15	**10.38** ± 0.68	**15.21** ± 0.11	**13.08** ± 1.18	**10.33**	**9.75** ± 0.26	**11.31** ± 0.37	**4.61**	**16.04**	**16.12** ± 0.09
MnO	**0.08** ± 0.02	**0.06** ± 0.01	**0.08** ± 0.02	**0.05** ± 0.02	**0.09**	**0.07** ± 0.02	**0.06** ± 0.02	**1.18**	**0.14**	**0.10** ± 0.02
NiO					**0.02**			**0.12**	**0.28**	**0.23** ± 0.02
CaO	**23.16** ± 0.14	**22.95** ± 0.21	**20.28** ± 0.09	**23.47** ± 0.13	**23.45**	**22.91** ± 0.08	**23.51** ± 0.11	**1.40**	**0.00**	**0.00** ± 0.00
BaO										
Na_2O	**0.35** ± 0.02	**0.40** ± 0.02	**1.07** ± 0.03	**0.35** ± 0.04	**0.36**	**0.40** ± 0.01	**0.41** ± 0.01			
K_2O	**0.01** ± 0.01	**0.00** ± 0.00	**0.01** ± 0.01	**0.00** ± 0.00	**0.04**	**0.01** ± 0.01	**0.01** ± 0.01			
P_2O_5										
Cl										
F										
H_2O										
Total	**98.48** ± 0.23	**98.27** ± 0.67	**98.96** ± 0.47	**99.03** ± 0.35	**100.02**	**98.36** ± 0.32	**99.49** ± 0.38	**98.45**	**102.78**	**102.11** ± 0.22
Atomic formulae										
Si	1.740	1.522	1.839	1.703	1.523	1.493	1.595	0.904	0.024	0.022
Ti	0.083	0.167	0.029	0.088	0.160	0.181	0.139	2.253	0.203	0.245
Al	0.283	0.517	0.265	0.325	0.526	0.550	0.435	2.083	6.936	8.204
Cr	0.001	0.005	0.002	0.002	0.000	0.000	0.007	0.027	7.525	6.005
Fe^{3+}								9.913	1.256	1.458
Fe^{2+}	0.227	0.267	0.173	0.217	0.278	0.285	0.247	4.989	2.310	2.383
Mg	0.739	0.602	0.841	0.740	0.589	0.567	0.644	1.872	5.575	5.523
Mn	0.002	0.002	0.003	0.002	0.003	0.003	0.002	0.273	0.028	0.019
Ni					0.000			0.026	0.053	0.042
Ca	0.947	0.956	0.806	0.955	0.961	0.957	0.962	0.410	0.000	0.001
Ba										
Na	0.026	0.030	0.077	0.026	0.027	0.030	0.030			
K	0.000	0.000	0.000	0.000	0.002	0.000	0.001			
P										
Total	4.048	4.067	4.036	4.058		4.066	4.061	22.750	23.910	23.900
Ca (trace)										
Cr/(Cr+Al)								0.013	0.520	0.423
Mg/(Mg+Fe)	0.765	0.693	0.830	0.773	0.679	0.665	0.723	0.273	0.707	0.699
Fo										
Wo	48.8	51.5	42.4	49.3	51.7	52.0	51.0			
En	38.1	32.4	44.3	38.2	31.7	30.8	34.2			
Fs	11.8	14.5	9.2	11.3	15.1	15.6	13.2			
Ac	1.3	1.6	4.1	1.3	1.5	1.6	1.6			

Table C.XI. Chemical composition of glass (gl) and groundmass (gm) in xenoliths.

sample	MXZH8			MXZH18		MXZH61		MXZH62	MXZH24			MXZH69	EB1
	glass1	glass2	gm3	glass1	glass2	glass	glass	glass	glass1	glass2		glass	glass rim
n	10	7	9	15	5	9	1	1	6	10		6	15
SiO_2	**39.40** ± 0.63	**41.09** ± 1.38	**40.53**	**40.28** ± 0.10	**39.98** ± 0.68	**40.97** ± 0.23	**38.04**	**48.03**	**41.43** ± 0.45	**40.99** ± 0.25		**42.42** ± 0.69	**41.71** ± 0.88
TiO_2	**3.49** ± 0.17	**4.23** ± 0.47	**2.38**	**3.28** ± 0.06	**3.22** ± 0.08	**3.29** ± 0.09	**0.11**	**0.83**	**3.63** ± 0.07	**3.65** ± 0.08		**3.39** ± 0.23	**3.19** ± 0.25
Al_2O_3	**14.20** ± 0.16	**11.67** ± 0.47	**13.87**	**13.26** ± 0.08	**14.98** ± 0.23	**15.43** ± 0.23	**34.45**	**21.98**	**15.29** ± 0.27	**15.24** ± 0.10		**16.34** ± 0.34	**16.52** ± 0.35
Cr_2O_3	**0.01** 0.01	**0.01** ± 0.01	**0.00**			**0.01** ± 0.01	**0.03**	**0.00**	**0.00** 0.01	**0.01** 0.01		**0.03** ± 0.02	**0.01** ± 0.01
Fe_2O_3													
FeO	**10.65** ± 0.85	**13.55** ± 1.32	**9.79**	**10.26** ± 0.14	**10.36** ± 0.28	**10.85** ± 0.54	**0.85**	**8.22**	**9.68** ± 0.29	**9.93** ± 0.21		**9.10** ± 0.40	**10.17** ± 1.08
MgO	**0.74** ± 0.06	**1.05** ± 0.15	**0.56**	**5.08** ± 0.09	**4.08** ± 0.18	**4.95** ± 0.41	**0.38**	**3.33**	**5.74** ± 0.08	**5.81** ± 0.09		**4.54** ± 0.38	**0.79** ± 0.09
MnO	**0.16** ± 0.02	**0.19** ± 0.02	**0.18**	**0.15** ± 0.03	**0.17** ± 0.02	**0.23** ± 0.02	**0.02**	**0.27**	**0.19** ± 0.02	**0.19** ± 0.03		**0.21** ± 0.03	**0.17** ± 0.02
NiO						**0.01** ± 0.01	**0.02**	**0.00**	**0.02** 0.01	**0.00** 0.00		**0.02** 0.02	
CaO	**15.99** ± 0.47	**14.85** ± 0.73	**16.57**	**17.42** ± 0.15	**14.10** ± 0.78	**15.03** ± 0.23	**6.06**	**4.37**	**15.30** ± 0.39	**16.01** ± 0.14		**13.86** ± 0.53	**13.40** ± 1.19
BaO	**0.05** ± 0.02	**0.01** ± 0.02	**0.64**	**0.09** ± 0.02	**0.12** ± 0.04	**0.17** ± 0.02	**0.04**	**0.16**	**0.20** ± 0.02	**0.18** ± 0.03		**0.16** 0.06	**0.02** ± 0.04
Na_2O	**3.65** ± 0.15	**0.49** ± 0.05	**6.83**	**2.97** ± 0.07	**2.57** ± 0.46	**3.95** ± 0.07	**6.18**	**5.92**	**3.61** ± 0.06	**3.79** ± 0.03		**4.07** ± 1.40	**6.20** ± 0.87
K_2O	**3.74** ± 0.22	**0.28** ± 0.10	**1.85**	**4.70** ± 0.14	**6.24** ± 0.67	**4.60** ± 0.09	**4.03**	**4.33**	**3.70** ± 0.11	**3.68** ± 0.04		**4.71** ± 1.46	**2.12** ± 0.50
P_2O_5	**1.15** ± 0.06	**1.27** ± 0.12	**1.31**	**0.98** ± 0.06	**1.16** ± 0.06	**1.34** ± 0.06	**0.55**	**0.73**	**0.96** ± 0.06	**1.00** ± 0.06		**1.01** 0.09	**1.51** ± 0.06
Cl	**0.12** ± 0.01	**0.01** ± 0.01	**0.05**	**0.27** ± 0.01	**0.35** ± 0.02	**0.36** ± 0.01	**1.67**	**0.50**	**0.28** ± 0.01	**0.27** ± 0.01		**0.30** 0.04	**0.06** ± 0.04
F	**0.01** ± 0.01	**0.00** ± 0.00	**0.00**	**0.00** ± 0.01	**0.24** ± 0.14	**0.01** ± 0.02	**0.00**	**0.07**	**0.03** ± 0.02	**0.00** ± 0.01		**0.02** 0.05	**0.00** ± 0.00
SrO	**0.00** ± 0.00	**0.00** ± 0.00	**0.45**										**0.06** ± 0.04
S	**0.06** 0.02	**0.02** ± 0.01	**0.13**										
Total	**93.39** ± 0.36	**88.71** ± 0.71	**95.11**	**98.68** ± 0.25	**97.39** ± 1.60	**101.09** ± 0.38	**92.04**	**98.58**	**99.98** ± 0.20	**100.71** ± 0.40		**100.13** ± 1.08	**95.93** ± 0.80
Atomic formulae													
Si													
Ti													
Al													
Cr													
Fe^{3+}													
Fe^{2+}													
Mg													
Mn													
Ni													
Ca													
Ba													
Na													
K													
P													
Total													
Ca (trace)													
Cr/(Cr+Al)													
Mg/(Mg+Fe)	0.110	0.121	0.093	0.469	0.413	0.449	0.442	0.419	0.514	0.511		0.471	0.122
Fo													
Wo													
En													
Fs													
Ac													

Table C.XII. Chemical composition and structural formulae of olivine crystals from Železná Hůrka.

sample	EB5-olivines					EB1	
	ol9-core	ol9-rim	sp-in-ol9	ol4-core	ol4-rim	ol-core	ol-rim
n	38	1	3	8	5	36	11
SiO_2	**40.43** ± 0.14	**39.75**	**0.10** ± 0.02	**38.77** ± 0.18	**39.52** ± 0.23	**39.15** ± 0.13	**39.80** ± 0.07
TiO_2	**0.01** ± 0.01	**0.05**	**1.38** ± 0.01	**0.03** ± 0.01	**0.03** ± 0.02	**0.02** ± 0.02	**0.02** ± 0.01
Al_2O_3	**0.04** ± 0.01	**0.04**	**22.65** ± 0.22	**0.04** ± 0.01	**0.04** ± 0.01	**0.04** ± 0.01	**0.04** ± 0.01
Cr_2O_3	**0.06** ± 0.01	**0.04**	**41.32** ± 0.26	**0.01** ± 0.01	**0.02** ± 0.02		
Fe_2O_3			**8.33** ± 0.10				
FeO	**10.57** ± 0.11	**14.24**	**12.36** ± 0.07	**17.12** ± 0.22	**13.83** ± 0.35	**16.23** ± 0.09	**13.53** ± 0.19
MgO	**48.87** ± 0.16	**45.83**	**15.27** ± 0.08	**43.61** ± 0.09	**46.04** ± 0.19	**43.85** ± 0.10	**45.76** ± 0.21
MnO	**0.15** ± 0.02	**0.22**	**0.10** ± 0.01	**0.24** ± 0.02	**0.20** ± 0.02	**0.16** ± 0.02	**0.15** ± 0.02
NiO	**0.28** ± 0.02	**0.13**	**0.17** ± 0.02	**0.09** ± 0.03	**0.12** ± 0.05	**0.13** ± 0.02	**0.13** ± 0.04
CaO	**0.17** ± 0.01	**0.33**	**0.01** ± 0.01	**0.15** ± 0.01	**0.25** ± 0.08	**0.14** ± 0.01	**0.26** ± 0.08
BaO							
Na_2O							
K_2O							
P_2O_5							
Cl							
F							
H_2O							
Total	**100.59** ± 0.25	**100.62**	**101.69** ± 0.24	**100.05** ± 0.31	**100.05** ± 0.20	**99.71** ± 0.17	**99.70** ± 0.28
Atomic formulae							
Si	0.991	0.990	0.025	0.985	0.988	0.993	0.996
Ti	0.000	0.001	0.248	0.000	0.001	0.000	0.000
Al	0.001	0.001	6.369	0.001	0.001	0.001	0.001
Cr	0.001	0.001	7.792	0.000	0.000		
Fe^{3+}			1.495				
Fe^{2+}	0.217	0.297	2.466	0.364	0.289	0.344	0.283
Mg	1.785	1.702	5.431	1.652	1.717	1.658	1.708
Mn	0.003	0.005	0.020	0.005	0.004	0.003	0.003
Ni	0.005	0.003	0.033	0.002	0.002	0.003	0.003
Ca	0.005	0.009	0.002	0.004	0.007	0.004	0.007
Ba							
Na							
K							
P							
Total	3.007	3.008	23.881	3.014	3.011	3.006	3.002
Ca (trace)							
Cr/(Cr+Al)			0.550				
Mg/(Mg+Fe)	0.892	0.852	0.688	0.820	0.856	0.828	0.858
Fo	88.6	84.5		81.5	85.0	82.4	85.2
Wo							
En							
Fs							
Ac							

Table C.XIII. Mineral-chemical composition and structural formulae for feldspar rich rocks (c - core, r - rim, i - intergrowth).

sample	XKZH1								XKZH2			
	fsp	opx-r	opx-c	opx-i	cpx-i	am	phl	rt	fsp	glass	glass	mag
n	5	8	4	2	4	4	4	4	4	3	4	1
SiO_2	**54.05** ± 0.30	**53.66** ± 0.22	**53.93** ± 0.22	**53.95** ± 0.07	**51.87** ± 0.86	**45.50** ± 0.87	**38.46** ± 0.25	**0.01** ± 0.01	**67.79** ± 0.19	**68.36** ± 0.83	**58.35** ± 0.99	**0.55**
TiO_2	**0.04** ± 0.04	**0.08** ± 0.01	**0.10** ± 0.01	**0.38** ± 0.01	**0.71** ± 0.24	**1.65** ± 0.02	**4.84** ± 0.08	**100.68** ± 0.37	**0.01** ± 0.01	**0.46** ± 0.09	**0.52** ± 0.28	**11.45**
Al_2O_3	**29.83** ± 0.16	**2.42** ± 0.07	**2.56** ± 0.08	**4.28** ± 0.34	**4.17** ± 1.22	**11.52** ± 0.24	**16.35** ± 0.05	**0.03** ± 0.02	**20.80** ± 0.01	**21.51** ± 0.07	**20.54** ± 0.09	**8.72**
Cr_2O_3		**0.03** ± 0.02	**0.07** ± 0.02	**0.16** ± 0.01	**0.14** ± 0.07	**0.05** ± 0.02	**0.04** ± 0.03	**0.06** ± 0.02		**0.01** ± 0.01	**0.01** ± 0.01	**0.06**
Fe_2O_3												**48.25**
FeO	**0.08** ± 0.04	**17.81** ± 0.14	**17.89** ± 0.27	**12.87** ± 1.00	**7.36** ± 0.66	**10.33** ± 0.19	**11.13** ± 0.23	**0.42** ± 0.29	**0.06** ± 0.03	**4.35** ± 0.52	**4.00** ± 0.52	**24.74**
MgO	**0.01** ± 0.01	**25.89** ± 0.12	**25.61** ± 0.07	**27.89** ± 0.94	**15.99** ± 0.82	**15.33** ± 0.18	**16.58** ± 0.25	**0.06** ± 0.09	**0.00** ± 0.00	**0.78** ± 0.09	**0.70** ± 0.11	**3.60**
MnO	**0.01** ± 0.01	**0.38** ± 0.05	**0.38** ± 0.03	**0.19** ± 0.02	**0.16** ± 0.02	**0.13** ± 0.03	**0.05** ± 0.04	**0.00** ± 0.00	**0.00** ± 0.01	**0.29** ± 0.04	**0.30** ± 0.06	**1.87**
NiO				**0.03** ± 0.02	**0.05** ± 0.03					**0.01** ± 0.01		**0.00**
CaO	**12.02** ± 0.05	**0.37** ± 0.03	**0.51** ± 0.05	**1.56** ± 0.06	**19.33** ± 0.81	**11.24** ± 0.08	**0.07** ± 0.03	**0.01** ± 0.01	**1.26** ± 0.03	**0.93** ± 0.06	**0.99** ± 0.12	**0.03**
BaO	**0.02** ± 0.01						**0.23** ± 0.07		**0.02** ± 0.01	**0.06** ± 0.00	**0.08** ± 0.01	
Na_2O	**5.13** ± 0.08	**0.01** ± 0.00	**0.03** ± 0.00	**0.05** ± 0.00	**0.55** ± 0.10	**1.96** ± 0.06	**0.80** ± 0.06		**10.88** ± 0.08	**2.70** ± 0.22	**8.70** ± 0.06	
K_2O	**0.18** ± 0.01	**0.01** ± 0.01	**0.00** ± 0.00			**0.55** ± 0.02	**7.82** ± 0.57		**1.06** ± 0.03	**1.15** ± 0.04	**3.66** ± 0.05	
P_2O_5										**0.06** ± 0.05		
Cl						**0.02** ± 0.00	**0.01** ± 0.01			**0.03** ± 0.01	**0.08** ± 0.02	
F						**0.00** ± 0.00	**0.00** ± 0.00			**0.00** ± 0.00	**0.00** ± 0.00	
H_2O							**4.17** ± 0.02	SrO	**0.08** ± 0.03		ZnO	**0.33**
Total	**101.36** ± 0.44	**100.66** ± 0.40	**101.06** ± 0.36	**99.97** ± 0.31	**100.09** ± 1.00	**98.25** ± 1.30	**96.38** ± 0.96	**101.27** ± 0.19	**101.95** ± 0.24	**100.70** ± 0.28	**97.91** ± 0.36	**99.60**
Atomic formulae												
Si	2.416	1.940	1.942	1.899	1.900	6.549	5.525		2.931			
Ti	0.001	0.002	0.003	0.010	0.020	0.179	0.523		0.000			
Al	1.572	0.103	0.108	0.178	0.180	1.954	2.768		1.060			
Cr		0.001	0.002	0.005	0.004	0.005	0.005					
Fe^{3+}												
Fe^{2+}	0.003	0.538	0.539	0.379	0.226	1.243	1.337		0.002			
Mg	0.000	1.395	1.375	1.463	0.873	3.289	3.550		0.000			
Mn	0.000	0.012	0.012	0.006	0.005	0.015	0.006		0.000			
Ni				0.001	0.001							
Ca	0.576	0.014	0.020	0.059	0.759	1.734	0.011		0.058			
Ba	0.000						0.013		0.000			
Na	0.444	0.000	0.002	0.004	0.039	0.547	0.223		0.912			
K	0.010	0.001	0.000			0.101	1.433		0.059			
P												
Total	5.024	4.006	4.002	4.001	4.007	15.614	15.392		5.022			
Ca (trace)												
Cr/(Cr+Al)												
Mg/(Mg+Fe)		0.722	0.718	0.794	0.795	0.726	0.726			0.242	0.237	0.206
Fo												
Wo or An	55.9	0.7	1.0	3.1	39.9				5.6			
En or Ab	43.1	71.2	70.6	76.6	45.9				88.7			
Fs or Or	1.0	28.1	28.3	20.1	12.1				5.7			
Ac		0.0	0.1	0.2	2.1							

Table C.XIII. (continued).

sample	XKZH3				
	cpx	fsp1	fsp2	ttn	ap
n	3	4	2	8	3
SiO_2	**52.18** ± 0.18	**67.49** ± 0.19	**68.38** ± 0.19	**30.60** ± 0.25	**0.27** ± 0.03
TiO_2	**0.19** ± 0.00	**0.01** ± 0.02	**0.01** ± 0.00	**37.80** ± 0.87	**0.00** ± 0.01
Al_2O_3	**1.65** ± 0.06	**19.26** ± 0.08	**20.02** ± 0.06	**1.34** ± 0.21	**0.01** ± 0.01
Cr_2O_3	**0.03** ± 0.01			**0.03** ± 0.02	**0.01** ± 0.01
Fe_2O_3				**2.03** ± 0.41	
FeO	**17.18** ± 0.03	**0.12** ± 0.02	**0.16** ± 0.00		**0.02** ± 0.01
MgO	**7.48** ± 0.05	**0.00** ± 0.00	**0.00** ± 0.00	**0.01** ± 0.02	**0.00** ± 0.00
MnO	**0.56** ± 0.01	**0.01** ± 0.01	**0.01** ± 0.01	**0.09** ± 0.02	**0.05** ± 0.01
NiO				**0.02** ± 0.03	**0.01** ± 0.01
CaO	**16.21** ± 0.04	**0.31** ± 0.02	**0.56** ± 0.03	**28.14** ± 0.29	**55.94** ± 0.11
BaO		**0.36** ± 0.04	**0.03** ± 0.01	**0.00** ± 0.00	**0.03** ± 0.02
Na_2O	**4.76** ± 0.08	**7.35** ± 0.03	**11.17** ± 0.12	**0.13** ± 0.04	**0.28** ± 0.02
K_2O	**0.01** ± 0.00	**6.23** ± 0.05	**1.21** ± 0.01	**0.00** ± 0.00	**0.00** ± 0.01
P_2O_5				**0.02** ± 0.02	**35.57** ± 0.67
Cl				**0.01** ± 0.01	**0.01** ± 0.01
F				**0.38** ± 0.17	**3.56** ± 0.02
H_2O	SrO	**0.12** ± 0.01	**0.11** ± 0.01		
Total	**100.25** ± 0.23	**101.25** ± 0.29	**101.68** ± 0.34	**100.45** ± 0.74	**94.27** ± 0.61
Atomic formulae					
Si	2.012	2.987	2.964		
Ti	0.005	0.000	0.000		
Al	0.075	1.005	1.023		
Cr	0.001				
Fe^{3+}					
Fe^{2+}	0.554	0.005	0.006		
Mg	0.430	0.000	0.000		
Mn	0.018	0.000	0.001		
Ni					
Ca	0.670	0.015	0.026		
Ba		0.006	0.001		
Na	0.356	0.630	0.939		
K	0.000	0.352	0.067		
P					
Total	4.122	4.999	5.025		
Ca (trace)					
Cr/(Cr+Al)					
Mg/(Mg+Fe)	0.437				
Fo					
Wo or An	33.0	1.5	2.5		
En or Ab	21.2	63.2	91.0		
Fs or Or	28.2	35.3	6.5		
Ac	17.6				

The amount of Fe^{3+} in spinel was calculated from stoichiometry by the algorithm in the CAMECA software. Natural and synthetic standards (Smithsonian Standards; Astimex Scientific Limited) were used for calibration. To test the degree of equilibration between and within mineral grains (intra-grain heterogeneity), a large number of point analyses and profiles were performed. The consistency of the data set was checked by repeated measurements for some samples. The accuracy of microprobe analyses is in the range of 0.05 to 0.2 wt.%. The matrix correction was done by the algorithm that is implemented in the software of the CAMECA microprobes (PAP algorithm; *Pouchou and Pichoir,* 1984). The results of the microprobe measurements are listed in Tables C.III to C.XIII.

Olivine analyses

The investigated olivines have forsterite contents between 0.82 and 0.88 (Tables C.III, C.IV, C.VII, C.X, C.XII) and differ from olivines in spinel lherzolites (0.90 to 0.91) from nearby localities in NE-Bavaria [*Huckenholz and Kunzmann,* 1993; own data], the Rhön [*Franz et al.,* 1997], and the Elbe Zone [*Medaris et al.*, 1997; *Kramer and Seifert,* 2000; own data]. Normal and reversed zoning of Mg and Fe could be observed in many of the investigated grains. CaO contents are relatively high in the analysed olivines from Mýtina (wehrlitic samples: 0.17 wt.%; megacrysts cores and MXZH66: 0.15 wt.%; phenocryst cores: 0.18 wt.%) comparable to olivines from Železná Hůrka (0.14 to 0.17 wt.%), whereas olivines in spinel lherzolites have lower CaO contents (Zinst-1: 0.09 wt.%; Go01-1: 0.04 wt.%). Rims of phenocrysts and megacrysts have CaO contents > 0.25 wt.%, but analyses may be influenced by the so-called phase boundary fluorescence effect.

Clinopyroxene analyses

Analysed clinopyroxenes can be classified as chromian or aluminian diopsides and augites, according to *Morimoto* [1988] (Tables C.III-C.VI, C.VIII, C.X, C.XII; Figure C.6). Cr-rich clinopyroxenes commonly belong to the spinel lherzolites, wehrlites or olivine-clinopyroxene-spinel cumulates. The composition of groundmass clinopyroxenes and rims is titanian aluminian diopsidic (up to > 6 wt.% TiO_2; up to 12 wt.% Al_2O_3). The Cr-content of clinopyroxenes within wehrlites (e.g., MXZH1) is highly variable, indicating magmatic/metasomatic overprinting of the samples.

Amphibole analyses

The investigated amphiboles (polycrystalline and megacrysts) are Fe-, Ti-rich calcic amphiboles (potassian titanian pargasites, according to *Leake et al.* [1978, 1997]; Tables C.III-C.V, C.IX, C.XIII). They show widespread K_2O/Na_2O ratios (composite samples 0.5 to 1.0; megacrysts 0.8 to 1.0). Mg/(Mg+Fe) values are 0.67 for clinopyroxene-hornblendites, 0.73 for hornblendite, 0.57 to 0.6 for hornblende-clinopyroxenites, and 0.79 for hbl-peridotite. Mg/(Mg+Fe) values of analysed amphibole megacrysts are close to 0.8. The TiO_2 content is about 2.5 wt.% in clinopyroxenites, > 3 wt.% in hornblendites as well as in sample MXZH66. TiO_2 content of megacrysts is 3.3 to 3.4 wt.%. Al_2O_3

varies between 12.7 wt.% (MXZH33) and 14.6 wt.% (MXZH66) for xenoliths, and between 13.8 and 14.7 wt.% for megacrysts. Only amphibole in sample MXZH66 (0.8 wt.%) and amphibole megacrysts (0 to 0.3 wt.%) contain significant amounts of Cr_2O_3.

A Fe^{3+}/Fe^{2+} ratio of 0.5 was determined for amphibole megacryst MXZH15 from the whole-rock chemistry (Table C.II). This sample and hornblendite sample MXZH68 also contain rounded Ni, Co, Pt and Cu bearing magnetite-sulphide inclusions (average sulphide analyses: 57.7 wt.% Fe, 38.7 wt.% S, 3.3 wt.% Ni, 0.2 wt.% Co, up to 4 wt.% Cu, up to 0.7 wt.% Pt; pyrrhotite). Such sulphide inclusions are common in metasomatized mantle xenoliths [e.g., *Shaw,* 1997] and may result from the immiscibility of sulphide liquids with the magma [*Deer et al.,* 1963].

Amphibole in the crustal xenolith XKZH1 has lower TiO_2 (1.65 wt.%), Al_2O_3 (11.5 wt.%) and K_2O (0.55 wt.%) than amphiboles in the other analysed (ultra-) mafic samples.

Phlogopite analyses

Micas, occurring as megacrysts and within xenoliths, are Ti-rich phlogopites (3.8 to 4.8 wt.% TiO_2, 18 to > 20 wt.% MgO; Tables C.V-C.VII, C.IX) [see also *Seifert and Kämpf*, 1994].

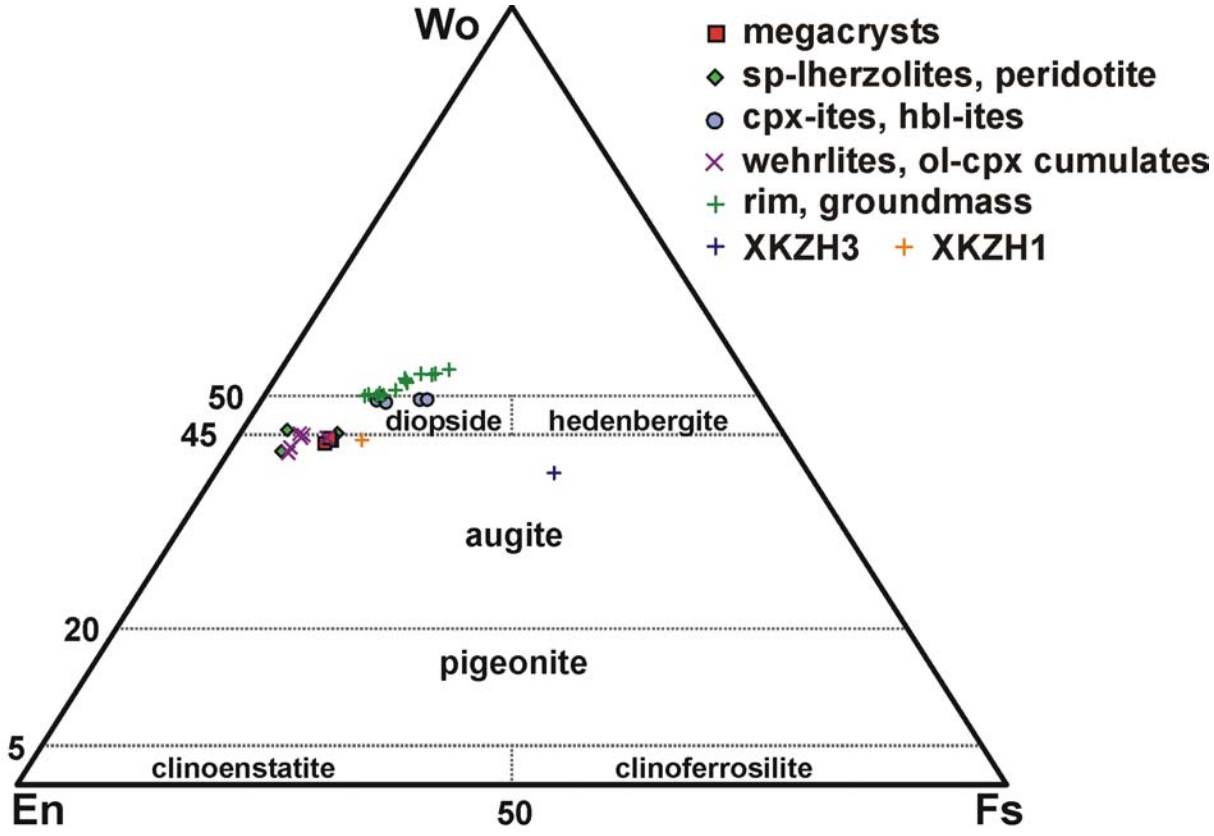

Figure C.6
Ternary classification diagram for clinopyroxenes [after *Morimoto,* 1988]. Cr-rich clinopyroxenes of spinel lherzolites, peridotite, wehrlites, olivine-clinopyroxene-spinel cumulates, and clinopyroxene in XKZH1 plot close to the augite-diopside boundary. Clinopyroxenes within clinopyroxenites and hornblendites can be classified as diopsides. Clinopyroxene rims and groundmass crystals plot above the 50% Wollastonite line due to very high Al and Ti contents. Sample XKZH3 contains Na-rich augitic clinopyroxene (aegirine-augite).

C.5 Interpretation of the petrological data

C.5.1 Composition and origin of xenoliths and megacrysts

Already in the 19th century, there was a controversy on the origin of the ultramafic nodules (mantle xenoliths) and megacrysts from Mýtina, whether they are true xenoliths or cumulates that crystallized in the host magma. Whereas *Reuss* [1852] argued that the olivine, amphibole, and augite nodules are evidence for a previous basaltic activity and that they were partly re-melted or became scoria-like, *Proft* [1894] favoured the early crystallization in the basaltic host magma.

C.5.1.1 Mantle xenoliths and cumulates

The magmatic textures of most ultramafic nodules indicate the crystallization from a melt not long before the entrainment into the host magma; otherwise textural equilibration and development of metamorphic fabric would be expected [*Best*, 2003]. The mineral chemistry (relatively low Mg content of olivine, low Cr_2O_3 contents of clinopyroxenes, high TiO_2 contents of diopsidic clinopyroxenes and amphiboles, widespread K_2O/Na_2O ratios of amphiboles) as well as the occurrence of titaniferous micas let me argue that the majority of the investigated samples are directly related to alkaline magmatism, associated with incompatible element enrichment of peridotite wall-rocks in the immediate vicinity of frozen conduits [see *Wilkinson and Le'Maitre,* 1987; *Witt and Seck,* 1989]. According to *Huckenholz et al.* [1992], amphiboles crystallized from basaltic magmas have a "convex-up shaped" Eu and Sm anomaly in the C1-normalized REE pattern; and amphiboles in veins, small dikes or selvages have lower mg-values and overlap for Na, K, Ti with megacrysts. The REE C1-normalized patterns of the analysed amphibole-bearing xenoliths (LREE enriched convex-upward; Figure C.5) resample that of vein amphiboles from ultramafic Alpine massifs and xenoliths, as compiled by *Downes* [2001], supporting the interpretation of a magmatic origin.

Pargasites within sample MXZH66 (mg 0.8, 0.5-0.8 wt.% Cr_2O_3) show some similarities to amphiboles of secondary origin, which commonly occur interstitially in the olivine-orthopyroxene-clinopyroxene-spinel matrix of peridotites (mg 0.82-0.94, >1 wt% Cr_2O_3; see *Huckenholz et al.,* [1993]). MXZH66 might represent a sample from near a hornblendite vein; such veins are widely observed in ultramafic Alpine massifs [e.g., Lherz massif, French Pyrenees; *McPherson et al.,* 1996; *Woodland et al.,* 1996; *Zanetti et al.,* 1996; *Fabries et al.,* 2001].

Some wehrlitic samples containing Cr-bearing diopside and olivine (Fo 88) and showing cumulus textures are possibly related to alkaline metasomatism (by alkaline-carbonatitic melts) of the uppermost mantle (see below). Generally, samples similar to the analysed (meta-) cumulates,

pyroxenites and hornblendites are also reported from the North Hessian Depression, the Eifel, the Urach and the Hegau volcanic fields [e.g., *Becker,* 1977; *Vinx and Jung,* 1977; *Mengel et al.,* 1991].

C.5.1.2 Megacrysts – high pressure precipitates or fragments of pegmatites or dikes ?

According to *Irving* [1984] and *Schulze* [1987], basaltic megacrysts can be divided into two groups: Group A, including aluminian augite, olivine, kaersutitic amphibole, may have been crystallized from the host basalts or similar magmas; and Group B, including Ti-rich mica, apatite, ilmenite, is considered to represent (pegmatitic) xenocrysts, belonging originally to more evolved magmas (possibly related to the host) intruded to shallower depths prior to the host magma [*Schulze,* 1987]. *Righter and Carmichael* [1993] argued that large, unzoned, inclusion-free megacrysts cannot have grown from the basalt host during ascent, because that would require unreasonable large growth and diffusion rates. According to *Righter and Carmichael* [1993], the unzoned nature of many megacrysts indicate a slow crystallization in magma chambers or as pegmatites. The growth of 1-cm crystals may last thousands of years, which requires long-lived magma chambers. In such reservoirs with stable temperature-pressure conditions close to mineral liquidus, small crystals of a specified mineral may dissolve and large crystals grow by the process of textural coarsening [e.g., *Higgins and Roberge,* 2003]. Arguments for a xenocryst origin of megacrysts are the fragmented or irregular edges in contact with the host basalt; some coarse xenocrysts show also fracturing [*Righter and Carmichael*, 1993]. Shape, composition and size indicate derivation from disaggregated gabbroic, pyroxenitic, wehrlitic dikes and pegmatites. Some coarse subhedral crystals could be real phenocrysts [*Righter and Carmichael*, 1993]. Furthermore, isotopic studies can be useful to clarify the relationship between megacrysts and the host rock [see *Schulze, 1987*].

Most of the olivine megacrysts from Mýtina show a narrow range in chemical composition of mineral cores (Fo 82 to 83; see Table C.VII). The core composition of megacrysts differs strongly from core analyses of the magnesium rich phenocrysts in the host rock (Fo 88 to 89; Table C.X). Towards the rim many megacrysts are more magnesian (Fo 85 to 86) indicating changing chemical conditions [see *Kämpf et al.,* 1993], magmatic overprinting (diffusion), or further crystallization in the host magma. This rim composition of olivine megacrysts is similar to that of olivine crystals (both pheno- and xenocrysts) from the Železná Hůrka scoria (see Table C.XII). Generally, the existence of large melt inclusion can be interpreted as an effect of fast crystallization (skeletal growth) in a magma reservoir, but it cannot be excluded that this porosity is also an effect of magmatic resorption due to melt infiltration. The different core compositions of most phenocrysts and megacrysts from the Mýtina tephra let me argue, that they at least did not crystallize in one single magma chamber. Maybe the less magnesian megacrysts are related to shallower reservoirs.

Most single clinopyroxene megacrysts, sampled from the Mýtina tephra and the Železná Hůrka scoria, can be classified as aluminian augites (see Table C.VIII; Figure C.6). However, also large chromian diopside crystals occur in olivine-clinopyroxene-spinel aggregates (MXZH61, MXZH64). Narrow rims are always titanian diopsidic in composition, similar to Ti-rich diopside phenocrysts in the host rock. Aluminian augites are the most likely candidates for high-pressure phenocrysts [*Schulze*, 1987]. The equilibrium composition (with host melt) depends strongly on p-T conditions. For a primary origin of some clinopyroxene-megacrysts as phenocrysts argue the fact that they grew on smaller crystals (e.g., MXZH62: chromian augite xenocryst; EB2: olivine xenocryst). In the ternary Wo-En-Fs diagram (Figure C.6) aluminian augite megacrysts plot close the clinopyroxenes (chromian augites to diopsides) from wehrlitic samples and olivine-clinopyroxene cumulates.

The chemical composition of amphibole megacrysts from the Mýtina tephra is similar to that of amphiboles in clinopyroxenites and hornblendites (Tables C.IX and C.III-C.V). All samples can be classified as titanian pargasites [*Leake,* 1978, 1997], however Al and Cr contents vary between samples. Ti-rich amphibole is a near liquidus phase in alkali basaltic systems [e.g., *Allen et al.,* 1975] and could represent deep-seated phenocrysts.

The coarse grain size of Ti-rich ferromagnesian micas (phlogopite), which are relatively uncommon as megacrysts in alkali basalts [according to *Schulze*; 1987], may indicate their origin as phenocrysts.

C.5.1.3 Crustal rocks

Sample XKZH1 could be a rare fragment of feldspar-rich meta-intrusive rocks noritic in composition. Similar rock types (charnockitic, noritic, gabbroic), which might be related to magmatic intrusions into the lower crust, were described as xenoliths from the Elbe Zone and the Českе středohoři Mts. by *Opletal* [1967], *Kramer* [1988], *Opletal and Vrána* [1989], and *Kramer and Seifert,* [2000]. However, the ages of these rocks and therefore the times of intrusion are unknown. Sample XKZH1 shows weak metamorphic layering, which constrains an older age and implies that the samples are not directly related to the Tertiary-Quaternary volcanic/magmatic episode.

Upper crustal xenoliths (quartzites, phyllites, and mica schists) are most probably fragments of the uppermost kilometre(s) of the crust in the area around Mýtina. According to *Richter and Stettner* [1993] and *Fiala and Vejnar* [2004], the uppermost crust in the vicinity of Mýtina consists of an Upper Cambrian to Ordovician alternated stratification of quartzites and phyllites or mica schists (Figure C.7). *Lapp and Weber* [1992] described a similar metagreywacke-phyllite-unit (about 250 m thick) from a core drilled near Neualbenreuth (south of Mýtina). Assuming no thin-skinned tectonic

stacking and the eruption of the tephra from the Železná Hůrka vent, which is located within the Cambrian mica schist units [cb; see *Bayerisches Geologisches Landesamt,* 1998], the samples should not originate from the stratigraphical higher Frauenbach and Phycoden units. The REE pattern of XKZH60 (pronounced negative Eu anomaly; see Appendix C.iii) shows similarities to the "muscovite gneisses" of the Erzgebirge. The magmatic protoliths of these gneisses were probably derived from high-silica per-aluminous rhyolites [see *Mingram et al.,* 2004].

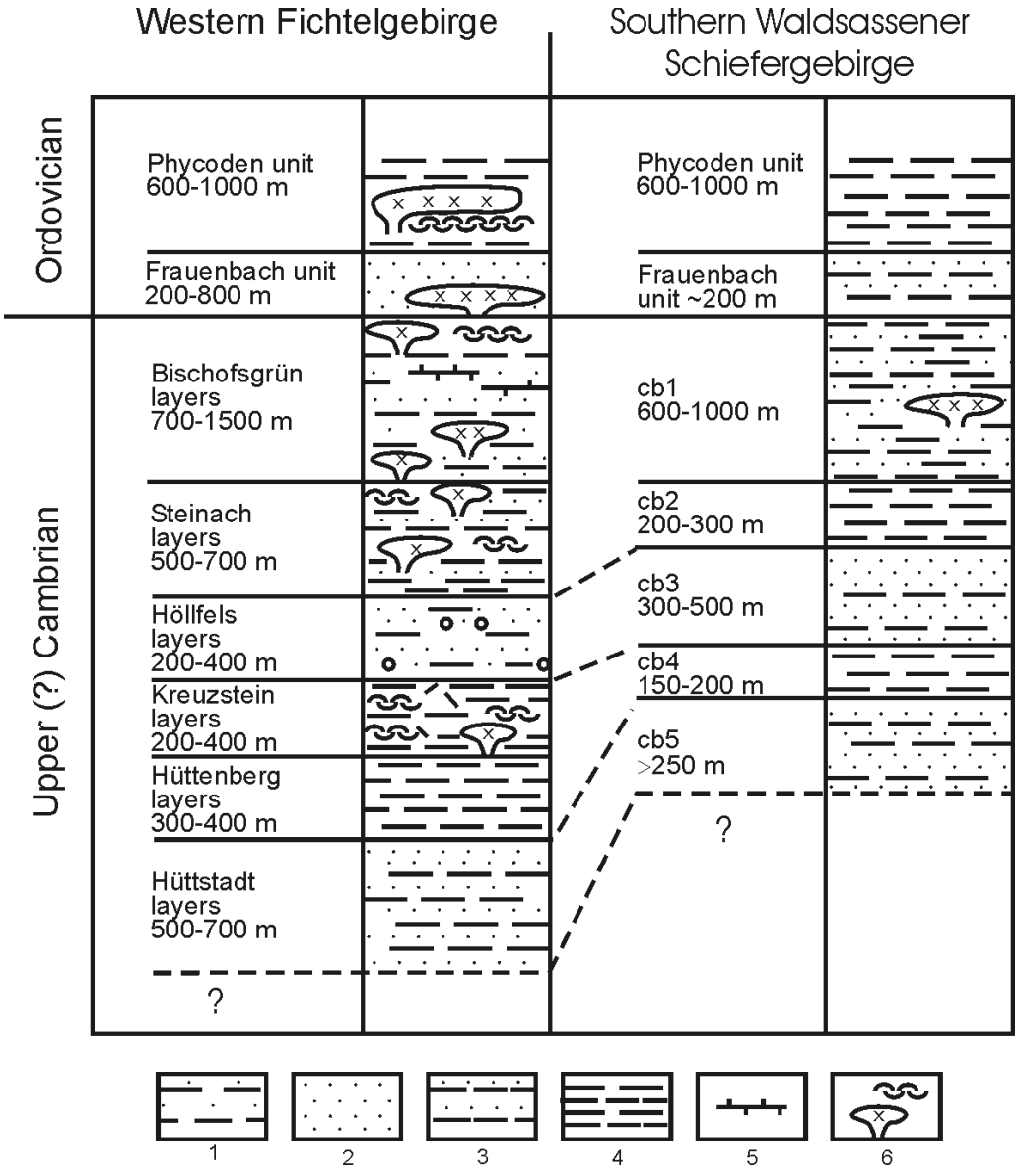

Figure C.7
Lithostratigraphical section of the uppermost crust in the vicinity of Neualbenreuth (southern Waldsassener Schiefergebirge) in comparison to the western Fichtelgebirge [from *Richter and Stettner*, 1993].
1 – shales and phyllites with silty layers; 2 – quartzites, quartzitic schists; 3 – alternated stratification quartzites/phyllites or mica schists; 4 – phyllite and mica schist; 5 – carbonate and calc-silicate intercalations; 6 – acid volcanics (tuffs, ignimbrites).
MXZH6, MXZH65, and MXZH66 (Plates 4, 5) might be samples from acid meta-tuffs, which belong to the "Neualbenreuth layers" in cb1 [*Richter and Stettner,* 1993]. Zircon enriched samples (e.g., XKZH51, 58, 59, 61 with Zr values >1000 ppm, see Appendix C.ii) might belong to zircon rich layers (placer like) in cb3. *Richter and Stettner* [1993] described zircon rich quartzite layers in the Frauenbach and the cb3 (cb5?) units.

C.5.2 Depth origin of xenoliths (geothermobarometry)

Geobarometric estimations for lower crust and upper mantle samples were performed because they may report more or less the conditions close to their formation or metamorphic overprinting at the present depth level. The results of the geothermobarometric calculations for the different types of (ultra-) mafic nodules (cumulates, hornblendites and megacrysts) are shown in Figure C.8 (amphiboles) and listed in Table C.XIV. No geothermobarometric calculations were carried out for upper crustal xenoliths in this study.

Different mineral pairs within one sample record sometimes different pressure-temperature conditions, which may be related to the formation, cooling history, or to later overprinting of the mineral assemblage. Now, I try to interpret the p-T estimates calculated for different samples and mineral pairs from the Mýtina ultramafic xenolith suite (Table C.XIV). However, this give only some constraints on the true pressure-temperature conditions, because the geothermobarometers based on inter-crystalline exchange of elements also show complex dependences on element concentrations.

Magma temperature (olivine-spinel and phlogopite-glass thermometry)

The olivine-spinel thermometers are strongly sensitive to sub-solidus reactions, however from spinel inclusion in olivine phenocrysts it should be possible to estimate the temperature during crystallization of the mineral pair. Values of about 1100°C and 1170°C can be calculated for spinel inclusions within olivine phenocrysts (samples EB5-9, MXZH17) using the geothermometric formulation of *Ballhaus et all.* [1991] and *O'Neill and Wall* [1987], respectively. Because of the fast undercooling during ascent and eruption, I think that sub-solidus reactions did not take place and these values can be assumed to be the temperature of the magma (liquidus). A similar temperature range (1130 to 1150°C) was estimated using the phlogopite-glass geothermometer of *Righter and Carmichael* [1996] for samples MXZH24 and MXZH69. A temperature of 1140°C can be estimated for the combination MXZH21 (phlogopite megacryst) and My1 (nephelinite).

Hbl-peridotite (p-T; MXZH66)

For the amphibole-bearing peridotite xenolith MXZH66 two pressure (depth) estimates were obtained. Using the Al/Ti diagram proposed by *Ernst and Liu* [1998] a pressure of 8 to 9 kbar (30 km depth) and a temperature of 960°C is indicated (Figure C.8a). Using the formulation of *Huckenholz et al.* [1993], the pressure estimate is about 15 kbar (50 km). The discrepancy in pressure estimates might be related to disequilibrium between the mineral phases (post-entrainment modification) or the fact that some assumptions of one of the geobarometers are not fulfilled. Maybe the elevated Cr (and Fe^{3+}?) content of the amphibole makes the sample not suitable to plot it in the Al-Ti diagram, or at least enforce some corrections before plotting. Because the clinopyroxene barometer of *Nimis and Ulmer* [1998] also gives values around 15 kbar (for a olivine-spinel temperature of 1060°C), I prefer this pressure

estimate. Temperatures calculated with the olivine-spinel thermometers of *Ballhaus et all.* [1991] and *O'Neill and Wall* [1987] are 950°C and 1060°C, respectively.

Hbl-clinopyroxenites and cpx-hornblendites, amphibole megacrysts (p-T)

The pressure-temperature conditions of formation of the amphibole-bearing samples (clinopyroxenites, hornblendites), including the amphibole megacrysts were estimated using the Al/Ti plot of *Ernst and Liu* [1998]. The polycrystalline samples plot almost all in a narrow p-T range (see Figure C.8a) of 6 to 8 kbar (22 to 29 km) and 900 to 970°C, only the apatite-bearing sample MXZH5 as well as sample MXZH66 show higher pressures of up to 10 kbar (about 35 km). The amphibole megacrysts plot between 7 and 10 kbar (25 to 35 km) at a very narrow temperature range around 970°C (Figure C.8b).

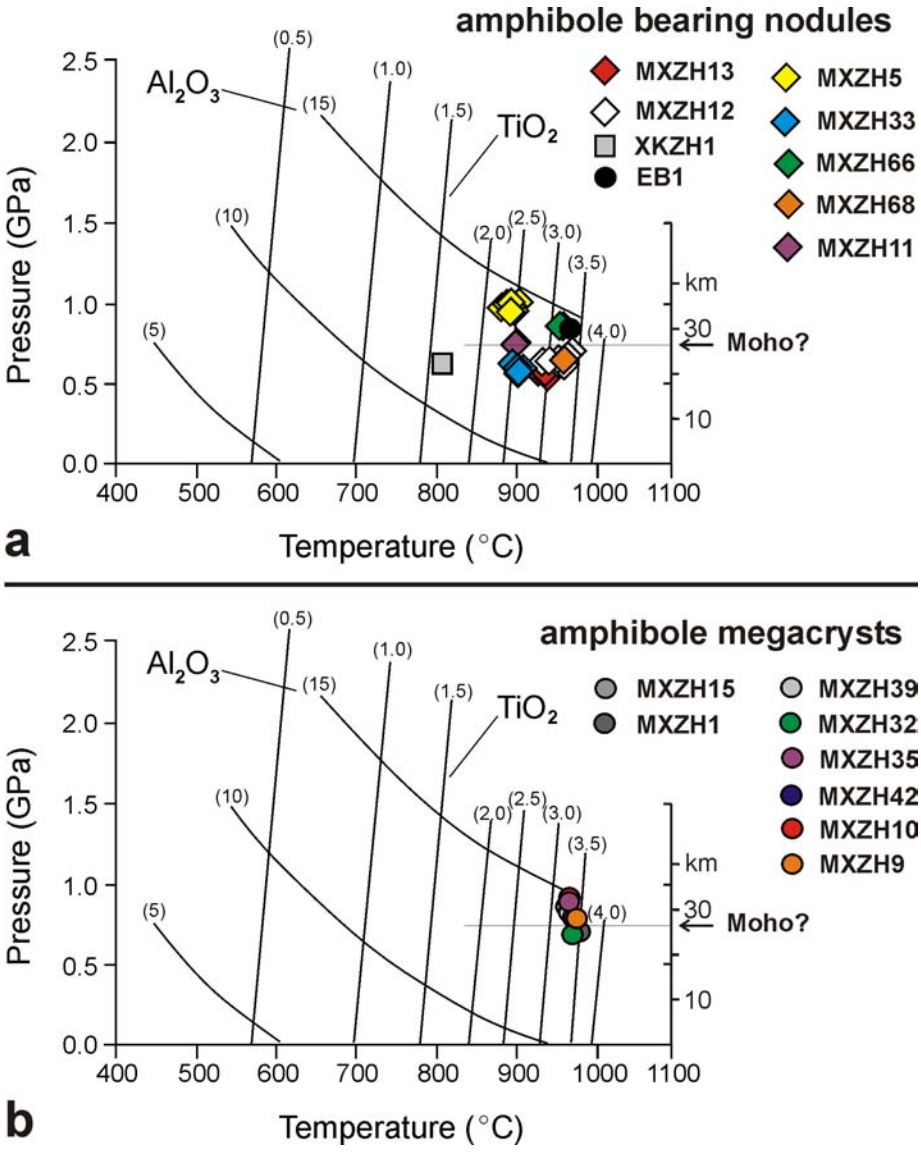

Figure C.8
Results from the Al-Ti amphibole thermobarometry [*Ernst and Liu,* 1998] **(a)** for amphibole-bearing xenoliths and **(b)** megacrysts.

Table C.XIV. p-T estimates of selected (ultra-) mafic nodules (xenoliths and cumulates) from the Mýtina tephra and the Železná Hůrka scoria cone using different geothermobarometers. Two spinel lherzolite samples from the Elbe Zone (Saxony) and from NE-Bavaria are included for comparison.
For the clinopyroxene barometry [NU; *Nimis and Ulmer*, 1998; *Nimis,* 1999] T_{cpxbar} = (1000-1150)°C was used, if no other temperature constraints were available.
T=1150°C was used for wehrlites (MXZH1, -2, -4) and ol-cpx cumulates (MXZH18, -64) and the olivine-clinopyroxene barometer [KB; *Köhler and Brey,* 1990].
At T=1130°C, pressure estimates for samples MXZH18 and MXZH64 coincide (10 to 11 kbar) using clinopyroxene and olivine-clinopyroxene barometry.

sample	rock type	temperature [°C]							pressure [kbar]					
		ol-sp	ol-sp	ol-sp	hbl	opx	2px	phl-gl	cpx-hbl	hbl	ol-cpx	cpxbar	T_{cpxbar}	p_{max}(sp)
		R1979	B1991	NW1987	E1998	BK1990	BKN	RC1996	H1992	E1998	KB	NU1998	°C	N81
Železná Hůrka												p(BH)		
EB1	ol-megacryst + am				960					8..9				
EB5-ol9	ol-phenocryst + sp	1180	1090	1160										29
Mýtina														
XKZH1	norite (primary)					810(r)..870(c)								
	norite (secondary?)				805	*1125*	970		6	6		4?	p(BA)	
MXZH66	hbl-peridotite	1290	950	1060	960				15	8..9	*?*	15..20	1060..960	24
MXZH5	hbl-clinopyroxenite				900				12	9.5..10		7.5..12.5	1000..900	
MXZH11	hbl-clinopyroxenite				900				11	7.5..8		7.5..12.5	1000..900	
MXZH33	hbl-clinopyroxenite				900				5	6		5..10	1000..900	
MXZH12	cpx-hornblendite				930..970				10	6..7		9..11	970..930	
MXZH13	cpx-hornblendite				930				8	5..6		7.5..9.5	970..930	
MXZH68	hornblendite				970					6..7				
MXZH1	wehrlite										10	10..18	1150..1000	
MXZH2	wehrlite										10..11	10..18	1150..1000	
MXZH4	wehrlite										(11)	7..15	1150..1000	
MXZH8	ol-cpx-cumulate											9..17	1150..1000	
MXZH18	ol-cpx-cumulate + sp	1170	1040	1110							13 (10)	11..14	1110..1050	27
MXZH64	ol-cpx-cumulate + sp	1180	1060	1120							13 (10)	11..14	1120..1060	27
MXZH61	ol-cpx-cumulate + sp	1300	1100	1190								10..12	1150..1100	27
MXZH17 (gm)	ol-phenocryst + sp	1270	1100	1170										27
MXZH24	ol-megacryst + phl, gl, cpx							1150				1..3	1150..1100	
	cpx-phenocryst (GM)											11..13	1150..1100	
MXZH69	ol-megacryst							1130						
MXZH21 + My1	phlogopite + nephelinite							1140						
sp-lherzolites														
Zinst-1	sp-lherzolite	1060	960	1000		1080	1105				21	16..21	1100..1000	25
Go01-1	sp-lherzolite (harzburgite)	1070	900	920		920	980				19	17..20	980..920	27

B1991 – *Ballhaus et al.;* 1991; BKN, BK1990 – *Brey and Köhler,* 1990; E1998 – *Ernst and Liu,* 1998; H1992 – *Huckenholz et al.,* 1992; KB – *Köhler and Brey,* 1990; NU1998 – *Nimis and Ulmer,* 1998; NW1987 – *O'Neill and Wall,* 1987; R1979 – *Roeder et al.,* 1979; RC1996 – *Righter and Carmichael,* 1996; N81 – *O'Neill,* 1981 (without Fe^{2+} correction).

Pressures calculated with the formulation of *Huckenholz et al.* [1993] give slightly higher pressure estimates between 5/8 and 12 kbar (22/29 to 40 km) for the clinopyroxene-amphibole-bearing samples. The differences between pressure estimates from both methods are within the given uncertainties. A comparison with experimental partitioning data for Ti, Ho, Lu, Sr between amphibole and basanitic melt from *Adam and Green* [1994] indicates the crystallization of amphibole megacryst MXZH15 at pressures above 1 GPa, assuming that the nephelinite sample My1 represents also the melt composition in the magma reservoir.

The relatively high temperatures obtained for the amphibole-bearing samples, possibly originating from near the crust-mantle boundary, are most probably crystallization (magmatic) temperatures. These values are valid for small dikes or intrusion at the time of their formation and do not necessarily represent temperatures valid for the crust-mantle transition and lower crust on the regional scale. If the amphibole megacrysts would be high-pressure precipitates of the host melt, then the p-T estimates provide constraints for the depth and temperatures of the palaeo-magma reservoirs near the crust-mantle boundary. The rounding of most amphibole megacrysts might be an effect of the upward transport (decompression) in a hotter and reactive melt.

Wehrlites, olivine-clinopyroxene aggregates and clinopyroxene-megacrysts (p-T)

For most wehrlitic samples (MXZH1, -2, -4), olivine-clinopyroxene aggregates (MXZH18, -64), and clinopyroxene megacrysts and phenocrysts (groundmass crystal in MXZH24), depths of origin of 29 to 38 km (8 to 11 kbar) could be estimated using the olivine-clinopyroxene barometer of *Köhler and Brey* [1990] and the clinopyroxene barometer of *Nimis and Ulmer* [1998]. However, both barometers are strongly temperature sensitive. Assuming a temperature of 1150°C, the estimates from both calibrations are more or less the same. This high temperature value (near liquidus) indicates that most samples are somehow related to the host magma or at least to the same Late Cainozoic magmatic activity. A comparison with experimental partitioning data for Ti and Ho between clinopyroxene and basanitic melt from *Adam and Green* [1994] indicates the crystallization of amphibole megacryst MXZH16 at pressures above 1 GPa, assuming that the nephelinite sample My1 represents also the melt composition in the magma reservoir.

Spinel lherzolites

The commonly applied geothermobarometers for spinel lherzolitic samples were tested on samples Go01-1 and Zinst-1, which are included in this study for comparison reasons.

The harzburgitic sample Go01-1 from the Elbe Zone was equilibrated at a pressure of about 19 kbar (more than 60 km depth), according to the formulation of *Köhler and Brey* [1990]. Temperature values (olivine-spinel, two-pyroxene) range from 920 to 980°C, depending on the formulation used. For the pressure calculation the temperature estimate from the two-pyroxene thermometer of *Brey and Köhler*

[1990] was used. The temperature estimate is closer to values reported from the eastern Erzgebirge than to values from the Elbe Zone [*Kramer and Seifert,* 2000]; the sample locality is close to the boundary of both areas.

A pressure of 21 kbar (approximately 70 km depth) was estimated for the sample from Zinst, NE-Bavaria. Calculated temperatures are in the range of 1000 to 1100°C, close to estimates from nearby localities (see references in section A.3.3, Table A.1).

Noritic xenolith (XKZH1)

For the noritic xenolith, depth and temperature estimation was possible using the Al/Ti-in-amphibole plot of Ernst and Liu [1998]. The sample plots at about 6 kbar (about 22 km) and 800°C (see Figure C.8a). An identical temperature (800°C) could be obtained using the Ca-in-orthopyroxene thermometer of *Brey and Köhler* [1990] and rim composition of the orthopyroxene close to the analysed amphibole. The core composition gives values of 860°C. This difference between rim and core might be related to cooling (after intrusion or during tectonic uplift) or a post-intrusion overprinting at lower temperatures. Temperatures between 700-900°C were also reported by *Mengel* [1990] for mafic and noritic granulites from the North Hessian Depression, which are interpreted as high-grade equivalents of subduction-related volcanics and cumulates.

Higher temperature values (970°C/1125°C) were obtained using analyses from areas of orthopyroxene-clinopyroxene intergrowth using two different formulations of *Brey and Köhler* [1990]. Because both temperature values differ strongly, the analysed minerals might not be in equilibrium. This may be an effect of magmatic overprinting (heating) of the sample in the host magma, or may be related to an earlier metasomatic event.

C.5.3 p-T data and regional geotherms

The p-T estimates for xenoliths can generally provide constraints on the recent thermal structure of the deep crust and uppermost mantle. As shown in Figure C.9, most analysed samples plot close to the alkaline province geotherm [*Jones et al.,* 1983], that means above proposed regional geotherms [*Čermák*, 1994] derived from surface heat-flow studies.

Moho temperatures, calculated from regional surface heat flow data differs from 450°C up to 750°C [see *Förster et al.,* 2003]. The problem in extrapolating the regional surface heat-flow data to depth is the strong influence of high-radioactive, heat-producing granitic rocks in the upper crust. Therefore, it is difficult to estimate the regional Moho heat-flow and temperatures [*Förster and Förster,* 2000]. However, from the p-T xenolith data, which is so far available for the area under investigation, it is impossible to construct a regional xenolith geotherm to get better constraints on the recent or at least Late Cainozoic thermal structure of the lower crust and upper mantle.

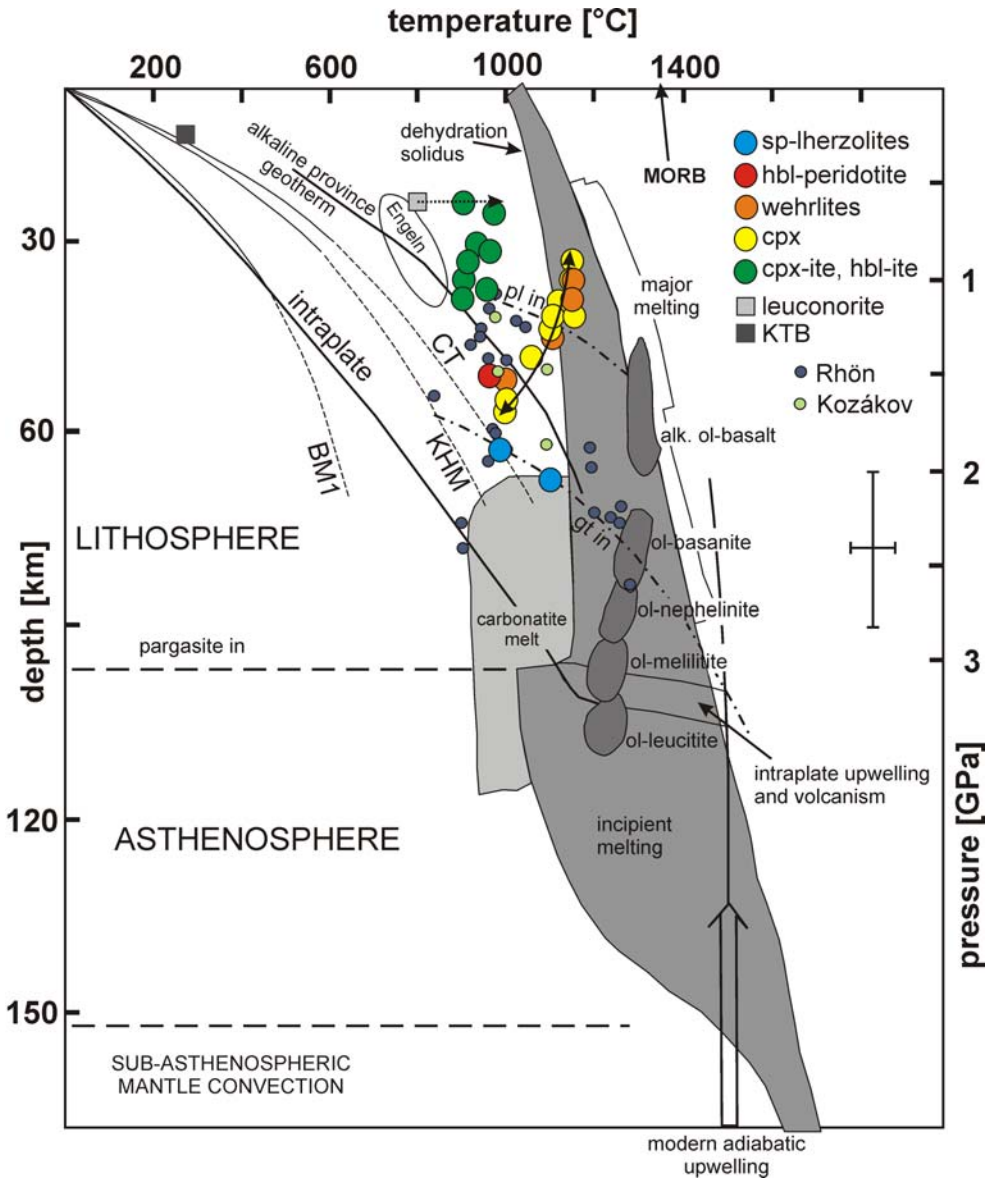

Figure C.9
Results of p-T calculations plotted into a diagram of *Green and Falloon* [1998]. The alkaline province geotherm [*Jones et al.,* 1983], regional geotherms (BM1 -Bohemian Massif minimum, KHM - Krušne Hory Mts., CT - Cretaceous Basin; *Čermák,* 1994), and one KTB-value [*Clauser et al.,* 1997] are included. The p-T field for granulite-facies metabasite ejecta from Engeln (Eifel, Germany) is shown for comparison with sample XKZH1 [adopted from *Jones et al.,* 1983; data from *Okrusch et al.,* 1979]. p-T estimates from the Rhön and the Kozákov are adopted from *Franz et al.* [1997] and *Medaris et al.* [1997], respectively.
Wilson and Downes [1992] described the frequently occurring/widespread melilite nephelinites as most likely candidates for primary melts from the asthenosphere/basal lithosphere. According to *Wilson et al.* [1995], melt coexisting with lherzolitic rocks at T >1025°C and pressures in the garnet stability field is in composition similar to ol-melilitite, whereas at lower pressures in the spinel stability field, silicate melt resamples ol-nephelinites.

C.6 Petrological indications for processes at the crust-mantle boundary

The p-T estimates indicate a depth origin of ultramafic nodules within the lower crust and uppermost mantle (approximately 20 to 50 km, with a maximum at 30 to 35 km). No orthopyroxene-bearing spinel-lherzolitic xenoliths could be found in the Quaternary volcanics; such xenoliths are thought to represent normal lithospheric upper mantle beneath Central Europe. The results indicate that possibly

large parts of the uppermost mantle beneath NW-Bohemia might be affected by mantle metasomatism around 0.3 Ma (due to infiltration of alkaline melts), which resulted in a mantle composition dominated by olivine and clinopyroxene (±amphibole, ±phlogopite).
The amphibole-rich nodules from about 20 to 35/40 km depth could represent fragments of magmatic dikes within the uppermost mantle and lower crust, which may be a more widespread phenomenon in the study area. According to *Barclay and Carmichael* [2004], isobaric crystallization of amphibole (hornblende) in a subduction related hornblende-basaltic melt near the base of the crust can influence the magma's capacity to flow (viscosity). And once amphibole crystallizes, the magma's ascent might be retarded by its high crystallinity. As *Barclay and Carmichael* [2004] pointed out, great proportions of basaltic bulk composition can crystallize as amphibole (as can be also seen in the similar chemical compositions of the pargasites and the nephelinitic host rock from Mýtina), and therefore most magma intrusions may stop in the lowermost crust due to cooling (freezing) by the surrounding "cold" crust. Maybe the uppermost mantle and lowermost crust beneath the western Eger Rift experienced many intrusions of small amounts of alkaline melt during the late Tertiary and Quaternary; only very few of these melts reached the surface.

The content and distribution of REEs in the nephelinitic host rock of the Mýtina tephra and from the Železná Hůrka scoria cone (Figure C.5) can be interpreted in terms of low percentage (approximately 1 %) of partial melting in a garnet-bearing source [according to *Rollinson,* 1993]. However, 1 % partial melt may be the amount of melt in the source region (90 to 100km depth?); more than 1 % could be present in the ponding region in the uppermost mantle (25 to 50 km depth), where it may form magma reservoirs. High "porosity", which can be observed in some ultramafic nodules, may indicate that this samples originate as "wall rock" of magma chambers, as discussed by *Tait* [1988] or may represent itself parts of a sponge-like magma reservoir.

Origin of CO_2 – related to alkaline-carbonatitic mantle metasomatism ?

According to *Green and Falloon* [1998], olivine-nephelinitic to olivine-melilitic melts originate at depths of about 90 to 100 km in a garnet-bearing source region (asthenosphere). Garnet remains in the residuum (might be inferred from the REE pattern). The ascending melts crystallize amphibole and phlogopite. This modal metasomatism of garnet/spinel lherzolite might leave carbonatitic residual melts, which react with enstatite and spinel to form olivine + (diopside + jadeite) + chromite + CO_2. The metasomatic lithosphere becomes enriched in clinopyroxene, illustrated by the formation of wehrlites (olivine + clinopyroxene + apatite + chromite) [see also *Yaxley et al.,* 1991, *Rudnick et al.,* 1993]. The CO_2 is released and migrates to the surface. This might be a possible scenario for the study area as well. However, up to now there are no further indications for the involvement of carbonatitic melts, as for instance carbonate inclusions in olivine and clinopyroxene or carbonate globules in silicate glass as observed by *Seifert and Thomas* [1995] in samples from the Elbe Zone, Germany.